Nano Energy 159 (2026) 112383

Contents lists available at ScienceDirect

Nano Energy

journal homepage: www.elsevier.com/locate/nanoen

Review

# Flexible wearable sensors for pulse wave monitoring: Principles, designs, and applications in disease assessment

Menghan Li [a,1], Xuandi Deng [a,1], Puqing Yao [a], Lei Jia [a], Xingyao Lv [a], Yu Song [b], Yuxiang Wu [c,*], Zhou Li [d,e,**], Zhuo Liu [a,**]

[a] Key Laboratory for Biomechanics and Mechanobiology of Ministry of Education, School of Biological Science and Medical Engineering, School of Engineering Medicine, Beihang University, Beijing, China
[b] Department of Biomedical Engineering, College of Biomedicine, City University of Hong Kong, Hong Kong, China
[c] Institute of Intelligent Sport and Proactive Health, Department of Health and Physical Education, Jianghan University, Wuhan, China
[d] Vita Tech Innovation Center, Tsinghua Changgung Hospital, School of Clinical Medicine, Tsinghua University, Beijing, China
[e] School of Biomedical Engineering, Tsinghua Medicine, Tsinghua University, Beijing, China

ARTICLE INFO

*Keywords:*
Pulse wave
Flexible sensors
Wearable devices
Machine learning
Disease diagnosis

ABSTRACT

Arterial pulse waves arise from the cyclic contraction of the heart and subsequently spread along the arterial tree, carrying abundant physiological information related to vascular mechanics, hemodynamics, and autonomic regulation. In recent years, advances in flexible wearable electronics have enabled continuous, non-invasive, and high-fidelity pulse wave monitoring under daily-life conditions. This review systematically analyzes the physiological principles underlying pulse wave generation and detection, and summarizes the structural designs and recent progress in pulse-wave-based disease assessment across multiple clinical scenarios. Particular emphasis is placed on the role of machine learning as a key enabler for pulse signal analysis, diagnostic algorithm development, and estimation of clinical parameters. Finally, current challenges and future perspectives toward multimodal sensing, intelligent signal analysis, and clinical translation are discussed. Overall, this review brings together sensing technologies, pulse signal characteristics, and disease-related applications, aiming to support more informed sensor design and the practical translation of wearable pulse monitoring systems.

## 1. Introduction

Arterial pulse waves arise from the periodic contraction of the heart and propagate through the arterial tree as pressure waves generated by the interaction between pulsatile blood flow and the arterial wall. Their propagation and morphology are jointly shaped by cardiac ejection, arterial compliance, peripheral resistance, and wave reflection, allowing pulse-wave signals to convey information about both cardiac and vascular function [1]. The clinical value of the arterial pulse has long been recognized, with records dating back to the sixth century BCE describing radial artery palpation in ancient Chinese, Indian, and Egyptian medicine [2]. With the development of modern sensing and signal-analysis techniques, pulse assessment has evolved from qualitative palpation toward quantitative waveform analysis. Characteristic features such as the systolic upstroke, diastolic decay, dicrotic notch, and pulse wave velocity (PWV) can provide information on cardiac contractility, arterial stiffness, peripheral vascular resistance, and wave reflection dynamics [3,4]. The importance of accessible cardiovascular monitoring is further underscored by the growing global burden of cardiovascular diseases (CVDs). CVDs remain the leading cause of death and disability worldwide, with approximately 626 million prevalent cases, 19.2 million deaths, and 437 million disability-adjusted life years (DALYs) reported globally in 2023 [5,6]. Moreover, the number of people living with CVDs has more than doubled since 1990, highlighting the increasing need for practical approaches to early risk assessment, longitudinal disease management, and continuous physiological monitoring. In this context, arterial pulse waves are particularly attractive because they can be acquired non-invasively and repeatedly, while

* Corresponding authors.
** Corresponding author at: Key Laboratory for Biomechanics and Mechanobiology of Ministry of Education, School of Biological Science and Medical Engineering, School of Engineering Medicine, Beihang University, Beijing, China.
*E-mail addresses:* yxwu@jhun.edu.cn (Y. Wu), li_zhou@tsinghua.edu.cn (Z. Li), liuzhuo@buaa.edu.cn (Z. Liu).
[1] M. Li and X. Deng contributed equally to this work.

https://doi.org/10.1016/j.nanoen.2026.112383
Received 23 July 2026; Received in revised form 1 September 2026; Accepted 7 September 2026
Available online 9 September 2026
2211-2855/© 2026 Elsevier Ltd. All rights are reserved, including those for text and data mining, AI training, and similar technologies.

retaining beat-to-beat information on cardiovascular dynamics. Importantly, the physiological information contained in arterial pulse waves is not restricted to cardiovascular disease. Pulse-wave morphology and timing are influenced by broader changes in vascular tone, autonomic regulation, metabolic status, and systemic hemodynamics. Accordingly, alterations in pulse-derived features have also been associated with stroke [7,8], metabolic syndrome [9–11], organ dysfunction and failure [12–16], and mental health disorders [17–19]. Although such associations do not necessarily imply disease-specific diagnostic capability, they indicate that pulse-wave sensing may provide useful information for screening, monitoring, and risk assessment across a broader range of physiological and pathological conditions. These characteristics have expanded the role of arterial pulse sensing from conventional cardiovascular assessment toward continuous and cross-system health monitoring.

Despite the well-established diagnostic value of pulse-derived information, its widespread adoption in both clinical practice and daily life remains significantly limited. Conventional pulse monitoring methods typically rely on intermittent measurements, require cumbersome instrumentation, and offer restricted wearing comfort, thereby largely confining their use to controlled clinical settings [20]. Moreover, contextual influences such as the white-coat effect, wherein patients exhibit elevated physiological readings due to anxiety in medical settings, further compromise their reliability for long-term physiological assessment [21]. Addressing this challenge has driven successive technological innovations in pulse sensing. Optical methods emerging with photoplethysmography (PPG) have enabled their widespread use in wearable devices [22,23]. In parallel, advances in flexible materials and microfabrication gave rise to diverse mechanical sensing strategies, including piezoelectric, piezoresistive, and capacitive sensors [24]. The introduction of flexible polyvinylidene fluoride (PVDF)-based piezoelectric sensors and, more recently, triboelectric nanogenerators (TENGs) further expanded the design space for high-sensitivity, low-power pulse monitoring [25]. Machine learning techniques further enable automatic feature extraction and pattern recognition from complex physiological signals, thus boosting the practical value of pulse waveform analysis in disease screening and health assessment [26–28]. Collectively, these developments herald a new class of wearable pulse sensing systems for continuous, personalized, and context-aware health monitoring.

Recent progress in flexible wearable pulse sensing technologies and their health monitoring applications is systematically surveyed herein. The physiological basis of arterial pulse wave generation is first introduced. Major sensing strategies are then comparatively examined, with emphasis on their operating principles, material innovations, and structural design considerations. These strategies can be broadly divided into optical techniques and electromechanical transduction mechanisms. The latter group includes piezoresistive, capacitive, piezoelectric, and triboelectric approaches. Each offers distinct advantages for wearable integration. Building on these technological foundations, recent progress in pulse-wave-based disease assessment is summarized across multiple clinical domains, including cardiac rhythm disorders, abnormalities in hemodynamic load and vascular mechanics, autonomic and cardiorespiratory coupling dysfunctions, microcirculatory and metabolic regulation disorders, and systemic multi-organ conditions. The role of machine learning in pulse signal processing and model development is discussed in this context, highlighting its contribution to feature extraction, disease classification, and cuffless estimation of clinical parameters. This review also examines key challenges (e.g., motion artifacts, signal stability, and clinical validation) and outlines promising future directions, including multimodal sensing, edge intelligence, and integrated self-powered systems. Overall, this review aims to assist in choosing, optimizing, and clinically translating flexible wearable pulse sensing technologies.

## 2. Physiological basis and sensing mechanisms of arterial pulse waves

### 2.1. Generation, propagation, and morphological characteristics of arterial pulse waves

The arterial pulse wave originates from cardiac contraction. During this process, blood ejection produces a pulsatile flow that travels through the arterial system. This propagation is shaped by two key factors: the conversion of kinetic energy into lateral pressure against the vessel wall due to peripheral resistance, and the wave-like movement of the blood itself, which undergoes reflection at sites where arterial geometry or elasticity changes [29,30]. The combination of forward transmission of cardiac pressure impulses and the return of the peripheral vasculature between the large and resistance vessels (arteries and arterioles) constitutes the shape of the pulse waves in the respective arteries [31,32]. Consequently, the amplitude and flow waveform of pulse wave signals vary with the arterial geometry and distensibility, the amplitude and duration of cardiac ejection, and microvascular impedance. When recorded at the radial artery (a distal, superficial vessel readily accessible at the wrist, illustrated in Fig. 1a), the pulse waveform retains characteristic morphological segments commonly observed in peripheral arteries [33].

As shown in Fig. 1b, the pulse waveform is composed of the systolic and diastolic periods, and three characteristic peaks can be identified: the systolic peak (point I), the tidal peak (point II), and the diastolic peak (point IV). The morphology of the waves is related to the compliance of the vessel wall and changes in intraluminal blood pressure. The width of the systolic peak reflects the duration of the increase in aortic pressure, and the time corresponding to the ascending limb is called the rapid ejection phase. At the end of this phase, aortic dilation ceases, and a slowed ejection phase begins. As blood inflow into the aortic root becomes lower than outflow, aortic volume gradually decreases, leading to a fall in pressure. The elastic vessel wall gradually retracts, resulting in the descending branch of the pulse waveform signal. Peripheral pulse wave morphology is modified by reflected waves from distal vascular beds. These retrograde waves superimpose on the descending limb, creating the characteristic tidal wave, which forms the tidal peak. At diastole onset (point III), left ventricular pressure plummets during myocardial relaxation, causing abrupt aortic valve closure. This hemodynamic transition produces the dicrotic notch, an incisura preceding the dicrotic wave [34]. The subsequent brief pressure rebound arises from blood column deceleration against the closed aortic valve, generating a secondary pressure wave that forms the diastolic peak. During diastole, continuous peripheral runoff driven by arterial elastic recoil gradually reduces aortic volume and pressure, ultimately returning to the pre-systolic baseline. The diastolic blood pressure corresponds to the minimal pressure before the next cardiac cycle [35].

The slope and amplitude of the systolic upstroke predominantly reflect left ventricular contractility and aortic filling dynamics, while the configuration of the anacrotic phase, particularly the position of the anacrotic shoulder, serves as an important feature of arterial compliance and systemic vascular resistance [36,37]. The amplitude of the pulse wave correlates strongly with peripheral resistance magnitude, while double-peaking in the diastolic complex suggests aortic valve dysfunction or reduced arterial compliance [34]. These multidimensional morphological features provide critical insights into cardiovascular hemodynamics, arterial wall viscoelasticity, and peripheral tissue perfusion characteristics, establishing pulse waveform analysis as a non-invasive modality for evaluating integrated cardiocirculatory function [38–41]. At the body surface, these cardiovascular dynamics manifest as changes in blood volume, blood flow, optical properties, and tissue deformation, which can be captured by different optical and mechanical sensing technologies. The following sections therefore introduce these sensing mechanisms according to their distinct physical measurands and pulse-related outputs.

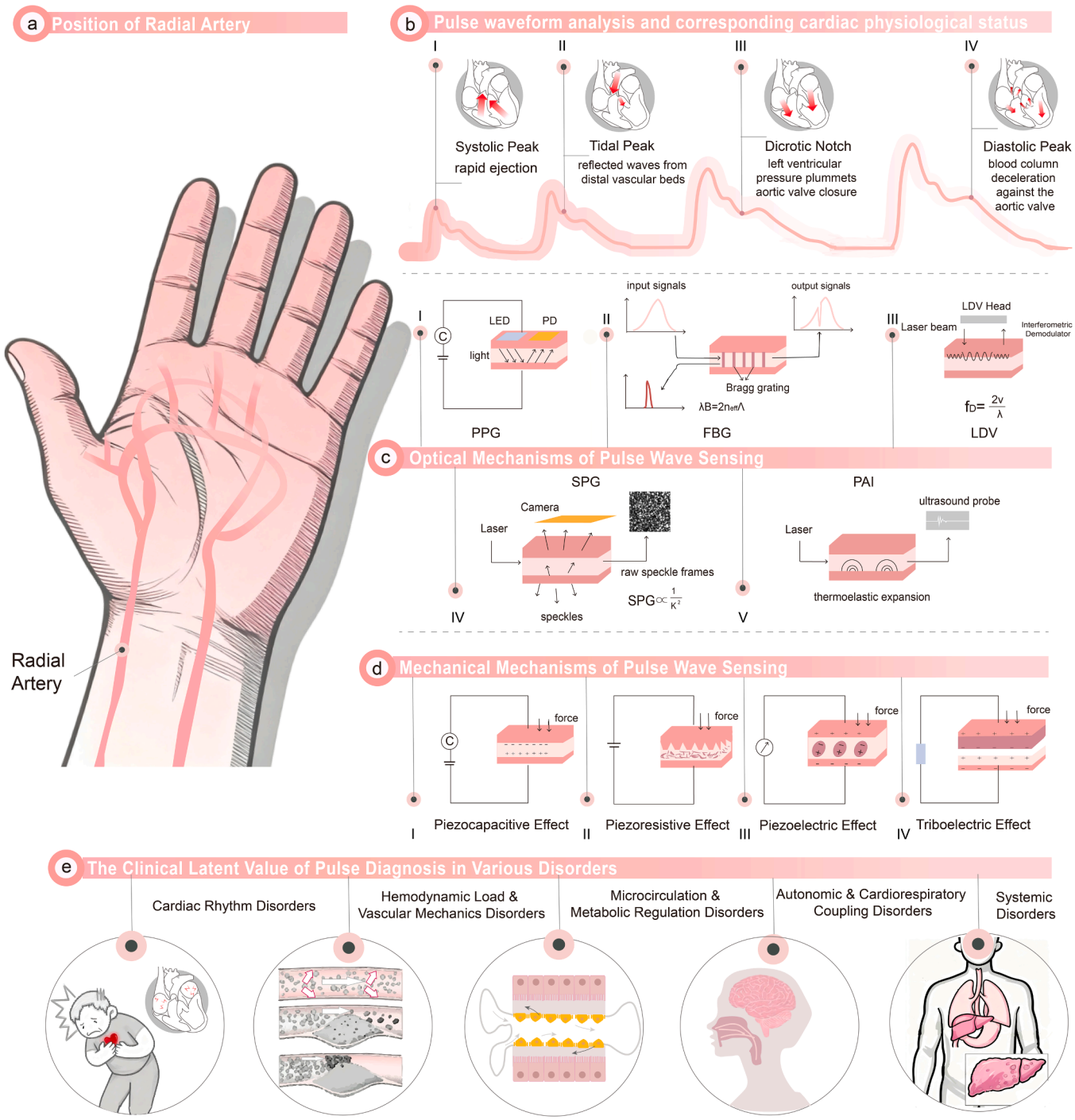



**Fig. 1.** Principles of pulse wave generation and measurement mechanisms. (a) Illustration of the position of the radial artery. (b) Pulse waveform analysis and corresponding cardiac physiological status. (c) Schematic illustrations of optical sensing mechanisms for pulse wave detection. (d) Schematic illustrations of mechanical sensing mechanisms for pulse wave detection. (e) The clinical value of pulse monitoring in disease diagnosis.

### 2.2. *Optical sensing mechanisms*

Optical pulse sensing operates by monitoring changes in the interaction between light and biological tissues, thereby capturing pulsatile physiological information. PPG represents one of the most widely adopted optical technologies in both consumer wearables and clinical devices. As schematically illustrated in Fig. 1c(I), a typical reflective-mode PPG sensor comprises a light-emitting diode (LED) and a photodetector (PD). It operates by emitting light into the skin and measuring the intensity variations of the back-scattered light. Pulsatile blood flow causes periodic changes in subcutaneous blood volume, modulating light absorption and generating the PPG signal. The acquired PPG waveform contains an alternating component (AC), which reflects arterial pulsation and encodes vascular compliance, and a direct component (DC), influenced by static tissues, venous blood, and ambient factors [42]. Utilizing the Beer-Lambert law, dual-wavelength PPG can estimate oxygen saturation ($SpO_2$) by analyzing the pulsatile-to-baseline absorbance ratio at distinct wavelengths [43,44]. Although PPG is appreciated for its simplicity and low cost, it remains vulnerable to motion artifacts.

In contrast, fiber Bragg grating (FBG) sensors constitute an alternative optical technique. An FBG system includes a laser source and an

interrogator. As shown in Fig. 1c(II), input signals from arterial pulsations induce mechanical strain on the fiber, altering the period (Λ) of the internal diffraction grating. This causes a shift in the reflected Bragg wavelength ($\lambda_B = 2n_{eff}\Lambda$), which is detected as the output signal and used to reconstruct the pulse wave [45]. This mechanism enables high-sensitivity measurement of mechanical pulses and inherent immunity to electromagnetic interference, making FBG suitable for environments like Magnetic Resonance Imaging (MRI) [46]. However, conventional silica optical fibers are brittle and prone to breakage under bending or extension, which limits their mechanical robustness and comfort when worn on the body [47]. Moreover, such fibers cannot withstand routine washing or vigorous movement without encapsulation, and their rigidity relative to skin presents challenges for long-term wearable use [48]. In addition, FBG wearable platforms face practical challenges, including temperature cross-sensitivity and limited wear resistance, which remain obstacles for widespread consumer adoption [49].

Beyond PPG and FBG techniques, several optical sensing approaches based on dynamic light scattering have been developed to probe blood flow pulse dynamics. laser Doppler velocimetry (LDV), as illustrated in Fig. 1c(III), operates by directing a coherent laser beam onto the skin surface. The light scattered by moving red blood cells undergoes a frequency shift, known as the Doppler shift (Δf), which is directly proportional to the flow velocity. The relationship can be expressed as $\Delta f \propto 2v/\lambda$, where v is the flow velocity, and λ is the laser wavelength. By detecting these frequency shifts, LDV enables continuous, non-invasive

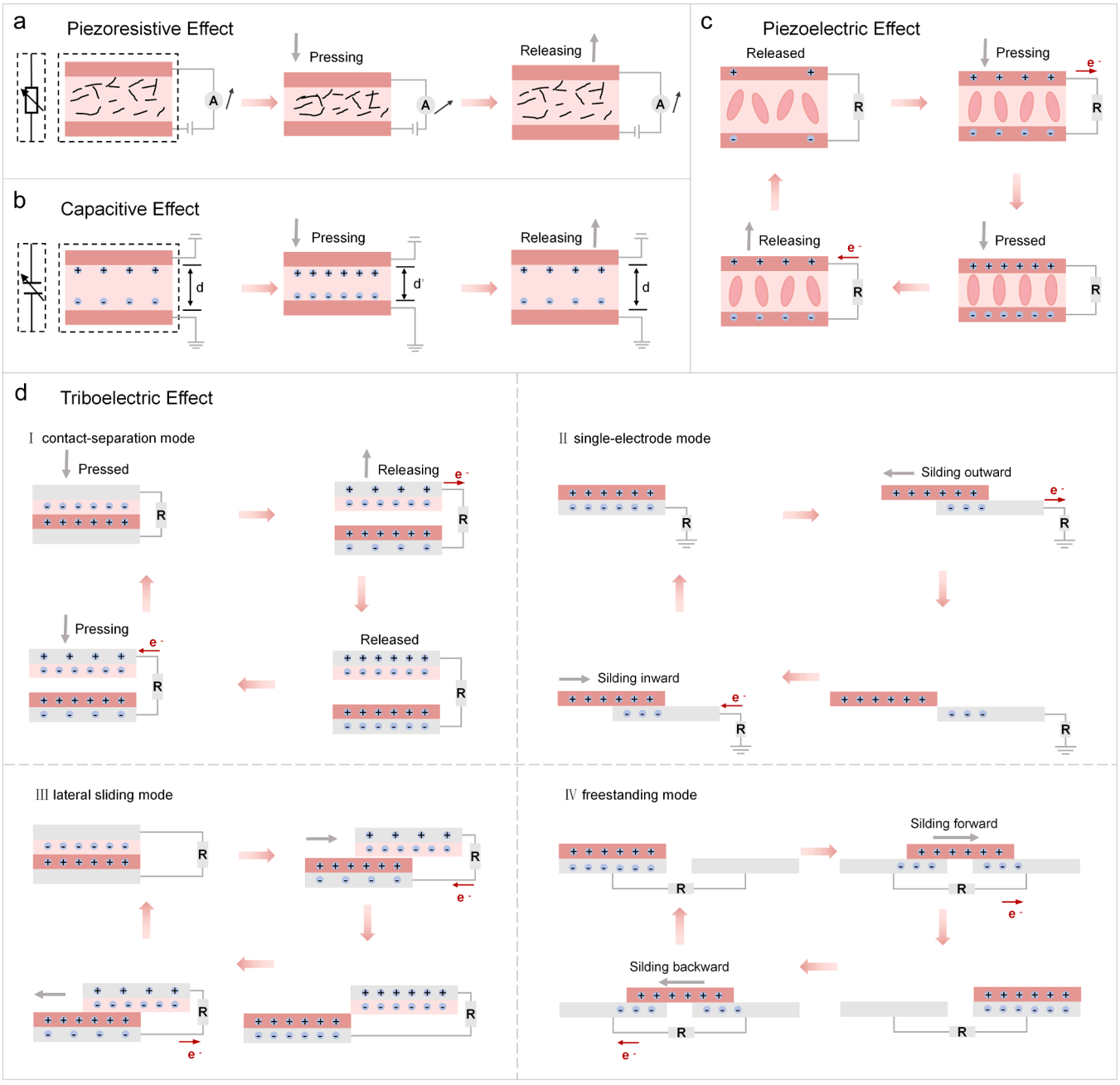



**Fig. 2.** Schematic illustrations of mechanical transduction mechanisms in wearable pulse wave sensors. (a) Piezoresistive sensing based on deformation-induced changes in electrical resistance. (b) Capacitive sensing based on pressure-induced changes in capacitance. (c) Piezoelectric sensing based on the direct piezoelectric effect, in which applied mechanical stress generates electrical charges. (d) Triboelectric sensing based on contact electrification and electrostatic induction, including four fundamental working modes: (I) contact-separation mode, (II) single-electrode mode, (III) lateral sliding mode, and (IV) freestanding mode.

quantification of blood flow velocity and microcirculatory dynamics with high temporal resolution, and has been widely used for assessing tissue perfusion and vascular reactivity in physiological and clinical studies [50,51]. Speckle-based optical techniques exploit the dynamic interference patterns generated when coherent laser light is scattered by biological tissue. In speckle plethysmography (SPG), as shown in Fig. 1c (IV), a laser source illuminates the tissue while a camera captures raw speckle images over time. The physiological pulse wave is extracted by analyzing temporal fluctuations in the speckle pattern statistics, which arise from motion-induced phase variations caused primarily by red blood cell dynamics [52]. Quantitatively, the extracted SPG signal is often related to the inverse square of the spatial frequency magnitude (SPG signal $\propto 1/K^2$). While promising, LDV and SPG systems typically require coherent laser sources, precise optical alignment, and high-speed detection or imaging hardware, resulting in increased system complexity, power consumption, and susceptibility to motion-induced artifacts [53–55]. These constraints currently limit their translation beyond controlled laboratory or clinical environments, despite their strong potential for high-precision physiological assessment. Another emerging modality is photoacoustic imaging (PAI). This hybrid technique, also illustrated in Fig. 1c (V), involves pulsed laser irradiation. Light absorption by hemoglobin causes thermoelastic expansion, generating broadband ultrasound waves that are captured by an ultrasound probe [56]. PAI uniquely provides detailed vascular images and oxygenation data from deeper tissues, but is currently limited to clinical and research settings due to high cost and limited portability.

In summary, optical pulse sensing technologies are progressively evolving from simple, single-point detection towards multidimensional, imaging-based, and even non-contact strategies. Future progress will likely hinge on multimodal integration, advanced signal processing, and system miniaturization to bolster clinical utility and daily health monitoring accessibility.

### 2.3. Mechanical sensing mechanisms

Mechanical pulse sensors detect arterial pulsation by converting pulse-induced pressure, strain, or tissue deformation into electrical signals. As illustrated in Fig. 2, the major transduction pathways include piezoresistive, capacitive, piezoelectric, and triboelectric mechanisms. In general, the sensing process can be understood as a sequence starting from mechanical input, going through structural and material response, and ending with electrical output. This sequence underlies their distinct response characteristics, sensitivities, and application scenarios.

#### 2.3.1. Piezoresistive effect

Specific schematic illustrations of piezoresistive sensors are demonstrated in Fig. 2a. In piezoresistive sensors, applied pressure is transferred into a variation in electrical resistance. This variation arises from three primary factors: the contact resistance between electrode and sensing material, the intrinsic resistance of the sensing material, and the resistance of the electrode [57]. The total resistance of the system can be expressed as:

$$R_{total} = R_{contact} + \rho\frac{L}{A} + R_{electrode} \quad (1)$$

where $\rho$ is the resistivity of the sensing material, L is the effective conductive path length, A is the cross-sectional area of the conductive pathway, $R_{contact}$ represents the interfacial contact resistance between the electrode and the sensing material, and $R_{electrode}$ is the resistance of the electrode itself. Mechanistically, piezoresistive pulse sensors typically operate through two representative routes [58,59]. The first relies on interfacial contact modulation. Under an applied pulse force, surface microstructures or conductive asperities deform, thereby increasing the effective contact area between conductive layers and reducing the contact resistance. The second relies on deformation of conductive networks within bulk or porous composites, such as MXene-, CNT-, graphene-, or metal-nanowire-based porous structures [60–62]. In these systems, pressure-induced compression changes the number and quality of conductive pathways and can also alter tunneling distances between adjacent conductive domains, resulting in a pronounced resistance change. Because of this direct electromechanical conversion pathway, piezoresistive sensors are particularly attractive for pulse monitoring due to their simple readout, high sensitivity, and ease of structural design. However, their performance may be affected by hysteresis, baseline drift, and limited linearity, especially when large deformation or viscoelastic substrates are involved.

#### 2.3.2. Capacitive effect

A typical capacitive pressure sensor is illustrated in Fig. 2b. In its simplest form, two conductive electrodes sandwich a soft dielectric layer, forming a deformable parallel-plate capacitor. When an external pulse pressure is applied, the capacitance changes because the electrode spacing, effective overlap area, or dielectric properties are altered. The basic capacitance relationship is given by:

$$C = \varepsilon_0\varepsilon_r\frac{A}{d} \quad (2)$$

where A is the overlapping area of the two plates, $\varepsilon_0$ is the vacuum permittivity, $\varepsilon_r$ is the relative permittivity of the intervening dielectric, and d is the plate separation distance. Unlike piezoresistive sensors, capacitive sensors do not rely on charge transport through a conductive network, but instead detect pulse signals through deformation-induced modulation of the electric field distribution. In wearable pulse applications, the most common mechanism is compression of the dielectric layer, which reduces $d$ and thereby increases capacitance. Microstructured dielectrics, porous elastomers, and low-modulus substrates are often introduced to amplify this deformation and improve low-pressure sensitivity. In some designs, changes in contact area between electrodes and dielectric microstructures also contribute to the capacitance response. Capacitive pressure sensors (CPSs) are valued for their high drift stability, simple architecture, and insensitivity to strain and temperature, positioning them as attractive candidates for high-performance flexible pressure sensing [63]. However, they may exhibit limited sensitivity (S), inadequate resolution in the low-pressure regime, or a saturating response under high pressures [64].

To address these limitations, a variant of capacitive sensing known as ionic capacitive sensing or iontronic sensing has emerged. While based on the same fundamental principle of measuring capacitance, iontronic sensors differ fundamentally in their structure and operating mechanism. Instead of using solid parallel plates, they typically employ a soft ionic material (e.g., ionogel, hydrogel) as both the dielectric and one of the electrodes. Under pressure, the formation of an ultra-thin electrical double layer (EDL) between the ionic material and a standard electrode results in an extremely high intrinsic capacitance [65]. The variation in contact area under pressure directly modulates this EDL capacitance. This mechanism endows iontronic sensors with a key advantage of higher sensitivity compared to conventional CPSs, especially in the low-pressure regime critical for physiological signals like pulse waves.

#### 2.3.3. Piezoelectric effect

The operating principle of a piezoelectric sensor is schematically shown in Fig. 2c. Piezoelectric sensing is based on the ability of certain materials to generate electrical polarization when subjected to mechanical stress, a phenomenon known as the direct piezoelectric effect. Conversely, these materials can deform under an applied electric field, which is referred to as the converse piezoelectric effect. For sensing applications, the direct effect is the relevant mechanism. At the material level, piezoelectricity arises from a non-centrosymmetric crystal or molecular structure [66]. When the material is compressed, stretched, or bent, the centers of positive and negative charges shift relative to each

other, producing a net dipole moment and surface-bound charges. Electrodes collect these charges and convert them into a measurable current or voltage output. Commonly used piezoelectric materials include natural crystals like quartz, ceramic compounds such as lead zirconate titanate (PZT) [67] and barium titanate ($BaTiO_3$) [68,69], as well as polymers like PVDF [70–72]. Ceramics usually provide high piezoelectric coefficients, whereas polymers offer greater flexibility and mechanical compliance for wearable integration. The theoretical behavior of piezoelectric materials can be described using coupled constitutive equations involving physical quantities such as strain (S), stress (T), electric displacement (D), and electric field (E), along with parameters including the piezoelectric coefficient (d), elastic compliance (s), and dielectric permittivity (ε). Superscript notations $s^E$ and $\epsilon^T$ denote values measured under constant electric field or constant stress conditions.

$$\begin{bmatrix} \delta \\ D \end{bmatrix} = \begin{bmatrix} s^E & d^t \\ d & \epsilon^T \end{bmatrix} \tag{3}$$

An important feature of piezoelectric sensors is that they respond most strongly to dynamic or transient mechanical stimuli. This makes them especially suitable for capturing the rapid upstroke and fine temporal details of pulse waveforms. At the mechanistic level, the piezoelectric response comprises intrinsic contributions, arising from polarization extension and rotation, and extrinsic contributions, associated with domain wall motion or phase boundary movement [73,74]. While domain wall motion can significantly enhance the piezoelectric constant, it often introduces hysteresis and energy dissipation. Thus, a balance between sensitivity and linearity or energy efficiency must be carefully considered in the design of high-precision sensors. The exploration of nanostructured piezoelectric materials, such as zinc oxide (ZnO) nanowires, offers a distinct approach to modulating these contributions, as evidenced by their foundational role in pioneering piezoelectric nanogenerator (PENG) [75]. These devices showcase the feasibility of converting mechanical energy into electricity at nanoscales through a mechanism wherein strain-induced polarization charges propel electron flow in an external circuit [76]. This progress opens up avenues for self-powered sensors and wearable piezoelectric devices.

In summary, key engineering parameters such as anisotropy, poling treatment, domain structure, and thermal stability must be systematically evaluated when employing piezoelectric materials in sensor applications.

### 2.3.4. Triboelectric effect

The triboelectric sensing mechanism, together with its four basic operating modes, is illustrated in Fig. 2d. Triboelectric sensors convert mechanical stimulation into electricity through the combined action of contact electrification and electrostatic induction [77,78]. When two materials with different tendencies to gain or lose electrons come into contact, charges are generated at the interface. At the macroscopic level, this contact electrification can be treated as a stable interfacial charge layer over the time scale of one operating cycle, regardless of whether the microscopic origin arises predominantly from electronic, ionic, or mechanochemical processes [79]. Once the tribo-charges are established, subsequent mechanical motion modulates the spatial distribution of these charges and the capacitance between electrodes. This geometrical and dielectric reconfiguration breaks electrostatic symmetry and induces a time-dependent potential difference between electrodes, driving electrons through the external circuit to restore electrostatic equilibrium. Within the Maxwell framework, the process is described by a displacement current associated with the time-varying electric displacement field, which is continuous with the conduction current in the load [80]:

$$J_D = \frac{\partial D}{\partial t} = \varepsilon_0 \frac{\partial E}{\partial t} + \frac{\partial P}{\partial t} \tag{4}$$

where $J_D$ is the displacement current density, $D$ denotes the electric displacement, $\varepsilon_0$ is the vacuum permittivity, $E$ represents the electric field E, and $P$is the polarization density. Thus, a device based on triboelectric effect can be rigorously regarded as a variable-capacitance, polarization-modulated electromechanical transducer rather than a purely friction-driven generator.

On this unified physical basis, the working modes of triboelectric sensors are commonly categorized into four fundamental configurations: contact-separation [25,81], single-electrode [82,83], lateral sliding [84,85], and freestanding [86] modes, as well as their derived structures [87,88]. In the contact–separation mode (Fig. 2d(I)), two triboelectric layers with different electron affinities are brought into contact under an external mechanical force, resulting in the formation of opposite surface charges at their interface. When the two layers subsequently separate along the normal direction, the spatial separation of these charges generates an electrostatic potential difference between the corresponding electrodes. This potential drives electrons through the external circuit until electrostatic equilibrium is approached. When the two layers are brought back into contact, the potential difference decreases and the electrons flow in the opposite direction. Repeated contact and separation therefore generate an alternating electrical output. Because arterial pulsation mainly produces small, repetitive out-of-plane deformation normal to the skin surface, this mode is particularly compatible with wearable pulse sensing. In the single-electrode mode (Fig. 2d(II)), only one triboelectric layer is connected to an electrode, while the counter surface, which may be the skin, clothing, or another moving object, is electrically referenced to ground through the surrounding environment or the human body [89]. Contact electrification produces opposite charges on the interacting surfaces. As the counter surface approaches or moves away from the triboelectric layer, the resulting variation in the local electrostatic field induces charge exchange between the sensing electrode and ground. Unlike the contact–separation mode, a paired counter electrode is not required, which simplifies the device architecture and facilitates direct integration with flexible substrates, textiles, and epidermal interfaces. This structural simplicity makes the single-electrode mode particularly attractive for wearable and self-powered physiological sensing. In the lateral-sliding mode (Fig. 2d(III)), the two triboelectric surfaces remain in contact or in close proximity while undergoing relative displacement parallel to the interface. After initial contact electrification, lateral motion changes the overlapping area between the oppositely charged surfaces. The resulting asymmetric charge distribution generates a time-dependent potential difference between the electrodes and drives electron transfer through the external circuit. When the sliding direction is reversed, the potential difference also reverses, thereby producing an alternating output. Compared with the contact-separation configuration, this mode is more sensitive to tangential displacement and shear motion and is therefore particularly useful for motion, tactile, and sliding-force sensing, although it is less commonly adopted for arterial pulse detection dominated by normal skin displacement. In the freestanding mode (Fig. 2d(IV)), a pre-charged or triboelectrically charged dielectric layer moves relative to two spatially separated stationary electrodes. As the charged layer approaches one electrode and moves away from the other, the electrostatic coupling between the moving dielectric and the two electrodes changes continuously. This position-dependent coupling redistributes induced charges between the electrodes and generates an alternating current through the external load. Importantly, the freestanding triboelectric layer does not need to maintain direct electrical contact with either electrode, which can reduce electrode wear and provide greater structural freedom for motion sensing. This mode is therefore advantageous for detecting translational or reciprocating motion over relatively large displacement ranges. Among these four configurations, the contact–separation and single-electrode modes are most frequently employed in wearable pulse wave sensors, because arterial pulsation is predominantly transmitted to

the skin as small-amplitude, low-frequency deformation normal to the body surface. Both configurations can efficiently convert such repetitive mechanical motion into measurable electrical outputs while maintaining simple structures, mechanical compliance, and compatibility with soft and conformal wearable platforms [90].

In summary, each sensing approach has distinct benefits and drawbacks, which must be evaluated during the design and development of wearable devices for pulse waveform analysis. Research is ongoing to discover novel materials, manufacturing techniques, and sensor architectures to enhance the sensitivity, response speed, and overall efficacy of these systems. The core objective is to create reliable, accurate, and user-friendly wearable sensors suitable for the continuous monitoring of medical health.

## 3. Wearable sensors for pulse wave detection

Wearable pulse wave sensing encompasses a diverse group of technologies that capture different physical manifestations of the same underlying cardiovascular pulsation. The measurement pathways can be understood according to three successive levels: the primary measurand, the resulting pulse-related signal or feature, and the physiological or clinical parameter subsequently derived from that information. For example, PPG detects optical intensity variations primarily associated with pulsatile blood-volume changes, whereas SPG and laser Doppler techniques probe blood-flow-related optical dynamics. PAI detects photoacoustic responses arising from hemoglobin absorption, while FBG sensors convert pulse-induced mechanical strain into shifts in Bragg wavelength. In contrast, flexible mechanical sensors directly transduce local pressure, strain, or tissue deformation through piezoresistive, capacitive, piezoelectric, or triboelectric mechanisms. Although these modalities originate from the same cardiovascular dynamics, their distinct primary measurands determine the pulse features they preserve, the physiological parameters that can be derived, and the sources of measurement uncertainty. Table 1 summarizes the relationship among the primary measurand, pulse features, and derived parameters, providing a common framework for comparing the wearable sensing technologies discussed below.

**Table 1**
Classification of Wearable Pulse Wave Sensing Technologies.

| Technology | Primary measurand | Pulse-related signal/features | Representative derived physiological/ clinical parameters |
|---|---|---|---|
| PPG | Pulsatile changes in optical absorption/ scattering associated primarily with peripheral blood-volume variation | Pulse amplitude, waveform morphology, beat interval, pulse arrival time | Heart rate, $SpO_2$, PAT-based indices, vascular features, AF screening, cuffless BP estimation |
| LDV | Doppler frequency shift arising from moving red blood cells or pulse-induced surface motion, depending on configuration | Pulsatile flow velocity, perfusion waveform, vibration waveform, pulse timing | Microvascular perfusion, vascular reactivity, PWV and related hemodynamic indices |
| SPG | Temporal speckle fluctuations associated with dynamic light scattering from moving blood cells | Pulsatile speckle-flow waveform, relative flow dynamics | Microvascular blood flow, vascular resistance-related indices, pulse timing/ hemodynamic assessment |
| PAI | Photoacoustic response generated by optical absorption, predominantly by hemoglobin | Photoacoustic amplitude, vascular images, pulsatile vascular changes | Vascular morphology, oxygenation, deep-tissue hemodynamic information |
| FBG | Pulse-induced mechanical strain encoded as Bragg-wavelength shift | Strain waveform, pulse morphology and timing | Pulse rate, waveform characteristics, PWV/BP-related indices |
| Piezoresistive | Local pressure/ strain/ deformation | Resistance change and reconstructed mechanical pulse waveform | Pulse morphology, arterial stiffness-related indices, BP-related parameters |
| Piezocapacitive / iontronic | Local pressure/ deformation | Capacitance change and pulse waveform | Pulse morphology, BP-related parameters, hemodynamic indices |
| Piezoelectric | Dynamic stress/ strain | Charge/voltage generated by dynamic deformation | Pulse timing, morphology, heart rate, dynamic BP-related features |
| Triboelectric | Contact/ deformation-induced charge redistribution | Voltage/current waveform generated by pulse-induced motion | Pulse rate, morphology, timing, BP-related features |

### 3.1. Optical sensors

Optical and optically mediated pulse wave sensors interrogate cardiovascular pulsatility through changes in light absorption, scattering, Doppler frequency, speckle dynamics, or optically encoded strain. Owing to their distinct primary measurands, these technologies provide complementary representations of arterial pulsation rather than interchangeable measurements of pressure. Among them, PPG remains the most widely adopted optical technology in wearables, with recent progress focusing heavily on the co-optimization of optical layouts, material platforms, and signal processing chains. In terms of optical geometry, the signal-to-noise ratio of PPG is critically dependent on the optical path design. For instance, green light (520–560 nm) is preferred for heart rate monitoring due to its high sensitivity to superficial capillary blood volume, whereas near-infrared dual-wavelength configurations (660/880–940 nm) are the standard for blood $SpO_2$ assessment, balancing tissue penetration with hemoglobin absorption [91,92]. Optimizing source–detector separation and incorporating optical isolation structures are critical hardware strategies to improve signal robustness and reduce motion artifacts. Material innovations are increasingly influencing the form factor and mechanical compliance of PPG sensors in response to the requirements of long-term epidermal integration. Early PPG systems primarily relied on rigid inorganic semiconductors such as Si [93], GaAs [94], Ge [95,96], which offer excellent optoelectronic performance but suffer from intrinsic mechanical mismatch with soft and deformable biological tissues [97–99]. This limitation has motivated growing interest in flexible optoelectronic materials, including organic light-emitting diodes (OLEDs [100]) and organic photodetectors (OPDs [101]), which enable conformal contact, reduced motion-induced artifacts, and improved wearing comfort in wearable implementations. Their molecular tunability and solution processability also enable seamless fusion with nanomaterials (e.g., quantum dots [102,103], ZnO [97] or PbS [104] nanoparticles). This synergy is pivotal for overcoming the intrinsic trade-off between mechanical compliance and photoelectric efficiency, leading to devices that are both highly deformable and sensitive. The ultimate manifestation of this trend is the emergence of ultrathin, self-powered epidermal patches [105], which are transitioning the vision of "skin electronics" from a concept to a tangible reality. Yet motion artifacts endure as a principal source of signal degradation, largely arising from variations in skin–sensor contact and relative movement. Strategies to mitigate these effects include optimizing sensor layout, employing signal processing

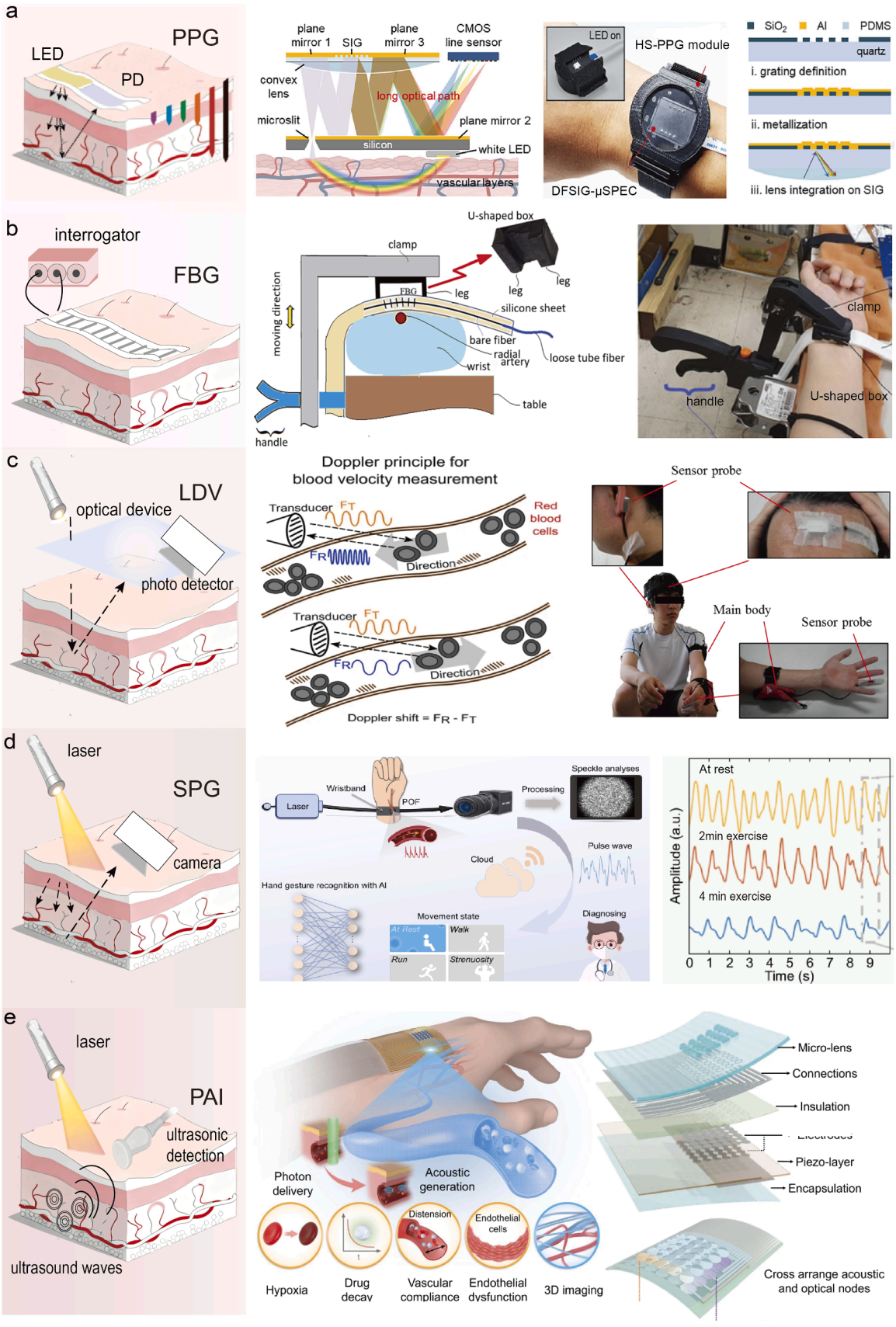
approaches like adaptive filtering or spectral analysis, and integrating auxiliary sensors such as accelerometers [106]. The pursuit of motion-robust PPG sensing has motivated innovations beyond conventional source–detector optimization. One representative example is the hyperspectral PPG module shown in Fig. 3a [107], which extends traditional single-wavelength photometry toward spectroscopic interrogation. By co-integrating a solid-immersion-grating microspectrometer with a broadband light-emitting diode, this system simultaneously acquires pulse-related information across 50 spectral bands. The resulting high-dimensional spectral data enable more effective separation of pulsatile components from motion-induced disturbances, allowing robust estimation of pulse transit time under dynamic conditions. As a result, sub-millimeter accuracy in blood pressure estimation has been demonstrated even during exercise, highlighting the potential of hyperspectral strategies for ambulatory and real-world monitoring. Alongside hardware optimization, algorithmic innovation, particularly the adoption of deep learning for adaptive filtering and signal quality assessment, has emerged as a key enabler of robust PPG performance [108,109]. As emphasized in recent reviews, the future of PPG no longer depends solely on hardware but on system-level integration, from high-quality dataset construction to disease-specific algorithm design, forming a closed development loop [110].

In parallel, FBG sensors provide a distinct sensing modality by detecting minute mechanical strains induced by pulsatile pressure [115]. Their operating principle is based on shifts in the Bragg wavelength under strain or temperature variations, necessitating sophisticated encapsulation to efficiently transmit vascular pulsations while suppressing thermal cross-sensitivity through reference gratings or algorithmic compensation [116]. Fig. 3b illustrates an optical power detection scheme based on dual FBGs for wrist pulse acquisition and blood pressure estimation [111]. Unlike conventional methods that rely on spectrometers to resolve wavelength shifts, this approach leverages the linear relationship between strain and the overlapping area of the reflection and transmission spectra of two identical FBGs, directly converting vascular pulsations into measurable optical power variations. This configuration simplifies system architecture, reduces cost, and enables automatic temperature compensation. These advances notwithstanding, several obstacles persist when applying FBG sensors in practical wearable scenarios. Although the optical power detection scheme reduces system cost, the miniaturization and integration of discrete components, such as the broadband light source, optical circulator, and photodetector, still require further development. Moreover, while the U-shaped clamping mechanism employed in this study ensures stable mechanical coupling, it compromises wearing comfort and long-term wearability. Future efforts directed toward flexible photonic integration, polymer optical fiber FBGs, and clamp-free conformal packaging may offer promising routes to overcoming these limitations.

Beyond volumetric and strain-based sensing, LDV and SPG extend optical biosensing by probing light scattering dynamics. LDV measures nanoscale vibrations on the skin surface to derive PWV, a gold-standard index of arterial stiffness. While its methodological reliability has been validated in controlled studies, conventional LDV setups remain bulky, sensitive to ambient vibration, and pose major challenges for wearable deployment. Fig. 3c (left) illustrates the principle of LDV [112], in which laser illumination of the bloodstream interacts with moving erythrocytes, acting as scattering centers. Scattered light experiences a frequency shift that depends on the velocity (v) of red blood cells in peripheral arteries. This shift, termed Δf, captures changes in v, and its sign reveals the direction of blood flow relative to the detection system. A seminal miniaturization effort by Li et al. [54] integrated a dual-beam homodyne LDV onto a compact silicon photonic chip (5 $mm^2$). This system-on-chip approach enables direct local PWV measurement by capturing signals at two carotid artery sites simultaneously, marking a critical shift from benchtop to chip-scale systems. However, this proof-of-concept also depends on external lasers and detectors, undermining full miniaturization. Iwasaki et al. [51] developed a MEMS-based laser Doppler flowmeter that eliminates optical fibers through a fully integrated probe with on-chip laser and photodiode, as is illustrated in Fig. 3c(right). Validation during treadmill running demonstrated stable signal acquisition at the forehead with effective separation of physiological signals from motion artifacts via time-frequency analysis, which underscores that achieving a robust, self-contained wearable LDV demands future breakthroughs in full system-on-chip integration and motion-immune packaging. SPG is an optical technique that analyzes spatiotemporal variations in speckle contrast arising from dynamic light scattering by moving red blood cells, enabling the generation of relative blood flow maps and complementary hemodynamic waveforms [117,118]. Fig. 3d illustrates one trajectory toward miniaturization of this technique [113], showing a compact smart photonic wristband implementation based on SPG that integrates dynamic speckle capture with hardware miniaturization for potential ambulatory monitoring applications.

PAI represents perhaps one of the most integrative optical approaches, coupling the high contrast of optical absorption with the depth penetration of ultrasound. By illuminating tissues with short laser pulses absorbed by chromophores such as hemoglobin, PAI generates ultrasonic waves that are reconstructed into maps of vascular morphology and oxygenation dynamics. Jin et al. [114] advanced PAI into a wearable format through a flexible optoacoustic blood "stethoscope" that enables noninvasive, multiparametric cardiovascular monitoring, as is illustrated in Fig. 3e. The device integrates a microlens array and piezoelectric sensors for conformal 3D vascular imaging, simultaneously tracking oxygen saturation, drug decay, venous compliance, and arterial dilation in both murine and human subjects. Although PAI has long been constrained by system complexity and tethering to external lasers and data acquisition, this work demonstrates significant progress toward wearable deployment.

Across these diverse optical modalities, common barriers remain, including motion artifacts, inter-individual variability, environmental interference, and the dependence of signal quality on optical coupling with biological tissues. Nevertheless, optical sensing offers distinct advantages for pulse wave monitoring, including non-invasive acquisition, high sensitivity to hemodynamic changes, electrical isolation, and, in some modalities, access to physiological information beyond pulse morphology, such as blood oxygenation and vascular structure. These characteristics make optical techniques particularly attractive for wearable and multimodal cardiovascular monitoring. Their performance, however, can be affected by skin pigmentation, ambient light, tissue composition, sensor–skin displacement, and relatively high power consumption associated with light sources and photodetectors. Multimodal sensor fusion may alleviate some of these limitations, for example by combining PPG with inertial measurement units for motion artifact rejection, coupling FBG with temperature sensors for real-time compensation, or integrating PAI with ultrasound to unify structural and functional information. These limitations have motivated the exploration of complementary mechanical sensing strategies for pulse wave acquisition. Fundamentally, arterial pulsation not only induces changes in tissue optical properties but also generates periodic mechanical deformation and pressure fluctuations at the skin surface. Mechanical sensors therefore provide a more direct route to capturing the physical manifestation of arterial pulsation, without relying on light–tissue interaction. In particular, resistive, capacitive, piezoelectric, and triboelectric sensors can translate subtle pulse-induced pressure or strain into electrical signals, offering potential advantages in structural simplicity, low power consumption, flexible form factors, and compatibility with conformal wearable devices. However, mechanical sensing introduces its own challenges, including sensitivity to contact pressure, sensor placement, mechanical hysteresis, and motion-induced deformation. Consequently, optical and mechanical approaches should be viewed as complementary rather than competing strategies for wearable pulse wave monitoring.




(caption on next page)

**Fig. 3.** Schematics of advanced wearable optical pulse sensors. (a) Hyperspectral PPG module integrating a solid-immersion-grating microspectrometer with a broadband LED for multi-wavelength pulse waveform acquisition. Reproduced with permission [107]. Copyright 2025, John Wiley and Sons. (b) A dual-FBG optical detection system that captures wrist arterial pulsations by converting mechanical deformation into measurable optical power variation. Reproduced with permission [111]. Copyright 2025, MDPI. (c) Doppler principle for blood flow measurement. Reproduced with permission [112]. Copyright 2022, IEEE. Running-ready wearable laser Doppler blood flow sensors. Reproduced with permission [51]. Copyright 2015, MDPI. (d) SPG wristband with internal laser illumination and camera detection for blood flow monitoring. Reproduced with permission [113]. Copyright 2024, Institute of Optics and Electronics, Chinese Academy of Sciences. (e) PAI setup combining pulsed laser excitation with ultrasound detection for deep-tissue vascular assessment. Reproduced with permission [114]. Copyright 2023, Springer Nature.

### 3.2. *Piezoresistive sensors*

The fundamental operating principle of resistive pressure sensors lies in converting mechanical stimuli into measurable electrical resistance changes. This can occur through variations in contact resistance between conductive electrodes or via the intrinsic piezoresistive effect within elastic composite materials. For pulse wave measurement, performance optimization strategies for these sensors primarily focus on three approaches: (i) depositing or patterning conductive active materials onto polymer surfaces to create microstructured sensing interfaces;

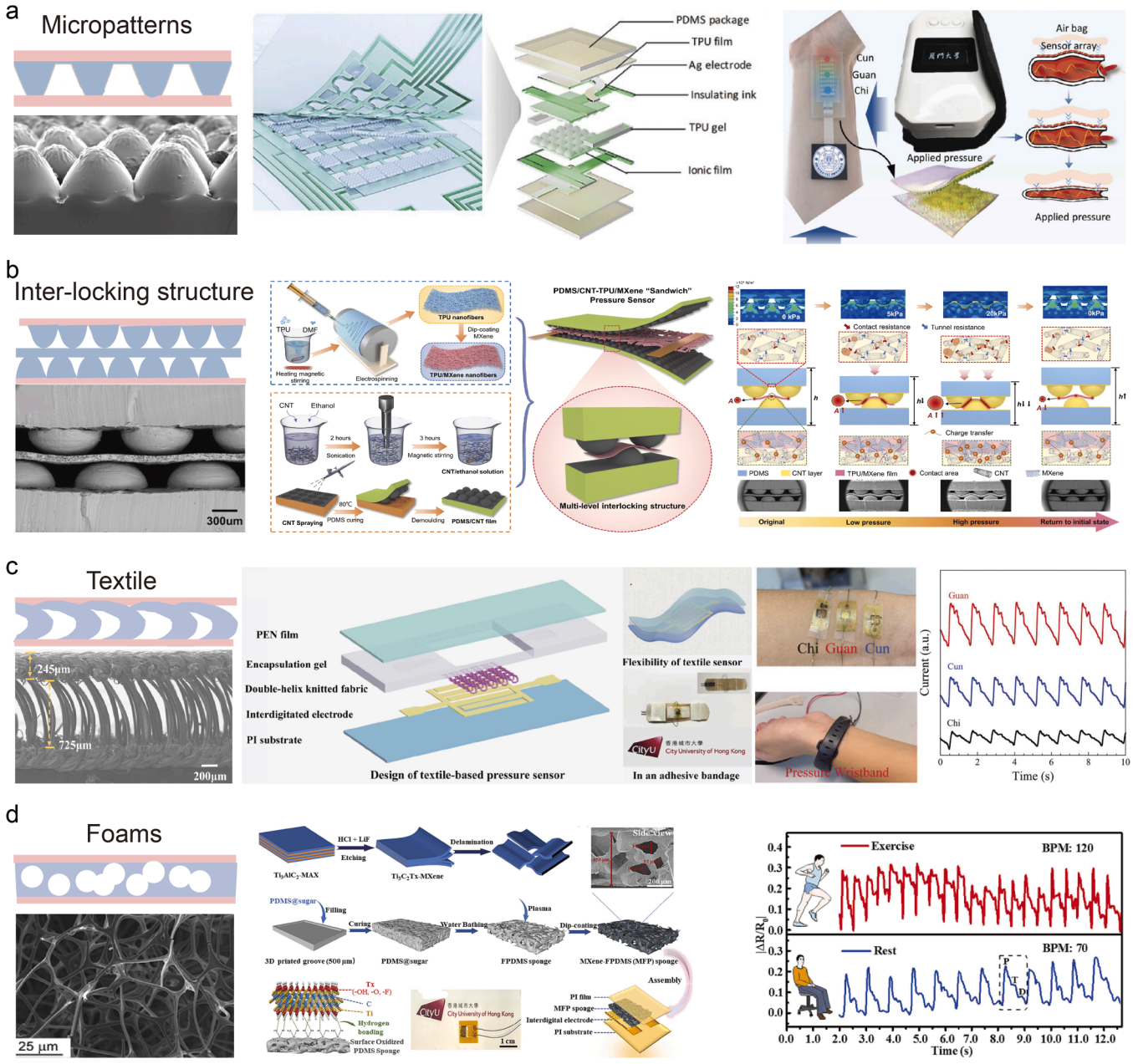



**Fig. 4.** Advanced piezoresistive sensor designs for pulse monitoring. (a) Dome-structured printed array inspired by TCM pulse diagnosis. Reproduced with permission [131]. Copyright 2024, Springer Nature. (b) Interlocking microdome sandwich with CNT/MXene hybrid network. Reproduced with permission [132]. Copyright 2024, Royal Society of Chemistry. (c) Double-helix yarn textile sensor with ultrafast recovery. Reproduced with permission [133]. Copyright 2021, John Wiley and Sons. (d) Plasma-engineered highly porous MXene/PDMS sponge with hydrogen-bonded interface for enhanced sensitivity and stability. Reproduced with permission from [134]. Copyright 2024, Elsevier.

(ii) dispersing conductive nanofillers into a soft, elastic matrix to form piezoresistive composites; and (iii) engineering porous or fibrous monolithic architectures to leverage their compressible three-dimensional networks. The evolution of microstructural design in piezoresistive sensors is fundamentally driven by the need to resolve the intrinsic conflict between high sensitivity and broad linear range. Early designs employing uniform, single-scale microstructures (e.g., pyramids, microcolumns, hemispheres [61,119]) exhibit high initial sensitivity through large contact area changes. However, their homogeneous mechanical response inevitably leads to rapid stiffening and signal saturation at elevated pressures [120–122]. This limitation has spurred a strategic shift towards mechanical heterogeneity and bio-inspired hierarchical architectures. Examples include petal-like [123], kirigami [124], interlocking structures [125], double helix structures [95], multi-level hemispherical microstructures [126] and multi-level pyramids [121]. These designs enable sequential engagement and cooperative deformation of structural units at different scales. These architectures effectively distribute stress and delay overall stiffening, thereby expanding the linear measurement range without sacrificing high sensitivity [123,127,128]. Beyond single-point sensing, multi-channel sensor arrays have emerged as a powerful tool for capturing spatial pulse characteristics [129,130]. Fig. 4a illustrates a fully printed, flexible pressure sensor array inspired by Traditional Chinese Medicine (TCM) pulse diagnosis [131]. This sensor employs a dense array (5 ×5) of dome-shaped microstructures on the sensitive layer, fabricated via screen printing, which contributes to its high sensitivity (3.997 $kPa^{-1}$) and excellent linearity ($R^2 = 0.999$) over a wide range (4.7–100 kPa). Fig. 4b provides a high-performance sensor built from a multi-layer interlocking sandwich design, consisting of upper and lower polydimethylsiloxane (PDMS)/carbon nanotubes (CNT) films with microdome arrays and a middle thermoplastic polyurethane (TPU)/MXene electrospun nanofiber membrane [132]. The staggered, complementary arrangement of the microdomes creates a constrained and cooperative deformation mechanism during compression, which significantly enlarges the effective contact area and delays structural stiffening. By incorporating CNT and MXene into a hybrid conductive network, the sensor achieves a high sensitivity of 82.17 $kPa^{-1}$ over a range of 0–25 kPa, along with fast response/recovery (100 ms).

Textile-based sensors, fabricated from conductive fibers or inks, offer superior wearability by seamlessly conforming to the body and leveraging cost-effective textile manufacturing [135,136]. Their hierarchical structure provides mechanical robustness, including high flexibility, fatigue resistance, and damage tolerance without crack propagation [137]. Additionally, their porous nature ensures breathability and thermal comfort, which are critical for wearable applications [138]. However, the stochastic nature of their fiber networks can lead to challenges in signal reproducibility and hysteresis. Addressing the hysteresis and reproducibility challenges inherent in the stochastic fiber networks of textile-based sensors, Fig. 4c demonstrated an innovative structural solution using DNA-inspired double-helix yarns [133]. This strategy eliminates the reliance on elastomeric polymer blending and introduces an alternative structural route for achieving mechanically resilient and comfortable textile sensors. Such an approach provides a viable design paradigm for high-performance epidermal pulse monitoring and holds particular promise for modernizing traditional pulse diagnostic practices, including those used in Traditional Chinese Medicine. Conversely, foam- or sponge-based sensors leverage their inherent high porosity and compressibility to achieve an exceptionally wide pressure range. Their electrical resistance in these systems changes dramatically as the porous network collapses under pressure. The conduction mechanism in these systems often relies on the quantum tunneling effect between neighboring conductive nanofillers (like carbon nanotubes or MXene) dispersed within the insulating polymer matrix like PDMS, polyurethane (PU).

At the materials level, constructing optimized and stable conductive networks is paramount. Nanoparticles and two-dimensional materials serve as ideal conductive fillers. Carbon-based materials (carbon black, CNTs, graphene) [139,140], conductive polymers (PPy, PEDOT: PSS) [141,142], metal nanomaterials (Ag nanowires, Au nanomaterials) [143], and emerging MXenes [61,144,145] are extensively used. They can be formulated into inks for printing on textiles, dispersed into polymers to create conductive composites, or coated onto foam skeletons. The emergence of laser-induced graphene (LIG) technology provides a viable solution for creating highly conductive, porous graphene foams directly on flexible substrates. Research shows that LIG sensors modified with silver nanoparticles exhibit significantly enhanced strain sensitivity and improved consistency in pulse waveform acquisition [146]. Nevertheless, a key challenge with nanoparticle-based composites is balancing high filler loading for conductivity against maintaining the mechanical compliance of the polymer matrix. Recent advances have focused on enhancing interfacial adhesion and structural stability in such systems. For example, Fig. 4d illustrates a thin MXene/PDMS sponge sensor using plasma-induced hydrogen bonding, which significantly improves mechanical robustness while enabling ultra-high sensitivity (14.2 $kPa^{-1}$) in the low-pressure regime [134]. This design achieves both high porosity (92.3%) and low modulus (9.7 kPa), effectively solving the trade-off between sensitivity and mechanical compliance.

In summary, piezoresistive sensors remain a dominant technology in wearable pulse monitoring, prized for their straightforward principle, high sensitivity, facile fabrication, and low cost. However, their path to long-term accuracy is fraught with significant temperature drift, inherent hysteresis in porous and textile structures, and nonlinear response. The research community has developed sophisticated strategies to circumvent these limitations. For instance, temperature drift is effectively suppressed by integrating sensing elements into Wheatstone full-bridge circuits [147], which compensate for common-mode thermal variations. Likewise, the vulnerability of single-point sensors to positioning errors is overcome by deploying active-matrix sensor arrays. These systems enable spatial mapping of the pulse wave, allowing for automatic artery localization and the selection of an optimally positioned sensor pixel for robust data acquisition. Looking forward, the development of flexible resistive pressure sensors for pulse monitoring is expected to follow several key trends. Multi-modal sensing systems, which integrate pressure sensing with temperature, humidity, or even biochemical marker detection, will provide more comprehensive physiological profiles. The synergistic advancement of these technological pathways is poised to accelerate their widespread use in daily health monitoring and precision medicine.

### 3.3. *Piezocapacitive sensors*

Considerable attention has been drawn to capacitive pressure sensors, especially iontronic sensors leveraging the EDL effect, for physiological signal monitoring owing to their high sensitivity, linearity over a broad regime, low power consumption, and unique transparency and wearability [148,149]. The pursuit of higher performance has driven capacitive sensing from conventional parallel-plate capacitors to iontronic sensors leveraging the EDL. While both rely on microstructural design, their optimization principles diverge. In conventional sensors, microstructures (pyramids, domes [150], cylinders [151], microcone [152], bio-inspired patterns replicated from plant leaves [153] or eggshells [63], and the combination of porous structures [154]) primarily amplify the rate of change in the macroscopic contact area (A). Despite extensive efforts to blend high-dielectric materials with nanomaterials (e.g., MXenes [155], carbon nanotubes [156], and Ag nanowires [157]), conventional capacitive designs often exhibit relatively modest sensitivity compared to their piezoresistive counterparts under similar conditions [158,159]. In stark contrast, iontronic sensors exploit the EDL's atomic-scale charge separation (~1 nm), making their capacitance exquisitely sensitive to minute changes in the interfacial contact area, particularly in the low-pressure regime critical for pulse waveforms

[148,149,64]. Since the electrical properties of ion conductors depend on the concentration of the ILs [160] and the measurement frequency [161], methods to improve sensitivity include blending ILs with high-polarity polymers (e.g.,poly(vinylidene fluoride-hexafluoro propylene) (PVDF-HFP [162,163]), TPU [164,165], PU [166], and polyvinyl alcohol (PVA) [150], employing electrode materials that exhibit ions intercalation such as $Ti_3C_2T_X$ [167], and structure engineering.

Representative structure strategies include laminating hierarchical microstructures for graded responsiveness [168,169], introducing secondary micro-features on micro-dome surfaces to amplify contact area variation [170,64,171], and engineering pores within the dielectric to improve compressibility [172]. Despite these advancements, the manufacturing of key microstructures still depends on complex processes like photolithography or the transfer of randomly structured microstructures, which hinders scalable production [163]. Recent research has thus explored alternative, cost-effective manufacturing routes, including high-precision 3D printing [64], digital light processing (DLP), screen-printing [173], and the development of pseudocapacitive iontronic sensors using MXene instead of conventional EDL materials [167]. Fig. 5a displays gradient pyramidal microstructures for iontronic sensors fabricated by a Gaussian-profile $CO_2$ laser, lowering the expense and fabrication difficulty compared with photolithography [170]. Beyond pursuing cost-effective fabrication, a more profound challenge lies in the fundamental interdependence of sensitivity, working range, and stability, a trilemma rooted in the limited compressibility of microstructures. Navigating this trade-off has largely been an empirical endeavor. Huang et al. presented a transformative approach by introducing programmability into sensor design itself [168]. As illustrated in Fig. 5b, their system enables the precise and customizable distribution of microstructures (e.g., pyramids, domes) across the sensing area. This approach allows local mechanical responses to be tailored to specific functional requirements, representing a transition from monolithic, fixed-function devices toward application-adaptive and designable sensing interfaces. Beyond microstructure geometry, innovative device architectures provide additional routes for improving signal stability under dynamic conditions. Fig. 5c illustrates a seminal shift from a traditional two-sided configuration to a one-sided electrode design [174]. This architecture, incorporating a low-friction soft-hard interface, is engineered to minimize shear-induced deformation and hysteresis of the dielectric layer during dynamic movement, which enables stable and accurate pulse monitoring even under conditions such as running.

Moving further from passive structural optimization, recent work highlights the importance of active and adaptive control of the sensor–tissue interface for achieving medical-grade accuracy. Fig. 5d demonstrates a flexible adaptive sensing tonometry that could autonomously maintain the ideal arterial compression by integrating capacitive arrays with a microfluidic actuator. It directly mitigates the primary source of error caused by variable contact pressure in cuffless monitoring, enabling the extraction of clinical-grade hemodynamic parameters, which represents a critical evolution from a static flexible sensor to an intelligent, self-optimizing diagnostic platform [175]. While planar configurations have dominated capacitive sensing, fiber-shaped sensors are now gaining traction as a strong candidate for textile-integrated wearables. Zhang et al. [176] developed a fiber-shaped capacitive strain sensor (FSFCSS) via direct ink writing, featuring helical Ag electrodes on a TPU fiber core encapsulated with high-dielectric BTO@Ecoflex. This helical design converts linear strain into bending strain, enabling an axial tensile range of 178% with 0.924 sensitivity and radial expansion sensitivity of 0.00086 $mmHg^{-1}$ for pressure sensing. The fiber geometry offers dual-mode detection (joint motion and hemodynamic signals) while maintaining compatibility with conventional textile manufacturing.

Despite these advances, the sensitivity–range–stability trilemma remains fundamentally unresolved. Designs employing nanoscale or sharp microfeatures can achieve exceptional sensitivity, but often at the expense of mechanical robustness and long-term linearity. In contrast, micro-roughened or porous architectures offer enhanced stability and overload tolerance, yet inherently exhibit reduced sensitivity. Hierarchical structures provide a rational compromise by sequentially engaging structural features across multiple length scales under increasing pressure. Future progress is therefore unlikely to arise from a single optimal geometry, but rather from application-specific hybrid designs that judiciously combine, for example, nanoscale sensitivity with the damage tolerance of a porous supporting matrix [177]. Practical application in pulse monitoring will require a shift from optimizing individual sensing elements toward integrated device and system co-design. This includes developing iontronic capacitive sensor arrays for spatial resolution, incorporating differential readout circuits to suppress thermal drift and motion artifacts, and using advanced signal processing algorithms for robust feature extraction. Furthermore, ensuring mechanical durability, biocompatibility, and stability under real-world conditions is crucial for clinical translation. The deep integration of microstructural engineering, material innovation, and system-level design will be key to unlocking the full potential of capacitive pressure sensors in wearable health monitoring.

### 3.4. Piezoelectric sensors

Piezoelectric sensors hold significant promise for pulse wave monitoring due to their unique ability to directly convert mechanical energy into electrical signals, enabling self-powered and highly responsive sensing of dynamic physiological activities. From the perspective of material properties, piezoelectric materials used in PENGs and sensors can be broadly categorized into inorganic ceramics, organic polymers, natural piezoelectric substances, and composite systems. Traditional inorganic materials, such as ZnO [75,178–180], aluminum nitride (AlN) [181], barium titanate ($BaTiO_3$) [182,183], lead PZT [184,185], and molybdenum disulfide ($MoS_2$) [186–189], are known for their high piezoelectric coefficients. However, most of the traditional inorganic piezoelectric materials are bulky and inherently brittle. To adapt them to wearable applications, researchers commonly employ thinning techniques (e.g., reducing piezoelectric films to micrometer thickness) and transfer or deposit them onto flexible substrates (e.g., polyimide [190]) to form heterogeneously integrated structures. The imperative for miniaturization and conformability is exemplified in Fig. 6a, which showcases a thin, flexible microsystem that heterogeneously integrates piezoelectric sensing units, signal processing, and wireless transmission on an ultra-thin (0.5 mm) substrate [191]. This system-level integration strategy is critical, as the achieved minimal bending radius of 3 mm enables conformal wrist attachment, which directly contributes to the suppression of motion artifacts caused by sensor displacement, thereby ensuring stable acquisition of high-fidelity pulse waveforms. In contrast, polymer-based piezoelectric materials have gained prominence over inorganic alternatives in wearable PENG development due to superior flexibility, tunable design parameters, lower processing temperatures, and enhanced manufacturability, all critically attributing for conformal bioelectronics. There are many piezoelectric polymers used for PENGs, including PLLA [192], polyamides (PA) [193], PVDF [70,151], and PVDF copolymers such as PVDF-HFP [194], polyvinylidene fluoride-trifluoroethylene (PVDF-TrFE) [195], etc. Nonetheless, their inherently weak electromechanical coupling and low piezoelectric coefficients limit energy conversion efficiency and sensing sensitivity [196]. To address this, strategies such as cold drawing, melt quenching, chemical modification [197], component regulation [198], and incorporation of functional fillers ($BaTiO_3$ [199], MXene [200], or other two-dimensional materials) have been employed to enhance piezoelectric output. Diversified morphological configurations, such as nanofibers [201,202], nanoparticles [203], laminates [204], and nanoyarn [205], have also been explored. Furthermore, environmental humidity poses a significant challenge to piezoelectric materials, as moisture ingress can

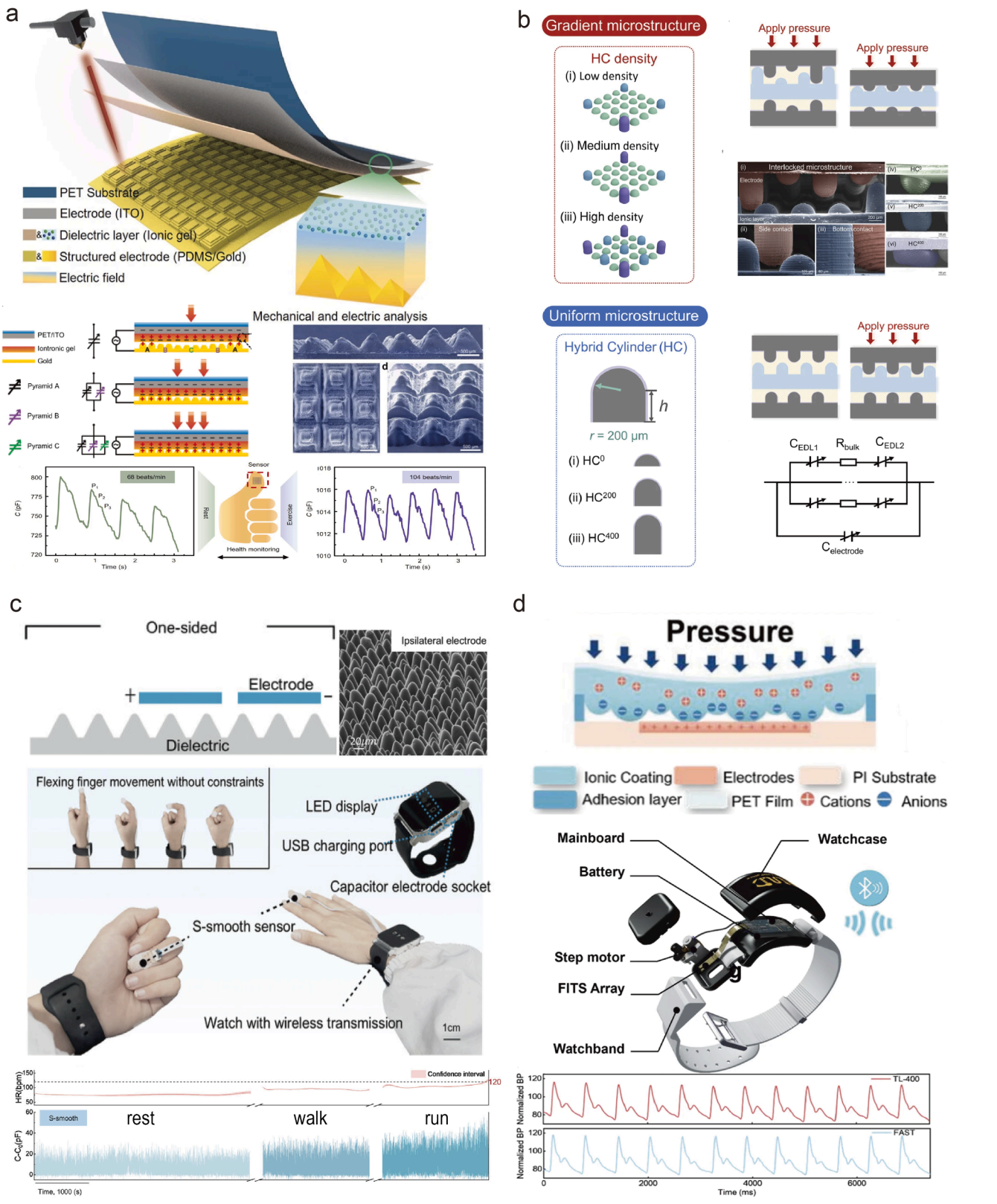



**Fig. 5.** Flexible capacitive sensors targeting pulse wave monitoring. (a) Programmable iontronic sensor with gradient pyramidal microstructures enabling customizable pressure-response characteristics for broad dynamic range sensing. Reproduced with permission [170]. Copyright 2023, Springer Nature. (b) Schematic illustration of the hybrid cylinders with different heights and different densities. Reproduced with permission [168]. Copyright 2025, Springer Nature. (c) Single-electrode capacitive configuration with low-friction soft-hard interface design for maintaining signal stability during dynamic motion. Reproduced with permission [174]. Copyright 2025, John Wiley and Sons. (d) Closed-loop hemodynamic monitoring system integrating a conformable capacitive sensor array with microfluidic actuation for automatic arterial positioning and optimal contact pressure control. Reproduced with permission [175]. Copyright 2024, Springer Nature.

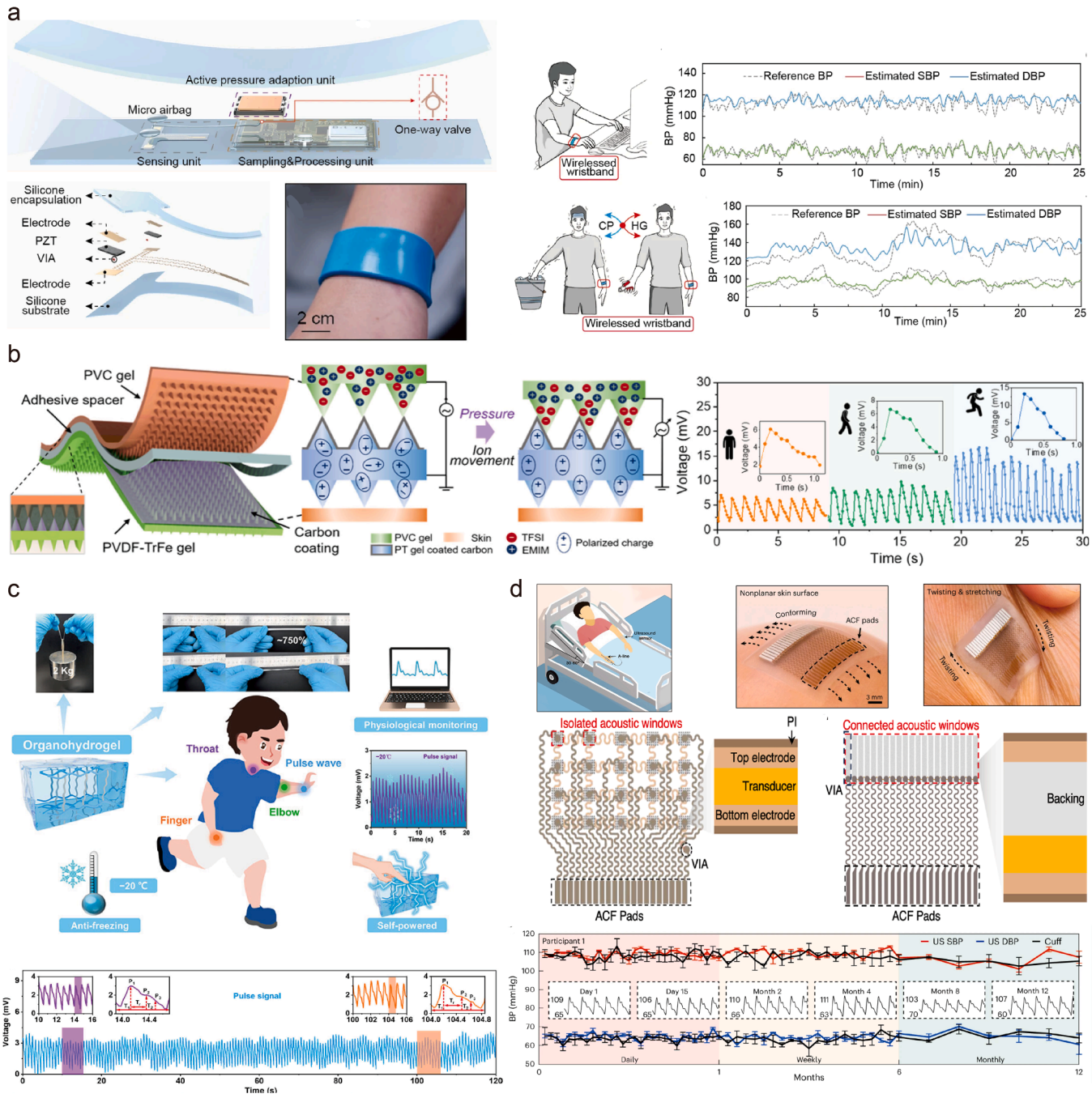



**Fig. 6.** Architectural and material innovations in wearable piezoelectric pulse sensors. (a) A thin, flexible microsystem heterogeneously integrating piezoelectric sensing units, signal processing circuits, and wireless transmission components on an ultra-thin substrate for conformal wrist attachment and motion-robust pulse monitoring. Reproduced with permission [191]. Copyright 2023, Springer Nature. (b) A self-powered, stretchable gel mechanosensor that mimics the mechanical properties of soft biological tissue, enabling stable mechanical coupling with the skin for accurate pulse monitoring during and after physical activity. Reproduced with permission [208]. Copyright 2021, American Chemical Society. (c) An anti-freezing organohydrogel-based sensor capable of reliable operation at temperatures as low as −20 °C, demonstrating enhanced environmental robustness for use in harsh conditions. Reproduced with permission from [209]. Copyright 2024, American Chemical Society. (d) A flexible large-area ultrasound array based on piezoelectric polymers, enabling continuous, non-invasive deep-tissue hemodynamic monitoring and central blood pressure waveform reconstruction. Reproduced with permission from [210]. Copyright 2024, Springer Nature.

severely compromise their electrical output. Conventional approaches to mitigating this issue rely on impermeable encapsulation. However, this inevitably compromises skin breathability, which is a fundamental requirement for comfortable long-term wearability. An emerging, more sophisticated strategy involves engineering the fabric architecture itself to manage moisture. For instance, 3D orthogonal woven fabrics can be designed with an asymmetric wetting structure, channeling moisture away from the active piezoelectric layer through capillary action while maintaining vapor permeability [206,207]. However, this introduces a new layer of complexity since the mechanical coupling of the piezoelectric element to the skin must be preserved amidst this dynamic moisture transport; otherwise, the very mechanical signals the sensor is meant to detect could be dampened or lost. This highlights the systems-level challenge of co-optimizing environmental robustness, comfort, and signal fidelity.

Incorporating piezoelectricity into gel or organohydrogel matrices

holds great promise for developing wearable electronics, as it offers a pathway to achieve enhanced conformability, biocompatibility, and even self-healing capabilities, which are particularly attractive for skin-interfaced applications [211,212]. Chun et al. [208] demonstrated this concept with a self-powered, stretchable gel-based mechanoreceptor sensor (Fig. 6b). Inspired by Merkel disks and cilia, the device features conical surface microstructures that enable conformal skin contact. This inherent skin-conformability allows it to maintain stable mechanical coupling with the epidermis during dynamic movement, addressing the drawback of conventional sensors that require the subject to remain stationary and enabling accurate post-exercise blood pressure measurement. The environmental robustness of such gel sensors is critically enhanced by formulating anti-freezing ionic conductors, a capability visualized in Fig. 6c [209]. Operation at temperatures as low as −20 °C extends the potential application range of wearable sensors from regulated indoor environments to harsh real-world conditions, including winter sports and polar activities. Flexible piezoelectric ultrasound transducer technology suggests a potential shift from monitoring surface phenomena toward deep-tissue imaging, as illustrated in Fig. 6d [210]. By enabling conformal, large-area arrays that can track vascular cross-sectional area changes in real-time, these devices unlock the ability to reconstruct central blood pressure waveforms continuously and non-invasively, a capability previously confined to clinical ultrasound systems [213–216]. This may facilitate the transition from consumer health tracking toward clinically relevant physiological monitoring.

In summary, future development of piezoelectric sensors for pulse monitoring should focus on three core directions: First, continued advancement in material hybridization (inorganic filler/polymer matrix) and microstructural design to simultaneously enhance sensitivity and mechanical compatibility. Second, vigorous development of scalable, low-cost advanced fabrication processes like thermal imprinting, roll-to-roll printing, and 3D printing, to enable mass production of high-performance flexible devices. Finally, and crucially for clinical translation, is the tight integration of arrayed, multimodal sensing hardware with intelligent algorithms based on signal decomposition, adaptive filtering, and machine learning models. Emerging directions, such as biodegradable piezoelectric materials and the incorporation of sensing platforms into closed-loop therapeutic systems, further highlight the trajectory toward multifunctional and clinically viable wearable technologies. Ultimately, the convergence of materials innovation, scalable fabrication, and intelligent data processing will be key to advancing the practical application and commercialization of piezoelectric sensors in dynamic health monitoring.

### 3.5. Triboelectric sensors

The proper selection of materials is a crucial starting point in developing wearable triboelectric pressure sensors for pulse wave monitoring. Beyond high electronegativity, key considerations must encompass pressure sensitivity, mechanical stability, and biocompatibility. Commonly used negative triboelectric layers include polytetrafluoroethylene (PTFE) [217], PDMS [218], polyimide (Kapton) [219] and PVDF [220,221], prized for their strong electron-accepting capability in the triboelectric series [222], while materials such as nylon and silk are frequently employed as positive layers. PDMS is often preferred due to its favorable transparency, stretchability, and biocompatibility [223]. Achieving an optimal balance among these properties is critical, as it directly influences skin-contact comfort, signal stability, and long-term wearability, which are fundamental prerequisites for acquiring high-quality pulse waveforms.

TENG-based sensors have seen tremendous advances. Nevertheless, their low output power poses a barrier to the development of high-performance sensors. Structural engineering across micro- and macro-scales provides an effective avenue for increasing the generated tribocharge density by precisely regulating contact-separation dynamics. At the microscopic level, the introduction of multi-level architectures (pyramid arrays [25] or nanorod patterns [224,225] on PDMS or PTFE surfaces) markedly increases the effective contact area, lowers the activation pressure, and improves charge transfer efficiency, thereby enabling the capture of fine fingertip pulse details. A triboelectric sensor featuring a multi-level microstructured PTFE layer enables unconstrained fingertip pulse monitoring via finger-touching on daily objects [226]. Its hierarchical design comprising microscale hexagonal prisms and nanowires, facilitates sufficient contact-separation even under large static forces, maintaining a high sensitivity of 0.15 mV/Pa and accurately capturing detailed pulse waveforms with characteristic peaks, which are essential for extracting cardiovascular parameters such as heart rate (Fig. 7a). On the macroscopic scale, fiber-based [222], kirigami-inspired [227], and layered configurations [228] impart remarkable stretchability and textile compatibility, allowing the sensor to accommodate joint movements and minimize motion artifacts. For instance, fiber-shaped TENGs can be woven into fabrics for stable arterial pulse monitoring [229], and PVDF-stitched structures have demonstrated superior triboelectric output compared to conventional film-based designs [220,230]. A flexible, stretchable, textile-based, self-powered triboelectric sensor with a kirigami architecture was fabricated to realize a wireless biological monitoring system [231]. Utilizing collected pulse wave signals, the system provides real-time cardiovascular assessment and visualization on mobile terminals, supporting both prediction and clinical diagnosis of heart-related conditions (Fig. 7b). Beyond conventional wearable scenarios, recent advances have extended pulse monitoring to extreme environments such as underwater diving. For instance, a Ni-MOF/PVDF composite nanofiber-based single-electrode TENG was developed with PDMS encapsulation, enabling fully waterproof operation and self-powered wireless transmission of pulse signals via Maxwell's displacement current in aquatic settings [70]. This system not only captures arterial pulse waveforms with high fidelity but also transmits data wirelessly through water without external power, demonstrating robustness against salinity, turbidity, and physical obstacles for real-time health monitoring of scuba divers (Fig. 7c).

Gel-based electrode systems (hydrogel- [233–236], organogel- [237], aerogel-based [238], and ionogel-based [239]) provide a promising platform for skin-conformal, self-powered triboelectric sensors because of their high transparency, flexibility, and flame resistance [234]. Ionogels, in particular, employ dual physical–chemical crosslinking networks with dynamic bonds. Imine bonds introduced via hyperbranched poly (ethylene imine) achieve stable voltage outputs (218 V) and power densities (e.g., 360 $mW{\cdot}m^{-2}$) in a broad temperature range (–40 °C to 80 °C), ensuring reliable operation under harsh environmental conditions [239]. Nevertheless, such gels often suffer from insufficient mechanical strength and poor elastic recovery, which limit their durability in dynamic wearing scenarios. Recent strategies to overcome these limitations include blending elastomers with hydrogels [240] or incorporating ionic/polymeric reinforcing phases, leading to improved mechanical integrity and electrical output stability.

When compared to piezoelectric hydrogels, triboelectric gel sensors operate primarily through interfacial contact electrification, generating signals from surface charge separation. This mechanism renders them highly sensitive to minute contact-release motions, making them particularly suitable for detecting superficial arterial pulsations. In contrast, piezoelectric hydrogels rely on stress-induced polarization changes and respond predominantly to dynamic mechanical deformation, thereby providing complementary information on transient pulse components. While triboelectric gels typically yield high signal-to-noise ratio AC outputs, they can be susceptible to contact pressure variations; piezoelectric hydrogels, however, provide concurrent information on steady and pulsatile components, aiding in the assessment of arterial stiffness. To mitigate interfacial instability, self-adhesive hydrogels such as PVA-PA-PDA have been integrated into sensor designs, forming conformal and robust skin contact that maintains high signal fidelity

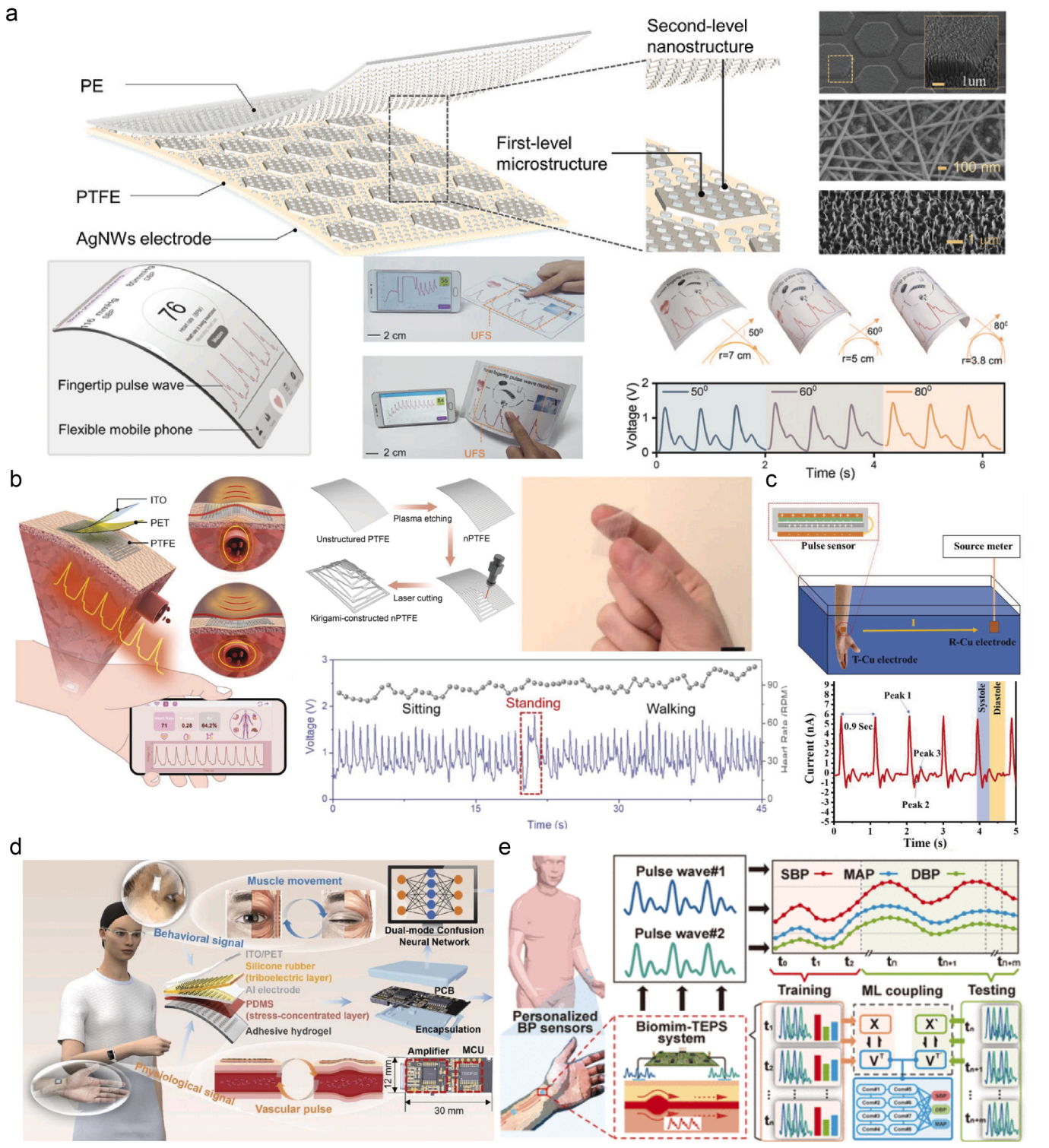



**Fig. 7.** Triboelectric sensors for pulse wave monitoring. (a) Schematic illustration of a three-layer ultrathin flexible sensor (UFS): PTFE and PE as the electrification layers, and AgNWs spin-coated on PTFE as the electrode. Reproduced with permission [226]. Copyright 2021, John Wiley and Sons. (b) A flexible textile-based self-powered triboelectric sensor with a kirigami structure, integrated into a wireless bio-monitoring system. Reproduced with permission [231]. Copyright 2022, John Wiley and Sons. (c) A Ni-MOF/PVDF composite nanofiber-based single-electrode TENG for underwater pulse monitoring. The device is encapsulated in PDMS for waterproof operation and utilizes Maxwell's displacement current for self-powered wireless signal transmission in challenging aquatic environments. Reproduced with permission [70]. Copyright 2023, John Wiley and Sons. (d) Self-adhesive hydrogel interface (PVA-PA-PDA) integrated into a stress-concentrated triboelectric sensor for stable skin contact. The design enhances signal fidelity and enables rapid measurement recovery (1.2 s) even under curved skin and dynamic motion. Reproduced with permission [232]. Copyright 2024, John Wiley and Sons. (e) Biomimetic nanopillar-based triboelectric pulse sensor coupled with personalized machine learning for cuffless continuous blood pressure monitoring. Reproduced with permission [224]. Copyright 2023, American Chemical Society.

during movement, as evidenced by pulse waveform amplification and rapid measurement recovery (1.2 s) even under curved skin surfaces [232] (Fig. 7d). Moreover, ionogels utilizing ionic liquids maintain conductivity and anti-freezing properties at subzero temperatures, whereas many piezoelectric hydrogels require cryoprotectants such as glycerol or glycols to prevent performance degradation.

Integrating high-performance triboelectric sensors with signal-processing circuitry and embedded algorithms constitutes a systems-level approach toward cuffless, continuous blood pressure monitoring [241]. Sandwich-structured sensor designs [242], for example, have achieved broad sensing ranges (e.g., 0.89 V/kPa in 0–35 kPa), low detection limits (1 g), and fast response times (32 ms), enabling precise extraction of detailed pulse wave features. Yao et al. developed a biomimetic nanopillar triboelectric pulse sensor coupled with personalized PLSR modeling to improve pulse-wave acquisition and account for inter-individual variability in blood pressure estimation (Fig. 7e) [224]. This work highlights the importance of jointly optimizing sensor performance and individualized signal analysis for reliable wearable monitoring. Although data-driven models provide powerful tools for pulse wave analysis and blood pressure estimation, the signal-to-noise ratio, sensitivity, and dynamic range of the sensor itself remain the hardware foundation for algorithmic efficacy. Therefore, enhancing the device-level output stability and interference immunity is essential for achieving reliable physiological monitoring in real-world wearable settings.

Looking forward, emerging research directions, such as the use of biodegradable triboelectric materials, mechanically adaptive structures inspired by kirigami/origami, and self-healing gel composites, are poised to further advance the wearability and environmental sustainability of these devices. The development of multimodal sensing systems that combine triboelectric with piezoelectric or other sensing mechanisms may offer richer physiological profiles from a single platform. Additionally, the pursuit of energy-autonomous operation through integrated energy harvesting and storage will be critical for realizing truly continuous, maintenance-free health monitoring systems. As these materials, structural, and systemic innovations mature, wearable triboelectric sensors are expected to play an increasingly important role in both personal health tracking and clinical-grade cardiovascular assessment.

### 3.6. Hybrid sensors

Despite substantial advances in individual sensing technologies, it remains difficult for a single sensing mechanism to simultaneously achieve high sensitivity, a wide operating range, stable signal acquisition, mechanical robustness, and reliable performance under real-world wearing conditions. [243,244] More importantly, different transduction mechanisms exhibit distinct response characteristics and failure modes, meaning that improvements in one performance metric are often accompanied by compromises in others. [245] These trade-offs have motivated a shift from optimizing isolated sensing elements toward multifunctional sensing architectures, in which complementary mechanisms or sensing modalities are integrated to broaden the measurable range, improve signal fidelity and robustness, and provide richer physiological information. The development of hybrid pressure sensors that integrate two or more transduction mechanisms is becoming a promising approach to overcome the intrinsic limitations of individual sensor types and to enhance the fidelity of pulse wave monitoring [246]. Capacitive–resistive hybrid designs exemplify this strategy by exploiting the high sensitivity of capacitance in the low-pressure regime and the superior resistance response at higher pressures. One approach exploits the intrinsic properties of porous composites. For instance, Ha et al. [247] engineered porous CNT–Ecoflex foams with ~86% porosity, where pore collapse induces resistive variations while pore compression modulates the dielectric constant, achieving wide dynamic range and pressure-resolved sensitivity suitable for arterial pulse detection (Fig. 8a). Another strategy includes engineering device architectures, where spatial deformation of microstructures simultaneously tunes interfacial capacitance and contact resistance, yielding linear responses across multiple orders of magnitude [248] (Fig. 8b).

Beyond conventional pressure transduction, hybrid triboelectric–piezoelectric systems leverage the complementary energy conversion properties of PVDF and functional nanomaterials such as $MoS_2$ and MXenes [252]. Recent fiber-based tribo–piezo hybrids demonstrated broad detection ranging up to 150 kPa with sensitivities above 3 V $kPa^{-1}$ , enabling accurate pulse monitoring under dynamic conditions [249] (Fig. 8c). More complex multimodal systems have also been realized. Sun et al. introduced a tribo–piezo–pyro hybrid device with a bio-inspired Ag nanowire leaf-venation electrode that simultaneously harvested mechanical and thermal fluctuations. The device allowed the integrated monitoring of radial pulse, respiration-driven temperature changes, and neuromuscular motions, offering a multifunctional diagnostic platform [250] (Fig. 8d).

The integration of optical and mechanical sensing further enhances cardiovascular assessment by combining volumetric information from PPG with local pressure fluctuations. Recent hybrid PPG–mechanical sensor systems demonstrated improved robustness against motion artifacts and inter-individual variability in cuffless blood pressure estimation, especially when paired with machine learning algorithms for feature extraction [253,254]. In a notable advancement aligned with this hybrid trend, Wang et al. recently created a dual-modal wearable device combining a PENG and a PPG sensor within a biomimetic fingertip architecture for sleep apnea monitoring [251]. A two-stage detection strategy is adopted in their system: the self-powered PENG continuously carries out initial screening, and the PPG sensor is triggered only when suspicious events are detected. This approach effectively combines the mechanical sensing advantages of PENG with the optical hemodynamic profiling of PPG, achieving 94.95% accuracy in sleep apnea detection while reducing overall power consumption by ~23% compared to continuous PPG operation (Fig. 8e). Conformal ultrasound-on-foil devices further extend this paradigm, providing cross-sectional vascular imaging that complements surface piezoelectric or triboelectric sensors for precise blood pressure waveform reconstruction [216].

Hybrid pulse sensors embody a convergence of materials innovation, device architecture, and multimodal signal integration. By harnessing complementary physical effects, these systems not only extend sensing range and sensitivity but also enable richer physiological information extraction. Based on an in-depth investigation of different sensing mechanisms, we observe significant variations in material choices, response characteristics, and key performance metrics. To systematically compare the advantages and limitations of each technological pathway, Table 2 summarizes representative sensors based on PPG, piezoresistive, piezocapacitive, piezoelectric, and triboelectric principles across core dimensions including responsivity, detectivity, linear dynamic range, response time, and stability. However, these device-level metrics should not be interpreted as direct indicators of on-body pulse-wave fidelity. The waveform recorded at the skin surface is determined by the entire mechanical or optical coupling pathway between the artery, surrounding tissue, skin, and sensor. For contact-based mechanical sensors, attachment pressure is particularly important [255]: insufficient pressure can result in poor mechanical coupling and low signal amplitude, whereas excessive pressure may deform the underlying tissue, alter arterial geometry, or even partially compress the vessel, thereby distorting the pulse waveform [191,256]. Arterial depth and the mechanical properties of the intervening tissue further determine how strongly vascular pulsation is transmitted to the skin surface. Sensor thickness, flexibility, and mechanical impedance also influence conformal contact and deformation transfer, while strap tension determines the static preload applied during measurement. In addition, small variations in sensor position relative to the artery can substantially alter waveform amplitude and morphology, making positioning

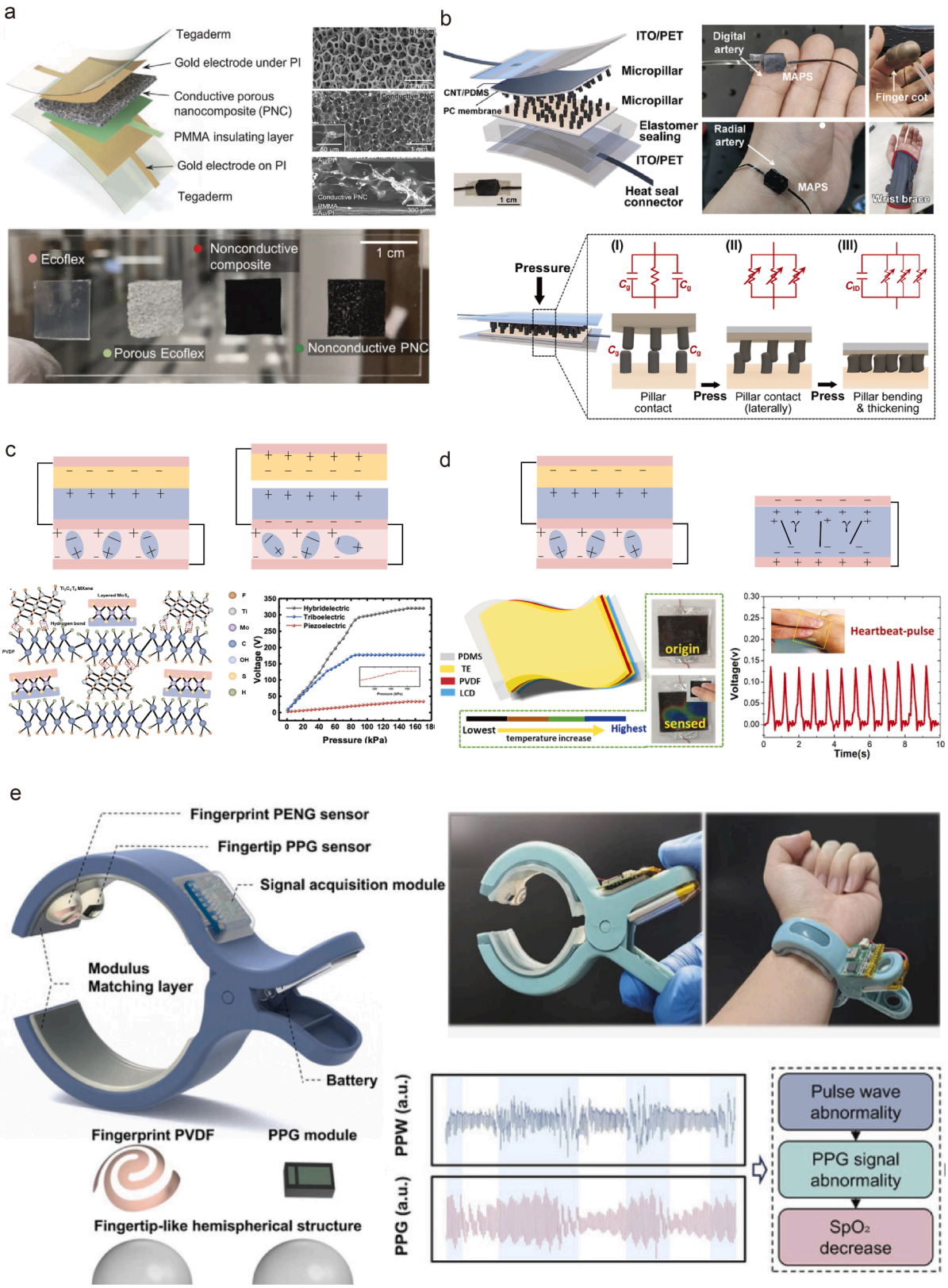



**Fig. 8.** Hybrid sensors for pulse wave monitoring. (a) Schematic illustration of the porous CNT–Ecoflex foam-based capacitive–resistive hybrid sensor. Reproduced with permission [247]. Copyright 2021, John Wiley and Sons. (b) Device architecture of a microstructure-based capacitive–resistive hybrid sensor. Reproduced with permission [248]. Copyright 2023, Royal Society of Chemistry. (c) Structure and performance of a fiber-based triboelectric–piezoelectric hybrid sensor. Reproduced with permission [249]. Copyright 2025, Elsevier. (d) Schematic of the bio-inspired tribo–piezo–pyro hybrid sensor with an Ag nanowire leaf-venation electrode. Reproduced with permission [250]. Copyright 2018, Elsevier. (e) Schematic of the biomimetic fingertip structure integrating PENG and PPG sensing units. Reproduced with permission [251]. Copyright 2025, John Wiley and Sons.

**Table 2**
Performance Comparison of Representative Wearable Pulse Wave Sensors.

| Categories | Material | Responsivity/ Sensitivity | Detectivity/ Detection limit | Linear dynamic range: | Response time | Stability (cycles) | Refs |
|---|---|---|---|---|---|---|---|
| PPG | Inorganic | 47.50 $A{\cdot}W^{-1}$ | $6.24 \times 10^{13}$ Jones | 83 dB | 0.81/2.03 ms. | 10,000 | [257] |
| | organic | 0.40 $A{\cdot}W^{-1}$ | $1.3 \times 10^{13}$ Jones | 130 dB | 10 μs | - | [258] |
| | Nanomaterials | 3891.80 $V{\cdot}W^{-1}$ | $2.10 \times 10^{12}$ Jones | 102 dB | 0.64/1.00 ms | 1,000 | [105] |
| | Hybrid | 8809.88 $A{\cdot}W^{-1}$ | $1.00 \times 10^{13}$ Jones | - | 23/29 ms | 10,000 | [259] |
| | Hybrid | 2.47 $A{\cdot}W^{-1}$ | $2.6 \times 10^{11}$ Jones | - | 40/45 μs | 2,000 | [260] |
| Piezoresistive | MXene | 652.10 $kPa^{-1}$ | 1 Pa | 0–60 kPa | 36/20 ms | 8,000 | [261] |
| | MXene | - | 10.20 Pa | 0–30 kPa | 11 ms | > 10,000 | [262] |
| | graphene | 37.30 $kPa^{-1}$ | 4 Pa | 0–1.4 MPa | 45/40 ms | > 30,000 | [263] |
| | graphene | 1875.53 $\cdot kPa^{-1}$ | 1.80 Pa | 0–40 kPa | 0.5/0.8 ms | > 15,000 | [264] |
| | CNT | 8775 $kPa^{-1}$ | 30.20 Pa | 0–1000 kPa | 11.6 ms 3.80 ms | 10,000 | [121] |
| | CNT | 18.09 $kPa^{-1}$ | - | - | 41.80/15.40 ms | > 50,000 | [265] |
| | AgNWs/WPU composite film PU | $1.04 \times 10^{6}$ $kPa^{-1}$ | 17 Pa | 0–27 kPa | 160 ms | > 1,000 | [266] |
| Capacitive | PDMS-CNTs | 0.15 $kPa^{-1}$ | 0.35 Pa | 0–450 kPa | 6/6 ms | > 10,000 | [267] |
| | MXene | 10.13 $MPa^{-1}$ | < 16 mg | - | 280/290 ms | 1,800 | [63] |
| | Iontronic Gel | 33.70 $kPa^{-1}$ | 0.36 Pa | 0–1700 kPa | 6/11 ms | > 4,500 | [170] |
| | iontronic sensor with microfeatures | 10 420.80 $kPa^{-1}$ | - | 0–300 kPa | 40/35 ms | ≥ 1,800 | [268] |
| | iontronic sensor with microfeatures | 37,347.98 $kPa^{-1}$ | 3.54 Pa | 0–151.6 kPa | 111/66 ms | 1,500 | [168] |
| Piezoelectric | PVDF | 1.34 $mV{\cdot}\ kPa^{-1}$ | ≤ 3 kPa | 3–176.84 kPa | 31/51 ms | > 5,000 | [209] |
| | PZT | 0.06 $kPa^{-1}$ | 0.40 kPa | 0–10 kPa | 23 ms | 50,000 | [269] |
| | PVDF | 0.41 $V{\cdot}kPa^{-1}$ (dry) 3.95 $V{\cdot}kPa^{-1}$ (sweat) | - | 1.25 kPa – 50 kPa | 100 ms (dry) /24 ms (wet) | > 20,000 | [207] |
| Triboelectric | CNT ( (+ ) FEP(-) | 0.21 $\mu A{\cdot}kPa^{-1}$ | 40 Pa | - | 40 ms | > 10,000 | [241] |
| | PTFE(+) Cu(-) | 1.65 $V{\cdot}kPa^{-1}$ | - | 0–1.3 kPa | 17 ms | > 4,500 | [270] |
| | PDMS( +) FEP(-) | 0.02 $V{\cdot}kPa^{-1}$ | - | 5 -1240 kPa | 33/102 ms | ≥ 1,000 | [245] |
| | cardboard (+ ) Silicone rubber(-) | 0.89 $V{\cdot}kPa^{-1}$ | 1 g | 0–35 kPa | 32 ms | - | [242] |
| | CNTs/PDMS ( + ) FEP(-) | 0.37 $nA{\cdot}kPa^{-1}$ | 1 kPa | 0–100 kPa | 7.99/8.98 ms | > 4,500 | [224] |
| Hybrid | porous nanocomposite (PNC) | 3.13 $kPa^{-1}$ | 0.07 Pa | 0.07 Pa - 125 kPa | 94 ms | 5,000 | [247] |
| | $BaTiO_3$ Nanoparticle | 3.71 $V{\cdot}kPa^{-1}$ | 0.10 kPa | 0.1–100 kPa | - | > 5,000 | [271] |

repeatability an important source of inter-session variability [125,175]. Similar interface-related effects are also relevant to optical sensing, where contact pressure, sensor placement, tissue optical properties, and motion can modify the detected PPG waveform. Consequently, a sensor exhibiting high sensitivity under calibrated benchtop loading does not necessarily provide superior physiological waveform reconstruction in vivo. On-body performance should therefore be evaluated using signal-level measures such as signal-to-noise ratio, waveform correlation with a reference signal, preservation of characteristic landmarks, timing accuracy, and repeated-wear reproducibility, in addition to conventional device metrics.

Against this distinction between device performance and physiological signal fidelity, the advantages and limitations of different sensing technologies can be interpreted more appropriately. Overall, piezoresistive and piezocapacitive sensors often exhibit high device-level sensitivity, which can facilitate the detection of weak mechanical stimuli under controlled conditions. However, this advantage should not be directly equated with superior on-body waveform fidelity, which additionally depends on sensor–skin coupling, positioning, tissue mechanics, and motion robustness. Specifically, piezoresistive sensors feature a direct mechanism and high sensitivity, but they typically possess a relatively narrow linear dynamic range and may face issues of hysteresis and drift under extremely high pressure. Piezocapacitive sensors, on the other hand, offer benefits such as low power consumption and good stability, but are more susceptible to environmental electromagnetic interference. Piezoelectric and triboelectric sensors, as paradigms of self-powered sensing, notably operate without an external power supply, making them particularly suitable for portable devices. Piezoelectric sensors, especially those based on PZT or PVDF, feature extremely fast response times, enabling precise capture of high-frequency details in the pulse waveform (such as the dicrotic notch). However, their response to static pressure is limited, and signals can decay easily. Triboelectric sensors are renowned for their diverse material choices and high output voltage, but still face challenges in terms of long-term stability and packaging technology. In contrast, PPG sensors, as a clinically established technology, hold the advantage of non-invasively acquiring blood volume change information directly. However, their signals are easily interfered with by ambient light, motion artifacts, and skin tone, often relying on algorithms for indirect estimation of blood pressure parameters. Regarding stability, optimized piezoresistive and piezocapacitive sensors can withstand tens of thousands of mechanical cycles, demonstrating reliable durability. In terms of response time, the response times reported for many mechanical sensors are sufficiently short for pulse waveform acquisition.

## 4. Clinical value of pulse wave detection

Each cardiac contraction generates pressure waves that propagate and reflect through the arteries, producing the pulse wave. This pulse wave carries extensive hemodynamic information about cardiac output, vascular compliance, and peripheral resistance [272], providing a viable means for the non-invasive and continuous assessment of arterial stiffness, valvular function, and early detection of hemodynamic abnormalities [273,274]. The convergence of flexible electronics, micro- and nano-scale sensing technology, and artificial intelligence has revolutionized wearable pulse sensing, transforming the traditional practice of

pulse palpation into a quantifiable and reproducible data stream. The clinical translation of this technology, however, is highly heterogeneous, with applications ranging from established screening to exploratory disease correlation studies. Given the substantial heterogeneity in study design and validation maturity, the clinical role of pulse wave sensing should be interpreted according to the level of evidence rather than classification accuracy alone. In this review, applications are therefore considered within four categories: screening, monitoring, risk stratification, and diagnosis. Screening refers to the preliminary identification of individuals who may require further clinical evaluation; monitoring denotes longitudinal tracking of physiological or disease-related changes; risk stratification involves estimating disease susceptibility, severity, or prognosis; and diagnosis requires sufficiently specific discrimination against accepted clinical reference standards in the intended-use population. Importantly, statistical associations between pulse-derived features and a disease state should not be interpreted as evidence of diagnostic specificity without independent and prospective clinical validation.

Pulse rhythm monitoring stands out as one of the most clinically substantiated applications of wearable pulse sensing. Atrial fibrillation introduces characteristic irregularities in pulse rhythm [275]. Consequently, PPG-based wearables (e.g., smartwatches) have become pivotal tools for atrial fibrillation (AF) screening [276,277]. Their core advantage lies in the ability to perform non-invasive, long-term continuous monitoring of pulse rhythm, identifying AF characteristics by detecting irregularities in pulse intervals. Large-scale prospective studies have confirmed that such algorithms exhibit high sensitivity and specificity for initial AF screening in the general population [278]. International clinical guidelines have increasingly recognized PPG-based rhythm monitoring within a pathway of initial screening followed by ECG confirmation. Accordingly, wearable PPG should currently be regarded primarily as a screening and longitudinal rhythm-monitoring tool rather than a standalone diagnostic modality. Its performance can also be compromised by motion artifacts and variations in skin optical properties, further emphasizing the need for confirmatory ECG and robust real-world validation.

Beyond rhythm disturbances, a major class of cardiovascular disorders manifests primarily through alterations in vascular mechanics and hemodynamic load [279]. Pulse waveform morphology, wave reflection, and PWV encode information related to arterial stiffness, blood pressure, and vascular aging, forming the physiological basis for assessing diseases such as hypertension, atherosclerosis, coronary heart disease (CHD), atrial septal defect (ASD) [280], heart failure [281], ventricular bigeminy, atrial flutter, and episodes of bradycardia and

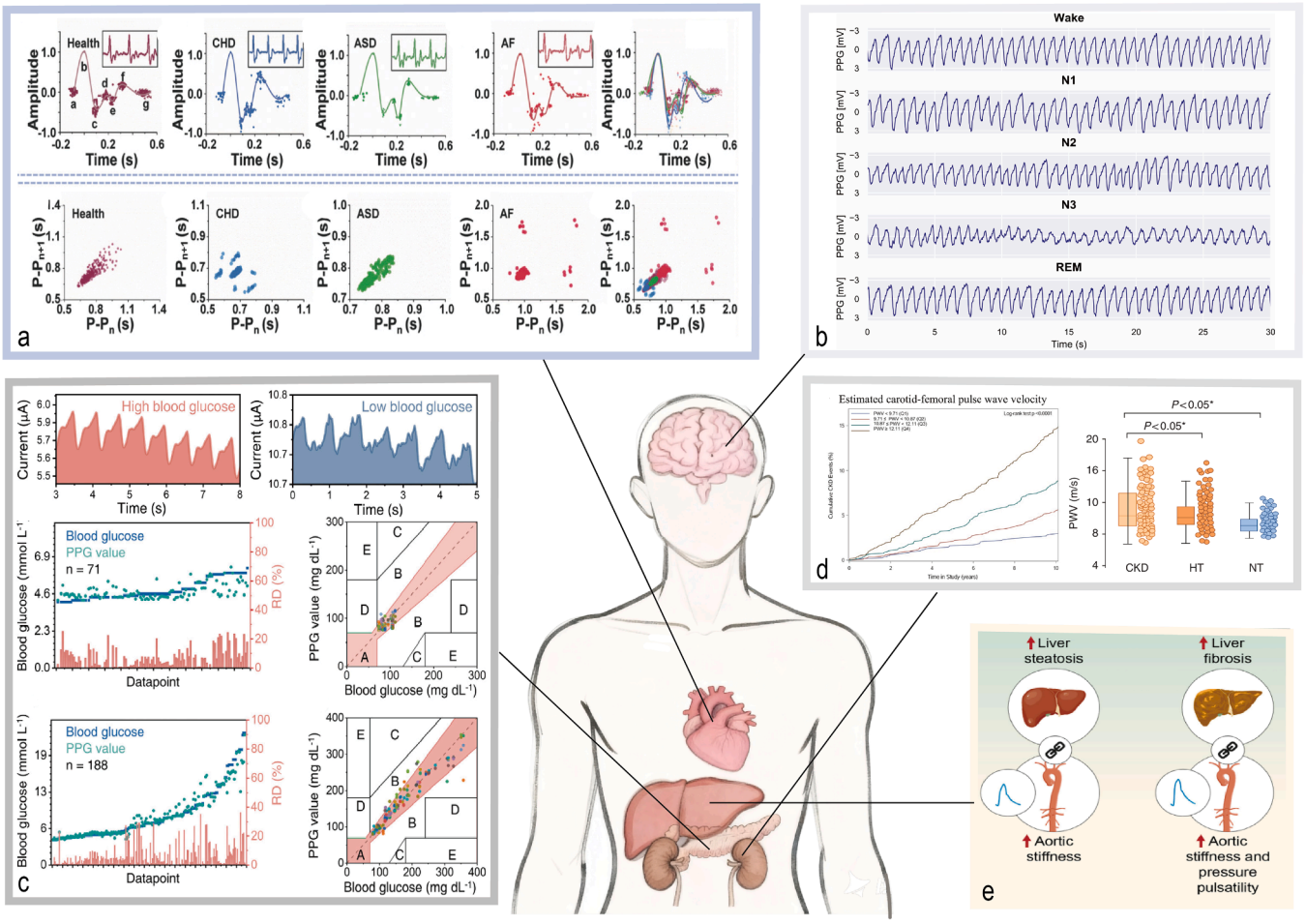



**Fig. 9.** Panoramic view of clinical diseases targeted by pulse detection. (a) Normalized pulse waveforms and the distribution of their characteristic points from a healthy volunteer and patients with CHD, ASD, and AF. Reproduced with permission [276]. Copyright 2017, John Wiley and Sons. (b) PPG signal examples from properly identified sleep phases. Reproduced with permission from [284]. Copyright 2020, Oxford University Press. (c) Raw PPG signals measured under high (red) and low (blue) blood glucose conditions, showing discernible morphological differences. Clarke Error Grid analysis demonstrates 93% of predictions remain in Zone A, with the rest in clinically acceptable Zone B. Reproduced with permission [285]. Copyright 2024, John Wiley and Sons. (d) Cumulative incidence of chronic kidney disease by quartiles of arterial stiffness measures. Reproduced with permission [286]. Copyright 2024, Springer Nature. And arterial stiffness phenotypes in CKD stages 2–5 patients compared with NT and HT controls. Reproduced with permission [287]. Copyright 2012, Elsevier. (e) Associations between vascular hemodynamic measures and liver fibrosis, stratified by cardiometabolic risk factors. Reproduced with permission [288]. Copyright 2024, Wolters Kluwer Health, LLC.

tachycardia [282]. Ouyang et al. [276] systematically demonstrated the potential of a triboelectric sensor for disease differentiation through characteristic point extraction and Poincaré plot analysis of pulse signals from healthy subjects and patients with CHD, ASD, and AF. Pulse contour analysis revealed significant differences in the distribution of characteristic points between disease groups (Fig. 9a), providing a foundation for AI-based pattern recognition and disease classification. Heart rate variability (HRV) Poincaré plot analysis offered an intuitive reflection of autonomic nervous system regulation. The plot geometries were consistent with ECG-based HRV analyses, indicating that such high-precision pulse sensors can serve as a valuable supplement to ECG. However, further application still needs large-scale clinical validation. Arterial stiffening in hypertension and atherosclerosis directly increases PWV, a gold-standard indicator of cardiovascular risk. Cuffless blood pressure estimation using PPG signals, primarily based on Pulse Transit Time (PTT), is an area of intense research. However, this technique faces fundamental challenges such as inter-individual model variability and the unresolved need for periodic recalibration. Moreover, negative results, such as those from Microsoft Research's Aurora project, indicate that ML models using radial artery tonometry, PPG, and ECG waveforms did not outperform strong baseline models that relied solely on calibrated cuff BP, highlighting the methodological hurdles [283]. For direct PWV assessment, LDV and wearable pressure sensor arrays can measure local PWV, but measurement accuracy is significantly influenced by factors like sensor spacing and temporal synchronization. The universal challenge in this domain is a lack of standardized validation protocols against international standards (e.g., ISO 81060–3, ESH guidelines).

Pulse waveform analysis also enables the assessment of autonomic nervous system regulation and cardiorespiratory coupling. PPG signals have been extensively investigated for detecting respiratory events associated with sleep apnea, commonly by deriving respiratory rate from pulse waveform modulation or estimating the apnea–hypopnea index using oxygen saturation dynamics [289,290]. However, PPG sensors require active illumination for signal acquisition, leading to substantial power usage. Scientists have investigated strategies for simplifying algorithm structure [291] and optimizing device design. A recent study employs a two-stage detection strategy by integrating a PENG and a PPG sensor [251]. Operating continuously, the self-powered PENG performs initial screening and only activates the PPG sensor when suspicious events occur. During apnea events, the nasal pressure airflow signal exhibits a significant reduction in waveform amplitude (>90%) or complete disappearance. Importantly, the information contained within the PPG signal extends beyond respiratory metrics to encompass the architecture of sleep itself. This is critically relevant, as sleep staging (the delineation of wake, rapid eye movement (REM), and non-REM sleep stages) is fundamental to diagnosing sleep disorders like obstructive sleep apnea (OSA) and assessing overall sleep quality. While conventional sleep staging relies on labor-intensive manual scoring of the electroencephalogram (EEG) during polysomnography (PSG), recent advances demonstrate that PPG can serve as a viable alternative. Korkalainen et al. [284] trained a deep learning model to perform sleep staging on the PPG signals obtained from diagnostic polysomnograms of 894 patients with suspected OSA. Fig. 9b displays sample PPG outputs recorded during various sleep stages. In these samples, the PPG signal during wakefulness is stable, showing fairly constant frequency and amplitude. During N1 sleep, however, irregular amplitude variation occurs and the frequency declines. Transitioning into N2 and then N3 sleep, the amplitude continues to drop and low-frequency oscillations emerge in the PPG signal. REM sleep closely resembles the wake state, albeit with slightly higher amplitude variability. Although these sleep-stage-related changes in PPG profiles may be challenging to distinguish by eye, rule-based or AI-enabled algorithms can reliably discriminate between sleep stages [292,293].

In metabolic disorders, pulse-based sensing primarily reflects changes in microcirculation and vascular responses rather than disease-specific biochemical information. PPG is particularly sensitive to pulsatile blood-volume variations and has therefore been explored for detecting physiological changes associated with glucose fluctuations [294]. For example, Zheng et al. [285] developed a highly sensitive NIR PPG sensor based on a vapor-deposited perovskite photodetector and used a Gradient Boosting Decision Tree model to estimate glucose levels from pulse wave morphology, reporting a MARD of 2.48% in an individual dataset and predictions within Zone A of the Clarke Error Grid (Fig. 9c). However, such results demonstrate an association between pulse wave characteristics and glycemic state rather than glucose-specific diagnostic capability. Because pulse morphology is also influenced by vascular tone, temperature, autonomic regulation, tissue optical properties, and other metabolic or hemodynamic factors, substantially larger and more diverse validation cohorts are required before pulse-based glucose estimation can be considered clinically equivalent to established biochemical measurements. At present, its more appropriate clinical positioning is therefore as an exploratory monitoring or risk-screening approach rather than a standalone diagnostic method or replacement for invasive blood glucose testing.

The potential applications of pulse wave analysis have also been extended to broader systemic diseases [13,295]. In these settings, however, pulse wave alterations should be interpreted primarily as nonspecific manifestations of systemic vascular and hemodynamic changes, rather than disease-specific biomarkers. Studies have reported differences in pulse-derived features among individuals with cirrhosis, fatty liver disease, and corresponding control groups [296–299], but these findings currently support exploratory screening or risk stratification rather than definitive diagnosis. A similar distinction applies to kidney and liver disease. Measures of arterial stiffness, including aortic PWV, estimated carotid–femoral PWV, and aortic pulse pressure, were independently associated with incident chronic kidney disease, with chronic kidney disease (CKD) incidence increasing across higher quartiles of these vascular measures (Fig. 9d) [286,287]. These observations indicate potential value for cardiovascular risk stratification and longitudinal assessment of vascular deterioration in populations at risk of CKD, but they do not establish CKD-specific diagnostic capability. Likewise, carotid–femoral PWV was independently associated with fatty liver disease and, more strongly, with liver fibrosis after adjustment for cardiometabolic risk factors (Fig. 9e) [288]. The stronger associations observed in individuals with obesity, diabetes, or metabolic syndrome further suggest that these pulse-derived vascular changes may reflect shared cardiometabolic and hemodynamic pathways rather than liver-specific pathology. Therefore, their current value lies primarily in risk stratification and complementary disease assessment, rather than standalone diagnosis of liver fibrosis.

In oncology, exploratory studies using pulse wave features and machine-learning classifiers have reported differences between patients with lung cancer and control populations [300]. However, the biological specificity of these pulse signatures remains unclear, and current evidence is insufficient to support pulse wave sensing as a diagnostic modality for cancer. Such approaches should therefore be considered preliminary screening or phenotyping tools that require prospective multicenter validation against established oncological reference standards.

Overall, most studies linking pulse wave features to non-cardiovascular systemic diseases remain retrospective, single-center, or limited in sample size. Their observed signals are likely influenced by shared processes such as chronic inflammation, autonomic dysfunction, vascular stiffening, altered peripheral resistance, and metabolic dysregulation. Consequently, current evidence supports their use primarily for screening, monitoring, or risk stratification, whereas disease-specific diagnosis will require prospective validation, external replication, and demonstration of incremental diagnostic value beyond established clinical tests. Different sensing modalities support distinct clinical roles because they capture different aspects of cardiovascular physiology. Mechanical sensors, including piezoresistive and piezoelectric

devices, are particularly suited to resolving detailed pulse wave morphology; PPG provides complementary information on peripheral blood-volume and microcirculatory dynamics; and ultrasound-based techniques can provide deeper vascular structural and hemodynamic information. Multimodal sensing may further improve robustness by combining complementary physiological measurements. Importantly, the clinical maturity of these applications varies substantially. PPG-based AF detection currently has the strongest evidence for screening and longitudinal rhythm monitoring, supported by a relatively well-established confirmatory pathway using ECG. Blood pressure and arterial-stiffness assessment are progressing toward monitoring and cardiovascular risk stratification, although standardized validation and calibration remain major challenges. Pulse-based assessment of metabolic disorders is still primarily exploratory and is better positioned for monitoring or risk screening. Applications involving CKD, liver fibrosis, cancer, and other systemic diseases remain at an early stage and should currently be regarded as exploratory screening or risk-stratification approaches rather than established diagnostic tools. Ultimately, progression from association to diagnosis will require demonstration of disease specificity, prospective multicenter validation, comparison with accepted reference standards, and evidence of clinically meaningful incremental value.

### 4.1. Machine learning for pulse wave

Pulse wave analysis has traditionally relied on well-established signal-processing and physiological feature-extraction techniques. Typical pipelines include signal filtering and artifact removal, beat segmentation, fiducial-point detection, and extraction of morphology- and timing-related parameters such as systolic peak amplitude, pulse width, pulse transit time (PTT), pulse arrival time (PAT), and pulse wave velocity (PWV). These features provide physiologically interpretable descriptions of cardiovascular function and remain widely used for estimating blood pressure, arterial stiffness, vascular resistance, and other hemodynamic parameters. However, such approaches depend strongly on predefined waveform landmarks and expert-designed features, whose reliability may deteriorate when waveform morphology changes across individuals, disease states, sensor locations, or real-world recording conditions. The increasing availability of continuous pulse wave data from wearable devices has therefore created a need for analytical methods capable of exploiting more complex and heterogeneous waveform information.

ML strategies for physiological parameter estimation have evolved from models based on explicit, physiology-inspired features to approaches that learn representations directly from data. Traditional ML models (e.g., linear regression (LR) [301], support vector regression (SVR) [302], K-Nearest Neighbors (KNN) [303], random forest (RF) [304]) rely on handcrafted features (e.g., PTT, morphological indices), which inherently bottle-neck performance by requiring expert knowledge and struggling to model intricate interactions. Compared with simple analytical or regression-based relationships, these models can capture more complex multivariate and nonlinear associations. Nevertheless, their performance remains constrained by the quality and completeness of the predefined features and may be sensitive to differences in population characteristics, sensor configurations, and calibration strategies. Benchmark studies across multiple datasets have further shown that apparently strong performance can depend substantially on data partitioning, subject overlap, and evaluation protocols, emphasizing the need for subject-independent and standardized validation [305,306]. These limitations have driven a gradual shift from feature-based ML toward representation learning from raw or minimally processed pulse waveforms. Convolutional Neural Networks (CNNs) [307] were naturally adopted to discern local morphological patterns (e.g., systolic peak, dicrotic notch) within a single pulse, while Recurrent Neural Networks (RNNs) and their variants (e.g., LSTMs) are adept at modeling temporal dependencies [308,309]. Hybrid CNN–RNN architectures have been widely adopted to jointly capture beat-level waveform morphology and temporal dependencies across successive cardiac cycles [310], both of which are essential for accurate pulse-based physiological estimation. Transformer-based models with attention mechanisms offer enhanced capabilities for long-range dependency modeling. However, their computational demands and energy consumption currently limit deployment on wearable edge devices. Lightweight strategies such as knowledge distillation [311,312], compression [313], and structural pruning provide viable paths for resource-constrained environments. Concurrently, generative models (Auto-encoder(AE)/ Variational Autoencoder(VAE)、U-Net [314]、Generative Adversarial Networks (GANs))show promise in data augmentation and domain adaptation, yet ensuring the physiological plausibility, statistical consistency, and clinical interpretability of generated signals remains a significant challenge [315].

The potential value of ML becomes clearer when it is compared directly with established signal-processing approaches under realistic monitoring conditions. PPG-based atrial fibrillation (AF) detection provides an illustrative example. Antiperovitch et al. compared a validated heuristic signal-processing algorithm with a convolutional deep neural network in 204 free-living participants monitored continuously for four weeks. Although the two approaches achieved nearly identical discrimination, the deep-learning model was able to analyze a substantially larger proportion of available PPG recordings and maintained strong performance in an external cohort acquired using a different sensor [316]. This finding suggests that the benefit of ML in mature pulse monitoring applications may not necessarily lie in a dramatic increase in nominal accuracy, but rather in improved tolerance to motion artifacts, waveform variability, and incomplete or heterogeneous real-world data. AF monitoring also represents one of the clearest examples of pulse wave algorithms progressing from methodological development toward commercial and clinical use. PPG-based rhythm analysis has already been incorporated into commercial smartwatches, where pulse irregularity can be used for opportunistic AF screening and, when necessary, followed by confirmatory single-lead ECG recordings. Recent prospective studies have extended these systems beyond proof-of-concept evaluation. In a multicenter randomized trial involving 437 older adults at elevated stroke risk, smartwatch-based monitoring increased the detection of previously unrecognized AF compared with standard care [317]. Continuous smartwatch PPG has also been evaluated against patch ECG in patients with established AF for estimating AF burden [318]. These studies demonstrate that, in selected applications, ML-assisted pulse sensing is beginning to move from retrospective algorithm development toward prospective validation in real clinical populations and commercially available devices.

The degree of clinical maturity, however, differs substantially across applications. Cuffless blood pressure estimation has attracted extensive ML research but remains less established than AF screening. To systematically compare the performance of different ML approaches discussed above, Table 3 summarizes representative data-driven models for estimating hemodynamic parameters, primarily blood pressure, from pulse waveforms. The comparison covers key aspects such as sensor type, model architecture, dataset characteristics, and estimation accuracy. Although many models report encouraging results under controlled validation conditions, strong performance does not necessarily translate to independent populations or free-living use. Models relying on one-time calibration or static demographic information may be particularly vulnerable to physiological changes over time and to differences among older adults, hypertensive patients, and individuals with comorbidities [305,306]. Nevertheless, clinically oriented validation of cuffless BP technologies is beginning to emerge. A recent prospective study evaluated a commercially available PPG-based chest-patch system in patients following cardiac surgery and compared tens of thousands of cuffless estimates with invasive arterial blood pressure measurements [319]. Such studies represent an important transition from retrospective database evaluation toward testing in real

**Table 3**
Summary of Data-driven Models for BP Estimation from Pulse Waveforms.

| Models | Sensor type | Dataset | Deviation (mmHg) | Ref |
|---|---|---|---|---|
| GRU + CNN | PPG | 154 normal individuals and 40 pregnant women | SBP: −0.17 ± 1.45 (ME ±SD) DBP: 0.27 ± 0.64 (ME ±SD) | [320] |
| Transformer | PPG | Mindray dataset MIMIC dataset II | SBP: 0.67 ± 4.29(ME ±SD) DBP:0.37 ± 2.46 (ME ±SD) | [321] |
| Multi-Scale Perception Network | FBG | MIMIC andh human subjects | SBP: −0.05 ± 2.15(ME ±SD) DBP: −0.19 ± 3.48(ME ±SD) | [322] |
| LR | piezoresistive | 20 human subjects for more than 50 min | SBP: 2.33 (MAE) DBP: 2.16 (MAE) MAP: 1.80 | [323] |
| Extreme Gradient Boosting (XGBoost) | piezoelectric | Dynamic evaluation of 87 subjects | SBP: 0.05 ± 4.61(ME ±SD) DBP: 0.11 ± 3.68(ME ±SD) | [191] |
| CNN | piezoelectric | 178 sets of data from 9 human subjects | SBP: 5.82 (MAE) DBP: 4.60 (MAE) | [67] |
| RFR | piezoresistive | 1128 sets of data from 28 human subjects | SBP: 0.87 ($R^2$) DBP: 0.79 ($R^2$) | [324] |
| CNN-BiLSTM | capacitive | 143 human subjects | SBP:0.0035 ± 3.3734(ME ±SD) DBP:0.4116 ± 1.9037(ME ±SD) | [325] |
| error back propagation (BP) neural network | triboelectric | 80 sets of data from 16 human subjects | SBP: 5.06 (MAE) DBP: 3.75 (MAE) | [326] |
| TradaBoost+RF | triboelectric | 5 subjects | 2.66 ± 1.35 (ME ± SD) | [327] |
| ANN | piezo-thermal | 260 sets of data from 18 human subjects | SBP: −0.03 ± 5.56 (ME ± SD) DBP: 0.12 ± 3.91 (ME ± SD) | [328] |
| Feedforward Neural Networks (FNN) | triboelectric | Public dataset | SBP: 3.06 (ME) DBP: 3.50 (ME) | [241] |
| Back Propagation Neural Network (BPNN) | FBG | 108 sets of data from the hospital | SBP: −0.35 ± 4.68 (ME+SD) DBP: −2.54 ± 4.07 (ME+SD) | [329] |

patient populations.

Despite promising results in controlled validation studies, most ML-driven physiological monitoring solutions remain at the proof-of-concept stage, with limited translation to widespread clinical practice [330]. Notably, negative results, such as those from Microsoft Research's Aurora project, indicate that ML models using radial artery tonometry, PPG, and ECG waveforms did not outperform strong baseline models that relied solely on calibrated cuff BP and time information for adult resting or 24-hour ambulatory monitoring [283]. Widespread adoption is hindered by several factors: limited model interpretability and insufficient incorporation of biophysical mechanisms [331,332]; inadequate generalization and robustness due to dataset biases and individual differences [333]; and a lack of standardization in calibration protocols, which vary significantly across studies in terms of the number of reference measurements and the time intervals between calibrations [334]. Furthermore, many algorithms are validated only in controlled settings, and their performance often degrades in real-world environments due to motion artifacts, ambient noise, and synchronization errors. The computational capacity and battery life of wearable edge devices also constrain the real-time inference of complex models [1].

While commercial devices allow patients to monitor physiological signals at home, continuous monitoring is not feasible with traditional approaches, making AI-enhanced wearables an attractive option. Developing this field requires establishing large-scale standardized datasets covering diverse populations and implementing unified evaluation standards for creating physiologically plausible models that can overcome performance degradation across different groups. Technologically, future efforts should focus on enhancing optical sensor stability through optimized anti-interference packaging and optical path design, integrating motion sensing units to suppress artifacts, and ensuring stable skin-device interface mechanics for highly sensitive pulse wave sensors. Algorithm development should focus on creating lightweight on-device inference solutions suitable for long-term monitoring, balancing computational efficiency and model performance through techniques like knowledge distillation and quantization. However, achieving true clinical translation requires moving beyond technical validation. Independent prospective studies following international standards and ultimately randomized controlled trials confirming patient outcome improvements are essential. Continuously collected data from wearable devices, including lifestyle metrics, sleep patterns, and daily activity data, provides new dimensions for enhancing traditional prediction models. Existing models primarily rely on clinical environment data, lacking dynamic monitoring information for important cardiovascular disease risk factors. Recent research shows significant correlations between parameters like step count, sleep duration and variability extracted from wearable devices, and health outcomes [335,336]. For example, increased step count on the first postoperative day strongly correlates with reduced hospital stay for major surgical patients [337]. Integrating real-time wearable data with electronic health records enables more representative health risk assessment models.

In terms of computational architecture, ML algorithm development has evolved from supercomputer reliance to cloud deployment. Cloud platforms like Amazon AWS and Google Cloud are increasingly used for medical data management due to cost-effectiveness and scalable resources. Research confirms that when directly integrated with electronic health record systems, high-performance cloud computing resources can efficiently facilitate the creation and implementation of complex predictive models [338,339]. This makes AI warning systems combining historical medical records and real-time wearable data feasible, though actual effectiveness still needs verification. Meanwhile, some computationally efficient "lean" algorithms can now process data directly on devices, providing new options for cloud-independent data analysis [340]. As illustrated in Fig. 10, the future outlook for wearable pulse wave sensors points toward intelligent closed-loop systems that integrate multimodal sensing, edge intelligence, and patient–sensor–AI–physician interfaces. Such systems are expected to enable continuous, personalized, and clinically actionable health monitoring.

The technology's clinical value ultimately depends on acceptance by both medical professionals and patients. Although clinicians show interest in new technologies, the "black box" nature of algorithms and difficulty explaining AI-generated conclusions to patients remain significant barriers [341]. In practical applications, nearly 90% of smartwatch alerts for abnormal pulse readings did not lead to a clinical

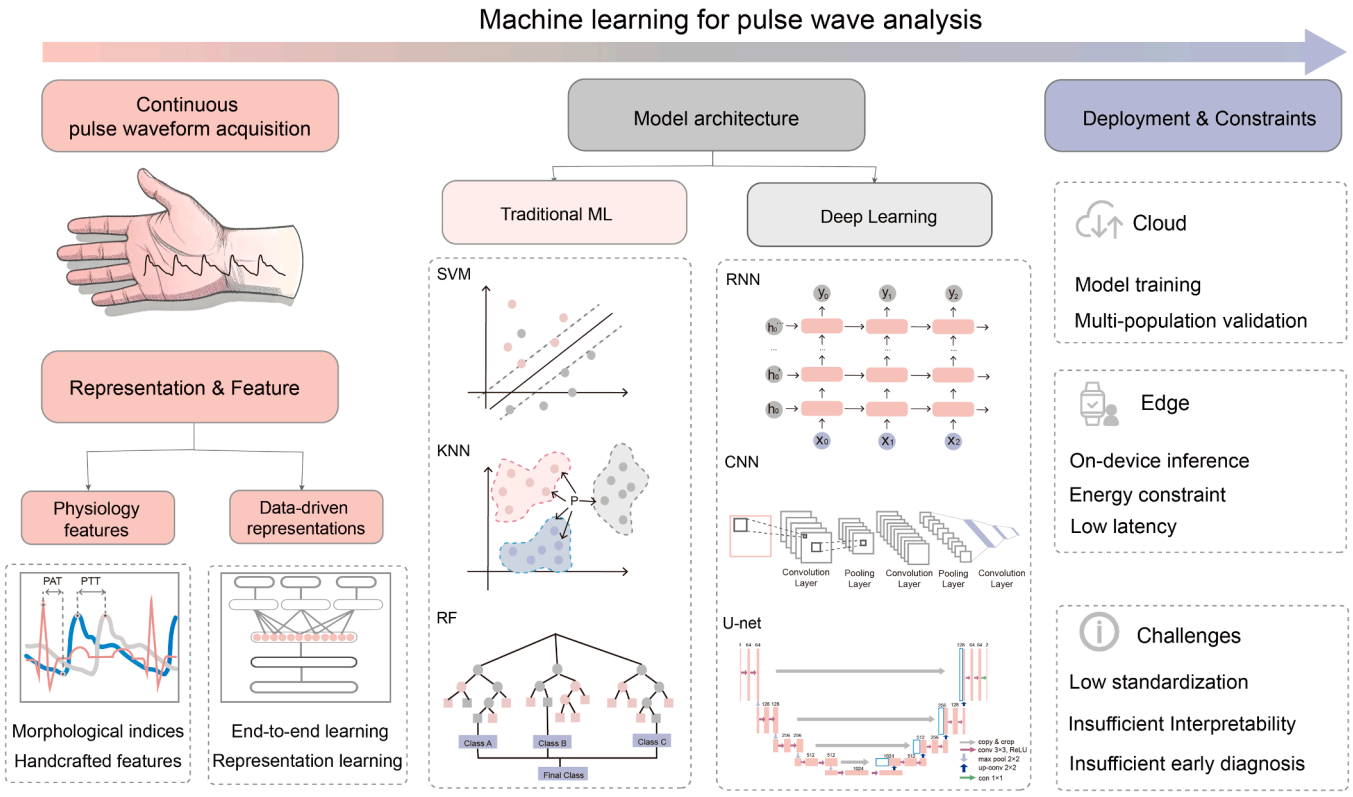



**Fig. 10.** Panoramic view of machine learning framework for pulse wave analysis.

diagnosis, raising concerns about low-value healthcare resource consumption. Patient surveys indicate only half view digital tools and AI as significant opportunities, while about 10% consider them threats [342]. Some patients worry technology misuse may undermine humanistic aspects of healthcare, particularly when using wearable devices without proper medical guidance, leading to high dropout rates and incomplete follow-up in large digital health projects - highlighting the need for enhanced patient education and engagement. Therefore, there is an urgent need to establish multi-parameter monitoring systems based on wearable devices, develop assessment pathways suitable for different clinical scenarios and patient groups, and ensure effective utilization of the technology system by both users and prescribing physicians through professional training.

## 5. Conclusion

This review focuses on optical and mechanical sensors, emphasizing their operating principles, material properties, structural designs, and clinical applications in pulse wave analysis. The advent of 5 G and the Internet of Things (IoT) promises enhanced device precision, accelerated clinical-grade data processing and transmission, and expanded storage capacity to facilitate inter-sensor communication. Nevertheless, despite significant research progress, several challenges must be urgently resolved before wearable pulse wave sensing devices can achieve clinically reliable, user-centered adoption, as outlined below.

Signal fidelity and noise management remain a significant bottleneck in wearable sensing systems. Measurements from both PPG and mechanical sensors are frequently compromised by a combination of intrinsic physiological variations (e.g., in skin properties and subcutaneous tissue) and extrinsic environmental factors (e.g., temperature, humidity), undermining accuracy and reproducibility [246]. Even ultrasound transducers, which directly interrogate arterial pulsations, introduce artifacts through probe pressure required for acoustic coupling and are prone to misalignment from minor movements. The performance of most existing wearable sensors is fundamentally constrained by a trade-off between high sensitivity and robustness against motion artifacts. This is exemplified by the prevalent difficulty in reliably capturing faint pulse signals during vigorous daily activities, which is a critical shortfall for continuous health monitoring, as these artifacts can lead to clinical misinterpretation. While emerging technologies like thermoelectric [328] and bioimpedance sensors [343,344] which directly leverage the body's inherent properties to reduce artifacts, offer promising alternative pathways, the core challenge of achieving both signal fidelity and operational stability in real-world settings persists. Active pressure devices like pneumatic cuffs partly mitigate sensor misalignment issues, yet compromise wearability, comfort, and measurement continuity. Furthermore, excessive external pressure risks arterial occlusion and signal distortion, while optimal pressure thresholds vary significantly with age, gender, and physiological fitness, making standardized quantification infeasible. These challenges also reveal a broader limitation in the current literature: wearable pulse sensors are often evaluated using heterogeneous protocols and device-centric metrics, making it difficult to compare performance across sensing mechanisms or to determine whether favorable benchtop characteristics translate into reliable physiological measurements. A unified benchmarking framework is therefore needed to evaluate wearable pulse wave sensors across the complete measurement chain, from transducer performance to on-body signal quality and clinical reliability. Such a framework should encompass five complementary levels. First, device-level characterization should report sensitivity or responsivity, detection limit, linear range, hysteresis, response/recovery time, frequency response, and cyclic durability under clearly defined loading conditions. Second, signal fidelity should be assessed against an appropriate reference waveform using metrics such as signal-to-noise ratio, waveform correlation, preservation of characteristic landmarks (e.g., systolic peak and dicrotic notch), and timing errors in pulse onset or peak detection. Third, motion resistance should be quantified under standardized perturbations, including wrist rotation, arm movement,

walking, and other representative daily activities, with changes in signal quality, feature error, and valid-data fraction reported rather than relying solely on qualitative demonstrations. Fourth, long-term stability should include baseline drift, repeated-wear reproducibility, mechanical fatigue, adhesion stability, environmental sensitivity to temperature and humidity, and the frequency of recalibration required during prolonged use. Finally, on-body validation should explicitly consider participant diversity, anatomical site, arterial depth and tissue characteristics, repeated measurement sessions, calibration strategy, and comparison with accepted clinical reference methods. Importantly, subject-independent and external validation should be distinguished from within-subject or within-session testing. Together, these criteria shift sensor evaluation from the question of whether a device can detect a pulse under idealized conditions to whether it can preserve physiologically meaningful waveform information reliably during realistic use.

Material structure and sensing innovation are pivotal to overcoming current limitations. Flexible pressure sensors face inherent sensitivity-range tradeoffs. As highlighted in our graphical abstract, nanomaterials (CNTs, metal oxide NPs), 2D materials (graphene, MXenes), and composite microstructures (iontronics, gel-based systems) offer promising pathways for enhancing performance. Nevertheless, despite numerous proposed microstructure designs (nanowire architectures and advanced fabric sensor arrays), their implementation in optical, triboelectric, and piezoelectric sensing platforms remains limited. Correlations between microstructure and sensitivity are still poorly understood, with current research relying heavily on empirical approaches rather than systematic design principles.

ML and system integration represent critical frontiers. Deep learning algorithms for pulse wave analysis remain constrained by insufficient training data and underutilization of the pulse wave's diagnostic richness. As visualized in our illustration, complementary sensor arrays not only fulfill ML input requirements but also reduce positioning precision

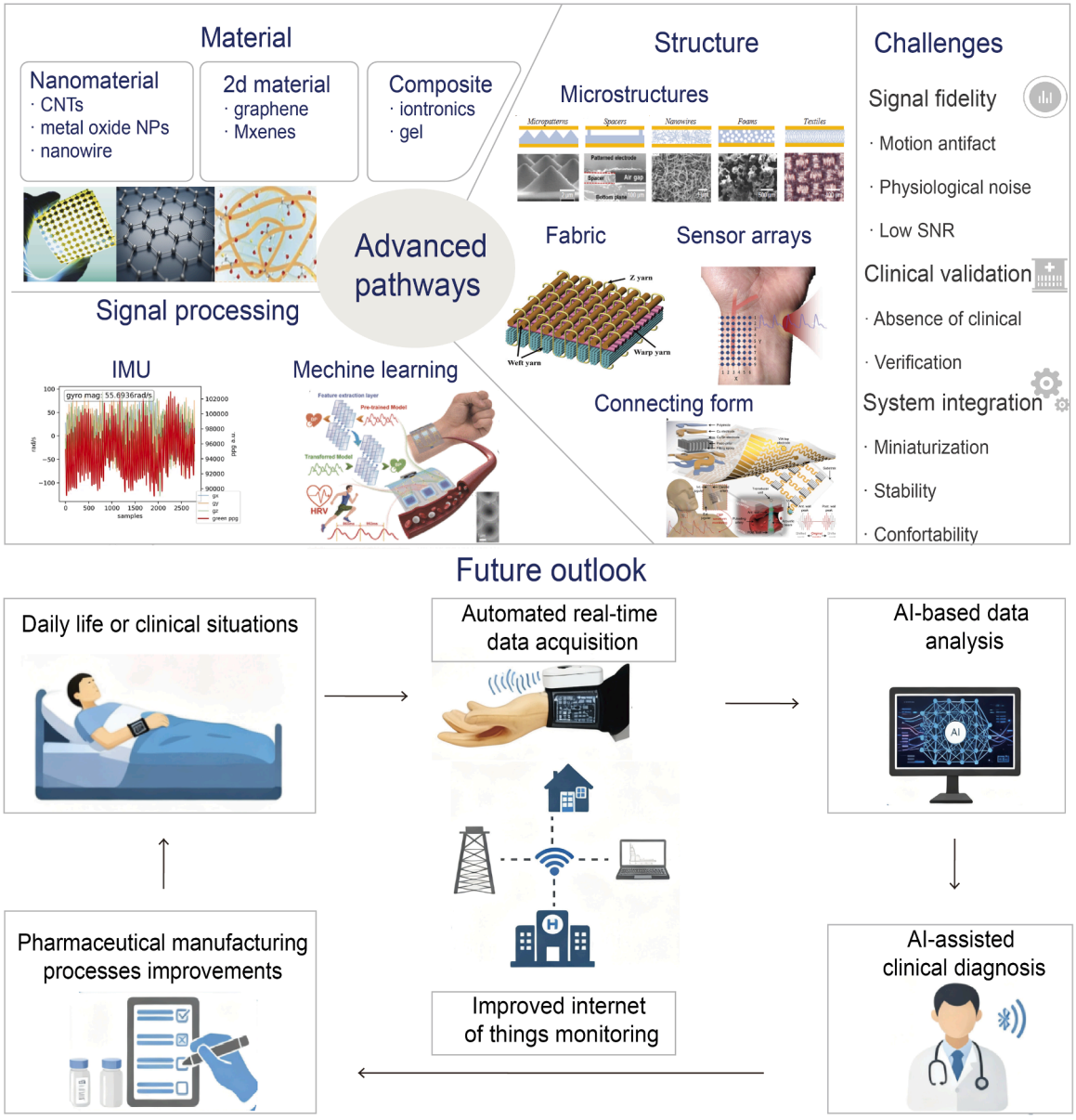



**Fig. 11.** Advanced strategies and key challenges for wearable pulse wave sensors, including materials innovation using nanomaterials, two-dimensional materials, and composites; structural engineering through microstructures [345], fabrics [206], sensor arrays and conformal integration [213]; and signal-processing approaches incorporating inertial measurement units (IMUs) and machine learning [109]. Microstructure images reproduced with permission [345]. Copyright 2022, American Chemical Society. Conformal-integration image reproduced with permission [213]. Copyright 2018, Springer Nature. Machine-learning image reproduced with permission [109]. Copyright 2025, American Chemical Society.

demands, enabling advanced signal processing and IMU-based motion compensation. Future work must optimize power-efficient algorithms capable of concurrent artifact suppression, baseline drift correction, and diagnostic pattern recognition to support clinical decisions. Furthermore, system integration faces substantial challenges in miniaturization, stability, comfortability, and compliance validation, all of which require thorough clinical testing.

The future outlook and clinical translation will be shaped by the development of intelligent closed-loop systems that seamlessly connect patients, sensors, and healthcare providers. Fig. 11 summarizes the key materials, structural designs, challenges, and advanced pathways discussed in this review, highlighting the convergence of nanomaterials, two-dimensional materials, composite microstructures, and machine learning toward next-generation wearable systems. As depicted in our illustration, next-generation ultra-thin tattoo-style devices with reliable epidermal adhesion will enable continuous, unobtrusive physiological monitoring in both daily life and clinical settings. These sensors, integrated with multi-parameter sensing capabilities and tunable optical properties, will form dense networks for automated real-time data acquisition, feeding comprehensive physiological information to cloud-based AI analytics platforms.

The envisioned patient-sensor-AI-physician-patient closed loop represents a paradigm shift in healthcare delivery. Real-time sensor data undergoes AI-based analysis to extract clinically actionable insights, which are then transmitted to healthcare providers for remote diagnosis and intervention. This continuous monitoring and feedback mechanism is particularly important for chronic disease management and elderly care, where early anomaly detection can trigger timely medical responses. Furthermore, the integration of such systems with pharmaceutical manufacturing processes enables real-time quality control and personalized drug delivery optimization. For scalable implementation, key challenges in low-cost materials, simplified manufacturing, and standardized IoT integration must be addressed. The convergence of advanced nanomaterials (CNTs, graphene, MXenes) and composite microstructures (hydrogels, iontronics) will push the boundaries of optoelectronic sensitivity, flexibility, and biocompatibility. Large-scale clinical validation remains imperative to demonstrate the reliability and efficacy of these integrated systems across diverse populations and use cases. Ultimately, the evolution toward miniaturized, multifunctional sensors embedded in intelligent closed-loop frameworks will transform personalized healthcare through continuous monitoring, AI-assisted diagnosis, and proactive medical intervention.

## CRediT authorship contribution statement

**Lei Jia:** Methodology. **Xingyao Lv:** Methodology, Investigation. **Menghan Li:** Writing – original draft, Visualization, Methodology, Investigation, Formal analysis. **Xuandi Deng:** Writing – original draft, Methodology, Investigation, Formal analysis. **Puqing Yao:** Methodology, Investigation. **Yuxiang Wu:** Writing – review & editing, Supervision. **Zhou Li:** Writing – review & editing, Supervision. **Zhuo Liu:** Writing – review & editing, Writing – original draft, Supervision, Project administration, Funding acquisition, Conceptualization. **Yu Song:** Methodology.

## Declaration of Competing Interest

The authors declare that they have no known competing financial interests or personal relationships that could have appeared to influence the work reported in this paper.

## Acknowledgments

The authors thank the support of National Natural Science Foundation of China (82372141), Beijing Nova Program (202604841178, 20250484871), Beijing Natural Science Foundation (Z240022, L245015), Scientific and Technological Innovation Project of China Academy of Chinese Medical Sciences (CI2023C020YL), Fundamental Research Funds for the General Universities.

## Data availability

Data will be made available on request.

## References

[1] L. Zhao, C. Liang, Y. Huang, G. Zhou, Y. Xiao, N. Ji, Y.-T. Zhang, N. Zhao, Emerging sensing and modeling technologies for wearable and cuffless blood pressure monitoring, npj Digit. Med. 6 (2023) 93, https://doi.org/10.1038/s41746-023-00835-6.

[2] N. Ghasemzadeh, A.M. Zafari, A brief journey into the history of the arterial pulse, Cardiol. Res. Pract. 2011 (2011) 164832, https://doi.org/10.4061/2011/164832.

[3] N. Pilz, V. Heinz, T. Ax, L. Fesseler, A. Patzak, T.L. Bothe, Pulse wave velocity: methodology, clinical applications, and interplay with heart rate variability, Rev. Cardiovasc. Med. 25 (2024) 266, https://doi.org/10.31083/j.rcm2507266.

[4] M.F. O'Rourke, A. Pauca, X.-J. Jiang, Pulse wave analysis, Br. J. Clin. Pharmacol. 51 (2001) 507–522, https://doi.org/10.1046/j.0306-5251.2001.01400.x.

[5] S.S. Martin, A.W. Aday, N.B. Allen, Z.I. Almarzooq, C.A.M. Anderson, P. Arora, C. L. Avery, C.M. Baker-Smith, N. Bansal, A.Z. Beaton, Y. Commodore-Mensah, M. E. Currie, M.S.V. Elkind, W. Fan, G. Generoso, B.B. Gibbs, D.G. Heard, S. Hiremath, M.C. Johansen, D.S. Kazi, D. Ko, M.H. Leppert, J.W. Magnani, E. D. Michos, M.E. Mussolino, N.I. Parikh, S.M. Perman, M. Rezk-Hanna, G.A. Roth, N.S. Shah, M.V. Springer, M.-P. St-Onge, E.L. Thacker, S.M. Urbut, H.G.C. Van Spall, J.H. Voeks, S.P. Whelton, N.D. Wong, S.S. Wong, K. Yaffe, L. P. Palaniappan, on behalf of the American Heart Association Council on Epidemiology and Prevention Statistics Committee and Stroke Statistics Committee, 2025 heart disease and stroke statistics: A report of US and global data from the American Heart Association, Circulation 151 (2025), https://doi.org/10.1161/CIR.0000000000001303.

[6] Global, Regional, and National Burden of Cardiovascular Diseases and Risk Factors in 204 Countries and Territories, 1990–2023, S0735109725074285, JACC (2025), https://doi.org/10.1016/j.jacc.2025.08.015.

[7] A.K. Boehme, C. Esenwa, M.S.V. Elkind, Stroke Risk Factors, Genetics, and Prevention, Circ. Res. 120 (2017) 472–495, https://doi.org/10.1161/CIRCRESAHA.116.308398.

[8] G.D. Friedman, D.B. Loveland, S.P. Ehrlich, Jr., Relationship of stroke to other cardiovascular disease, Circulation 38 (1968) 533–541, https://doi.org/10.1161/01.CIR.38.3.533.

[9] P.L. Huang, eNOS, metabolic syndrome and cardiovascular disease, Trends Endocrinol. & Metab. 20 (2009) 295–302, https://doi.org/10.1016/j.tem.2009.03.005.

[10] S. Mottillo, K.B. Filion, J. Genest, L. Joseph, L. Pilote, P. Poirier, S. Rinfret, E. L. Schiffrin, M.J. Eisenberg, The Metabolic Syndrome and Cardiovascular Risk, JACC 56 (2010) 1113–1132, https://doi.org/10.1016/j.jacc.2010.05.034.

[11] P. Zhang, Z. Zhang, J. Zhong, X. Zheng, J. Zhou, W. Sun, Cardiovascular diseases consequences of type 1, type 2 diabetes mellitus and glycemic traits: A mendelian randomization study, Diabetes Res. Clin. Pract. 208 (2024), https://doi.org/10.1016/j.diabres.2024.111094.

[12] L.S. Bhatia, N.P. Curzen, P.C. Calder, C.D. Byrne, Non-alcoholic fatty liver disease: a new and important cardiovascular risk factor? Eur. Heart J. 33 (2012) 1190–1200, https://doi.org/10.1093/eurheartj/ehr453.

[13] K. Marx-Schütt, D.Z.I. Cherney, J. Jankowski, K. Matsushita, M. Nardone, N. Marx, Cardiovascular disease in chronic kidney disease, Eur. Heart J. 46 (2025) 2148–2160, https://doi.org/10.1093/eurheartj/ehaf167.

[14] K. Matsushita, S.H. Ballew, A.Y.-M. Wang, R. Kalyesubula, E. Schaeffner, R. Agarwal, Epidemiology and risk of cardiovascular disease in populations with chronic kidney disease, Nat. Rev. Nephrol. 18 (2022) 696–707, https://doi.org/10.1038/s41581-022-00616-6.

[15] C. Matyas, G. Haskó, L. Liaudet, E. Trojnar, P. Pacher, Interplay of cardiovascular mediators, oxidative stress and inflammation in liver disease and its complications, Nat. Rev. Cardiol. 18 (2021) 117–135, https://doi.org/10.1038/s41569-020-0433-5.

[16] C. Zoccali, P.B. Mark, P. Sarafidis, R. Agarwal, M. Adamczak, R. Bueno de Oliveira, Z.A. Massy, P. Kotanko, C.J. Ferro, C. Wanner, M. Burnier, R. Vanholder, F. Mallamaci, A. Wiecek, Diagnosis of cardiovascular disease in patients with chronic kidney disease, Nat. Rev. Nephrol. 19 (2023) 733–746, https://doi.org/10.1038/s41581-023-00747-4.

[17] H. Ahn, S. Lee, E. Choi, N. Bae, H. Ahn, S. Kwon, S. Lee, K. Han, S. Oh, G. Lip, Increased risk of incident atrial fibrillation in young adults with mental health disorders: a nationwide population-based study, Eur. Heart J. 43 (2022) ehac544.634, https://doi.org/10.1093/eurheartj/ehac544.634.

[18] M. Goldfarb, M. De Hert, J. Detraux, K. Di Palo, H. Munir, S. Music, I. Piña, P. A. Ringen, Severe Mental Illness and Cardiovascular Disease, JACC 80 (2022) 918–933, https://doi.org/10.1016/j.jacc.2022.06.017.

[19] J.L. Treur, R.R. Veeneman, J.M. Vermeulen, K.J.H. Verweij, Unravelling the relation between mental illness and cardiovascular disease by triangulating evidence from different methods, Eur. Heart J. 44 (2023) 1851–1854, https://doi.org/10.1093/eurheartj/ehad049.

[20] J.P.L. Leenen, C. Leerentveld, J.D. van Dijk, H.L. van Westreenen, L. Schoonhoven, G.A. Patijn, Current evidence for continuous vital signs monitoring by wearable wireless devices in hospitalized adults: Systematic review, J. Med. Internet Res. 22 (2020) e18636, https://doi.org/10.2196/18636.
[21] J.R. Turner, A.J. Viera, D. Shimbo, Ambulatory Blood Pressure Monitoring in Clinical Practice: A Review, The American Journal of Medicine 128 (2015) 14–20, https://doi.org/10.1016/j.amjmed.2014.07.021.
[22] T. Aoyagi, Pulse oximetry: its invention, theory, and future, J. Anesth. 17 (2003) 259–266, https://doi.org/10.1007/s00540-003-0192-6.
[23] A.B. Hertzman, Photoelectric Plethysmography of the Nasal Septum in Man, Proceedings of the Society for, Exp. Biol. Med. 37 (1937) 290–292, https://doi.org/10.3181/00379727-37–9543 P.
[24] J.C. Kenry, C.T. Yeo, Lim, Emerging flexible and wearable physical sensing platforms for healthcare and biomedical applications, Microsyst. & Nanoeng. 2 (2016) 16043, https://doi.org/10.1038/micronano.2016.43.
[25] S. Wang, L. Lin, Z.L. Wang, Nanoscale Triboelectric-Effect-Enabled Energy Conversion for Sustainably Powering Portable Electronics, Nano Lett. 12 (2012) 6339–6346, https://doi.org/10.1021/nl303573d.
[26] C. Carini, A.A. Seyhan, Tribulations and future opportunities for artificial intelligence in precision medicine, J. Transl. Med. 22 (2024) 411, https://doi.org/10.1186/s12967-024-05067-0.
[27] M.M.H. Shandhi, J.P. Dunn, AI in medicine: Where are we now and where are we going? Cell. Rep. Med. 3 (2022) 100861 https://doi.org/10.1016/j.xcrm.2022.100861.
[28] F. Tasnim, A. Sadraei, B. Datta, M. Khan, K.Y. Choi, A. Sahasrabudhe, T.A. V. Gálvez, I. Wicaksono, O. Rosello, C. Nunez-Lopez, C. Dagdeviren, Towards personalized medicine: the evolution of imperceptible health-care technologies, Foresight 20 (2018) 589–601, https://doi.org/10.1108/FS-08-2018-0075.
[29] F.N. Van De Vosse, N. Stergiopulos, Pulse Wave Propagation in the Arterial Tree, Annu. Rev. Fluid. Mech. 43 (2011) 467–499, https://doi.org/10.1146/annurev-fluid-122109-160730.
[30] J.-J. Wang, A.B. O'Brien, N.G. Shrive, K.H. Parker, J.V. Tyberg, Time-domain representation of ventricular-arterial coupling as a windkessel and wave system, Am. J. Physiol. -Heart Circ. Physiol. 284 (2003) H1358–H1368, https://doi.org/10.1152/ajpheart.00175.2002.
[31] N. Westerhof, P. Segers, B.E. Westerhof, Wave Separation, Wave Intensity, the Reservoir-Wave Concept, and the Instantaneous Wave-Free Ratio, Hypertension 66 (2015) 93–98, https://doi.org/10.1161/HYPERTENSIONAHA.115.05567.
[32] N. Westerhof, P. Sipkema, G.C.V.D. Bos, G. Elzinga, Forward and backward waves in the arterial system, Cardiovasc. Res. 6 (1972) 648–656, https://doi.org/10.1093/cvr/6.6.648.
[33] Atlas of cardiovascular monitoring, J. Vasc. Surg. 29 (1999) 392–393, https://doi.org/10.1016/S0741-5214(99)70405-2.
[34] M. Nirmalan, P.M. Dark, Broader applications of arterial pressure wave form analysis, Contin. Educ. Anaesth. Crit. Care Pain. 14 (2014) 285–290, https://doi.org/10.1093/bjaceaccp/mkt078.
[35] C. Vlachopoulos, M. O'Rourke, W.W. Nichols. McDonald's Blood Flow in Arteries: Theoretical, Experimental and Clinical Principles, 6, CRC Press, 2011, https://doi.org/10.1201/b13568.
[36] M. Butlin, A. Qasem, Large artery stiffness assessment using SphygmoCor technology, Pulse 4 (2016) 180–192, https://doi.org/10.1159/000452448.
[37] G.F. Mitchell, H. Parise, E.J. Benjamin, M.G. Larson, M.J. Keyes, J.A. Vita, R. S. Vasan, D. Levy, Changes in Arterial Stiffness and Wave Reflection With Advancing Age in Healthy Men and Women: The Framingham Heart Study, Hypertension 43 (2004) 1239–1245, https://doi.org/10.1161/01.HYP.0000128420.01881.aa.
[38] J. Allen, Photoplethysmography and its application in clinical physiological measurement, Physiol. Meas. 28 (2007) R1, https://doi.org/10.1088/0967-3334/28/3/R01.
[39] M. Coutrot, E. Dudoignon, J. Joachim, E. Gayat, F. Vallée, F. Dépret, Perfusion index: Physical principles, physiological meanings and clinical implications in anaesthesia and critical care, Anaesth. Crit. Care & Pain. Med. 40 (2021) 100964, https://doi.org/10.1016/j.accpm.2021.100964.
[40] F. Roca, M. Iacob, I. Remy-Jouet, J. Bellien, R. Joannides, Evidence for a Role of Vascular Endothelium in the Control of Arterial Wall Viscosity in Humans, Hypertension 71 (2018) 143–150, https://doi.org/10.1161/HYPERTENSIONAHA.117.09870.
[41] X. Sun, H. He, M. Xu, Y. Long, Peripheral perfusion index of pulse oximetry in adult patients: a narrative review, Eur. J. Med. Res. 29 (2024) 457, https://doi.org/10.1186/s40001-024-02048-3.
[42] T. Pereira, N. Tran, K. Gadhoumi, M.M. Pelter, D.H. Do, R.J. Lee, R. Colorado, K. Meisel, X. Hu, Photoplethysmography based atrial fibrillation detection: A review, Npj Digit. Med. 3 (2020) 3, https://doi.org/10.1038/s41746-019-0207-9.
[43] Edward D. Chan, Michael M. Chan, Mallory M. Chan, Pulse oximetry: Understanding its basic principles facilitates appreciation of its limitations, Respir. Med. 107 (2013) 789–799, https://doi.org/10.1016/j.rmed.2013.02.004.
[44] M. Elgendi, On the Analysis of Fingertip Photoplethysmogram Signals, Curr. Cardiol. Rev. 8 (2012) 14–25, https://doi.org/10.2174/157340312801215782.
[45] A.D. Kersey, M.A. Davis, H.J. Patrick, M. LeBlanc, K.P. Koo, C.G. Askins, M. A. Putnam, E.J. Friebele, Fiber grating sensors, J. Light. Technol. 15 (1997) 1442–1463, https://doi.org/10.1109/50.618377.
[46] X. Zhang, C. Wang, T. Zheng, H. Wu, Q. Wu, Y. Wang, Wearable optical fiber sensors in medical monitoring applications: A review, Sensors 23 (2023), https://doi.org/10.3390/s23156671.
[47] F. Zhang, Y. Hao, A. Tian, Z. Yang, B. Zhang, T. Fukuda, C. Shi, Wearable fiber bragg grating sensors for physiological signal and body motion monitoring: A review, IEEE Trans. Instrum. Meas. 74 (2025) 1–24, https://doi.org/10.1109/TIM.2025.3558819.
[48] D. Jia, J. Chao, S. Li, H. Zhang, Y. Yan, T. Liu, Y. Sun, A fiber bragg grating sensor for radial artery pulse waveform measurement, IEEE Trans. Biomed. Eng. 65 (2018) 839–846, https://doi.org/10.1109/TBME.2017.2722008.
[49] K. Xiao, Z. Wang, Y. Ye, C. Teng, R. Min, PDMS-embedded wearable FBG sensors for gesture recognition and communication assistance, Biomed. Opt. Express 15 (2024) 1892–1909, https://doi.org/10.1364/BOE.517104.
[50] L. Antognoli, S. Moccia, L. Migliorelli, S. Casaccia, L. Scalise, E. Frontoni, Heartbeat Detection by Laser Doppler Vibrometry and Machine Learning, Sensors 20 (2020) 5362, https://doi.org/10.3390/s20185362.
[51] W. Iwasaki, H. Nogami, S. Takeuchi, M. Furue, E. Higurashi, R. Sawada, Detection of site-specific blood flow variation in humans during running by a wearable laser doppler flowmeter, Sensors 15 (2015) 25507–25519, https://doi.org/10.3390/s151025507.
[52] W. Heeman, W. Steenbergen, G.M. van Dam, E.C. Boerma, Clinical applications of laser speckle contrast imaging: A review, 080901–080901, J. Biomed. Opt. 24 (2019), https://doi.org/10.1117/1.JBO.24.8.080901.
[53] S. Seoni, P. Segers, S. Beeckman, M. Salvi, M. Romanelli, S. Badhwar, R.M. Bruno, Y. Li, S. Aasmul, N. Madhu, F. Molinari, U. Morbiducci, Real-time beat-to-beat pulse wave velocity estimation: a quality-driven approach using laser Doppler vibrometry, Med. & Biol. Eng. & Comput. (2025) 1–16, https://doi.org/10.1007/s11517-025-03417-8.
[54] Y. Li, P. Segers, J. Dirckx, R. Baets, On-chip laser Doppler vibrometer for arterial pulse wave velocity measurement, Biomed. Opt. Express 4 (2013) 1229–1235, https://doi.org/10.1364/BOE.4.001229.
[55] A. Garrett, B. Kim, N.Z. Gurel, E.J. Sie, B.K. Wilson, F. Marsili, J.P. Forman, N. M. Hamburg, D.A. Boas, D. Roblyer, Speckle Contrast Opt. Spectrosc. Improv. cuffless blood Press. Estim. Comp. Photo (2024), https://doi.org/10.1101/2024.08.16.608163.
[56] J. Park, S. Choi, F. Knieling, B. Clingman, S. Bohndiek, L.V. Wang, C. Kim, Clinical translation of photoacoustic imaging, Nat. Rev. Bioeng. 3 (2024) 193–212, https://doi.org/10.1038/s44222-024-00240-y.
[57] Z. Shi, L. Meng, X. Shi, H. Li, J. Zhang, Q. Sun, X. Liu, J. Chen, S. Liu, Morphological Engineering of Sensing Materials for Flexible Pressure Sensors and Artificial Intelligence Applications, Nano-Micro Lett. 14 (2022) 141, https://doi.org/10.1007/s40820-022-00874-w.
[58] B. Jafarizadeh, A.H. Chowdhury, M.S. Islam Sozal, Z. Cheng, N. Pala, C. Wang, Wearable System Integrating Dual Piezoresistive and Photoplethysmography Sensors for Simultaneous Pulse Wave Monitoring, ACS Appl. Mater. Interfaces 16 (2024) 65402–65413, https://doi.org/10.1021/acsami.4c17710.
[59] W. Li, X. Jin, X. Han, Y. Li, W. Wang, T. Lin, Z. Zhu, Synergy of Porous Structure and Microstructure in Piezoresistive Material for High-Performance and Flexible Pressure Sensors, ACS Appl. Mater. Interfaces 13 (2021) 19211–19220, https://doi.org/10.1021/acsami.0c22938.
[60] Y. Ma, N. Liu, L. Li, X. Hu, Z. Zou, J. Wang, S. Luo, Y. Gao, A highly flexible and sensitive piezoresistive sensor based on MXene with greatly changed interlayer distances, Nat. Commun. 8 (2017) 1207, https://doi.org/10.1038/s41467-017-01136-9.
[61] Y. Cheng, Y. Ma, L. Li, M. Zhu, Y. Yue, W. Liu, L. Wang, S. Jia, C. Li, T. Qi, J. Wang, Y. Gao, Bioinspired Microspines for a High-Performance Spray Ti3C2Tx MXene-Based Piezoresistive Sensor, ACS Nano 14 (2020) 2145–2155, https://doi.org/10.1021/acsnano.9b08952.
[62] J. Yan, Y. Ma, G. Jia, S. Zhao, Y. Yue, F. Cheng, C. Zhang, M. Cao, Y. Xiong, P. Shen, Y. Gao, Bionic MXene based hybrid film design for an ultrasensitive piezoresistive pressure sensor, Chem. Eng. J. 431 (2022) 133458, https://doi.org/10.1016/j.cej.2021.133458.
[63] X. He, Z. Liu, G. Shen, X. He, J. Liang, Y. Zhong, T. Liang, J. He, Y. Xin, C. Zhang, D. Ye, G. Cai, Microstructured capacitive sensor with broad detection range and long-term stability for human activity detection, Npj Flex. Electron. 5 (2021) 1–9, https://doi.org/10.1038/s41528-021-00114-y.
[64] N. Bai, L. Wang, Q. Wang, J. Deng, Y. Wang, P. Lu, J. Huang, G. Li, Y. Zhang, J. Yang, K. Xie, X. Zhao, C.F. Guo, Graded intrafillable architecture-based iontronic pressure sensor with ultra-broad-range high sensitivity, Nat. Commun. 11 (2020) 209, https://doi.org/10.1038/s41467-019-14054-9.
[65] J.-Y. Sun, C. Keplinger, G.M. Whitesides, Z. Suo, Ionic skin, Adv. Mater. 26 (2014) 7608–7614, https://doi.org/10.1002/adma.201403441.
[66] S. Trolier-McKinstry, Crystal chemistry of piezoelectric materials, in: A. Safari, E. K. Akdoğan (Eds.), Piezoelectric and Acoustic Materials for Transducer Applications, Springer US, Boston, MA, 2008, pp. 39–56, https://doi.org/10.1007/978-0-387-76540-2_3.
[67] M. Li, J. Aoyama, K. Inayoshi, H. Zhang, Wearable PZT Piezoelectric Sensor Device for Accurate Arterial Pressure Pulse Waveform Measurement, Adv. Electron. Mater. 11 (2025) 2400852, https://doi.org/10.1002/aelm.202400852.
[68] A. Sood, M. Desseigne, A. Dev, L. Maurizi, A. Kumar, N. Millot, S.S. Han, A Comprehensive Review on Barium Titanate Nanoparticles as a Persuasive Piezoelectric Material for Biomedical Applications: Prospects and Challenges, Small 19 (2023) 2206401, https://doi.org/10.1002/smll.202206401.
[69] Z. Wang, Z. Liu, G. Zhao, Z. Zhang, X. Zhao, X. Wan, Y. Zhang, Z.L. Wang, L. Li, Stretchable Unsymmetrical Piezoelectric BaTiO3 Composite Hydrogel for Triboelectric Nanogenerators and Multimodal Sensors, ACS Nano 16 (2022) 1661–1670, https://doi.org/10.1021/acsnano.1c10678.
[70] N.K. Das, M. Ravipati, S. Badhulika, Nickel Metal-Organic Framework/PVDF Composite Nanofibers-based Self-Powered Wireless Sensor for Pulse Monitoring of Underwater Divers via Triboelectrically Generated Maxwell's Displacement

Current, Adv. Funct. Mater. 33 (2023) 2303288, https://doi.org/10.1002/adfm.202303288.
[71] C. Han, H. Zhang, Q. Chen, T. Li, L. Kong, H. Zhao, L. He, A directional piezoelectric sensor based on anisotropic PVDF/MXene hybrid foam enabled by unidirectional freezing, Chem. Eng. J. 450 (2022) 138280, https://doi.org/10.1016/j.cej.2022.138280.
[72] T. Yang, H. Pan, G. Tian, B. Zhang, D. Xiong, Y. Gao, C. Yan, X. Chu, N. Chen, S. Zhong, L. Zhang, W. Deng, W. Yang, Hierarchically structured PVDF/ZnO core-shell nanofibers for self-powered physiological monitoring electronics, Nano Energy 72 (2020) 104706, https://doi.org/10.1016/j.nanoen.2020.104706.
[73] Y. Shi, Revisiting the phase diagram and piezoelectricity of lead zirconate titanate from first principles, Phys. Rev. B 109 (2024), https://doi.org/10.1103/PhysRevB.109.174104.
[74] B. Wu, H. Zheng, Y.-Q. Wu, Z. Huang, H.-C. Thong, H. Tao, J. Ma, C. Zhao, Z. Xu, Y.-X. Liu, Z. Xing, N. Liang, F.-Z. Yao, C.-F. Wu, K. Wang, B. Han, Origin of ultrahigh-performance barium titanate-based piezoelectrics: Stannum-induced intrinsic and extrinsic contributions, Nat. Commun. 15 (2024) 7700, https://doi.org/10.1038/s41467-024-52031-z.
[75] Z.L. Wang, J. Song, Piezoelectric Nanogenerators Based on Zinc Oxide Nanowire Arrays, Science 312 (2006) 242–246, https://doi.org/10.1126/science.1124005.
[76] Y.-M. Wang, Q. Zeng, L. He, P. Yin, Y. Sun, W. Hu, R. Yang, Fabrication and application of biocompatible nanogenerators, iScience 24 (2021) 102274, https://doi.org/10.1016/j.isci.2021.102274.
[77] C. Wu, A.C. Wang, W. Ding, H. Guo, Z.L. Wang, Triboelectric Nanogenerator: A Foundation of the Energy for the New Era, Adv. Energy Mater. 9 (2019) 1802906, https://doi.org/10.1002/aenm.201802906.
[78] L. Zhou, D. Liu, J. Wang, Z.L. Wang, Triboelectric nanogenerators: Fundamental physics and potential applications, Friction 8 (2020) 481–506, https://doi.org/10.1007/s40544-020-0390-3.
[79] J. Hu, M. Iwamoto, X. Chen, A Review of Contact Electrification at Diversified Interfaces and Related Applications on Triboelectric Nanogenerator, Nano-Micro Lett. 16 (2023) 1–25, https://doi.org/10.1007/s40820-023-01238-8.
[80] Z.L. Wang, On Maxwell's displacement current for energy and sensors: the origin of nanogenerators, Mater. Today 20 (2017) 74–82, https://doi.org/10.1016/j.mattod.2016.12.001.
[81] G. Zhu, C. Pan, W. Guo, C.-Y. Chen, Y. Zhou, R. Yu, Z.L. Wang, Triboelectric-Generator-Driven Pulse Electrodeposition for Micropatterning, Nano Lett. 12 (2012) 4960–4965, https://doi.org/10.1021/nl302560k.
[82] Y. Yang, H. Zhang, J. Chen, Q. Jing, Y.S. Zhou, X. Wen, Z.L. Wang, Single-Electrode-Based Sliding Triboelectric Nanogenerator for Self-Powered Displacement Vector Sensor System, ACS Nano 7 (2013) 7342–7351, https://doi.org/10.1021/nn403021m.
[83] Y. Yang, Y.S. Zhou, H. Zhang, Y. Liu, S. Lee, Z.L. Wang, A Single-Electrode Based Triboelectric Nanogenerator as Self-Powered Tracking System, Adv. Mater. 25 (2013) 6594–6601, https://doi.org/10.1002/adma.201302453.
[84] S. Wang, L. Lin, Y. Xie, Q. Jing, S. Niu, Z.L. Wang, Sliding-Triboelectric Nanogenerators Based on In-Plane Charge-Separation Mechanism, Nano Lett. 13 (2013) 2226–2233, https://doi.org/10.1021/nl400738p.
[85] G. Zhu, J. Chen, Y. Liu, P. Bai, Y.S. Zhou, Q. Jing, C. Pan, Z.L. Wang, Linear-Grating Triboelectric Generator Based on Sliding Electrification, Nano Lett. 13 (2013) 2282–2289, https://doi.org/10.1021/nl4008985.
[86] S. Wang, Y. Xie, S. Niu, L. Lin, Z.L. Wang, Freestanding Triboelectric-Layer-Based Nanogenerators for Harvesting Energy from a Moving Object or Human Motion in Contact and Non-contact Modes, Adv. Mater. 26 (2014) 2818–2824, https://doi.org/10.1002/adma.201305303.
[87] W. Yang, J. Chen, G. Zhu, J. Yang, P. Bai, Y. Su, Q. Jing, X. Cao, Z.L. Wang, Harvesting Energy from the Natural Vibration of Human Walking, ACS Nano 7 (2013) 11317–11324, https://doi.org/10.1021/nn405175z.
[88] G. Li, S. An, P. Wang, S. Xiong, J. Wang, S. Xu, H. Wu, K. Li, W. Li, L. Tong, C. Hu, Transverse-Asymmetric Electrode Structure Design to Eliminate Charge Transfer Loss for Enhancing Output Performance of Sliding Mode TENG, Adv. Funct. Mater. 35 (2025) 2413359, https://doi.org/10.1002/adfm.202413359.
[89] Y. Yang, H. Zhang, Z.-H. Lin, Y.S. Zhou, Q. Jing, Y. Su, J. Yang, J. Chen, C. Hu, Z. L. Wang, Human Skin Based Triboelectric Nanogenerators for Harvesting Biomechanical Energy and as Self-Powered Active Tactile Sensor System, ACS Nano 7 (2013) 9213–9222, https://doi.org/10.1021/nn403838y.
[90] X. Xiong, J. Liang, W. Wu, Principle and recent progress of triboelectric pressure sensors for wearable applications, Nano Energy 113 (2023) 108542, https://doi.org/10.1016/j.nanoen.2023.108542.
[91] K.B. Kim, H.J. Baek, Photoplethysmography in Wearable Devices: A Comprehensive Review of Technological Advances, Current Challenges, and Future Directions, Electronics 12 (2023) 2923, https://doi.org/10.3390/electronics12132923.
[92] D. Castaneda, A. Esparza, M. Ghamari, C. Soltanpur, H. Nazeran, A review on wearable photoplethysmography sensors and their potential future applications in health care, Int. J. Biosens. & Bioelectron. 4 (2018) 195.
[93] J. Kim, G.A. Salvatore, H. Araki, A.M. Chiarelli, Z. Xie, A. Banks, X. Sheng, Y. Liu, J.W. Lee, K.-I. Jang, S.Y. Heo, K. Cho, H. Luo, B. Zimmerman, J. Kim, L. Yan, X. Feng, S. Xu, M. Fabiani, G. Gratton, Y. Huang, U. Paik, J.A. Rogers, Battery-free, stretchable optoelectronic systems for wireless optical characterization of the skin, Sci. Adv. 2 (2016) e1600418, https://doi.org/10.1126/sciadv.1600418.
[94] O. Kwon, S. Moon, Y. Yun, Y. Nam, N. Kim, D. Kim, W. Choi, S. Park, J. Lee, Highly efficient thin-film 930 nm VCSEL on PDMS for biomedical applications, Sci. Rep. 13 (2023) 571, https://doi.org/10.1038/s41598-023-27589-1.
[95] M. Li, J. Lu, P. Wan, M. Jiang, Y. Mo, C. Pan, An Ultrasensitive Perovskite Single-Model Plasmonic Strain Sensor Based on Piezoelectric Effect, Adv. Funct. Mater. 34 (2024) 2403840, https://doi.org/10.1002/adfm.202403840.
[96] K. Zhou, B. Qi, Z. Liu, X. Wang, Y. Sun, L. Zhang, Advanced Organic–Inorganic Hybrid Materials for Optoelectronic Applications, Adv. Funct. Mater. 34 (2024) 2411671, https://doi.org/10.1002/adfm.202411671.
[97] X. Zhao, J. Wang, M. Liu, X. Ma, F. Zhang, Narrowband Organic Photodetectors: From Fundamentals to Prospects, Adv. Opt. Mater. 12 (2024) 2401087, https://doi.org/10.1002/adom.202401087.
[98] C. Li, Y. Bian, Z. Zhao, Y. Liu, Y. Guo, Advances in Biointegrated Wearable and Implantable Optoelectronic Devices for Cardiac Healthcare, Cyborg Bionic Syst. 5 (2024) 0172, https://doi.org/10.34133/cbsystems.0172.
[99] X. Zhang, J. Jiang, B. Feng, H. Song, L. Shen, Organic photodetectors: materials, device, and challenges, J. Mater. Chem. C. 11 (2023) 12453–12465, https://doi.org/10.1039/D3TC02028B.
[100] Y. Lee, J.W. Chung, G.H. Lee, H. Kang, J.-Y. Kim, C. Bae, H. Yoo, S. Jeong, H. Cho, S.-G. Kang, J.Y. Jung, D.-W. Lee, S. Gam, S.G. Hahm, Y. Kuzumoto, S.J. Kim, Z. Bao, Y. Hong, Y. Yun, S. Kim, Standalone real-time health monitoring patch based on a stretchable organic optoelectronic system, Sci. Adv. 7 (2021) eabg9180, https://doi.org/10.1126/sciadv.abg9180.
[101] B. Yin, X. Zhou, Y. Li, G. Hu, W. Wei, M. Yang, S. Jeong, W. Deng, B. Wu, Y. Cao, B. Huang, L. Pan, X. Yang, Z. Fu, Y. Fang, L. Shen, C. Yang, H. Wu, L. Lan, F. Huang, Y. Cao, C. Duan, Sensitive Organic Photodetectors With Spectral Response up to 1.3 μm Using a Quinoidal Molecular Semiconductor, Adv. Mater. 36 (2024) 2310811, https://doi.org/10.1002/adma.202310811.
[102] T.-H. Kim, C.-S. Lee, S. Kim, J. Hur, S. Lee, K.W. Shin, Y.-Z. Yoon, M.K. Choi, J. Yang, D.-H. Kim, T. Hyeon, S. Park, S. Hwang, Fully Stretchable Optoelectronic Sensors Based on Colloidal Quantum Dots for Sensing Photoplethysmographic Signals, ACS Nano 11 (2017) 5992–6003, https://doi.org/10.1021/acsnano.7b01894.
[103] H.S. Lee, B. Noh, S.U. Kong, Y.H. Hwang, H.-E. Cho, Y. Jeon, K.C. Choi, Fiber-based quantum-dot pulse oximetry for wearable health monitoring with high wavelength selectivity and photoplethysmogram sensitivity, Npj Flex. Electron. 7 (2023) 1–12, https://doi.org/10.1038/s41528-023-00248-1.
[104] A. De Iacovo, C. Venettacci, L. Colace, L. Scopa, S. Foglia, PbS Colloidal Quantum Dot Photodetectors operating in the near infrared, Sci. Rep. 6 (2016) 37913, https://doi.org/10.1038/srep37913.
[105] S. Li, J.H. Jang, W. Chung, H. Seung, S.I. Park, H. Ma, W.J. Pyo, C. Choi, D. S. Chung, D.-H. Kim, M.K. Choi, J. Yang, Ultrathin Self-Powered Heavy-Metal-Free Cu–In–Se Quantum Dot Photodetectors for Wearable Health Monitoring, ACS Nano 17 (2023) 20013–20023, https://doi.org/10.1021/acsnano.3c05178.
[106] L. Chen, Y. Wang, Y. Wen, L. Zhang, S. Liu, W. Xie, Organic photoplethysmography sensors for wearable health monitoring, Laser & Photonics Rev. 19 (2025) 2401992, https://doi.org/10.1002/lpor.202401992.
[107] J.-W. Park, J. Park, J. Jeon, S. Chae, G.B. Kim, G. Han, H.-S. Park, Y. Jeong, K.-H. Jeong, Wearable Hyperspectral Photoplethysmography Allows Continuous Monitoring of Exercise-Induced Hypertension, Adv. Sci. 12 (2025) 2417625, https://doi.org/10.1002/advs.202417625.
[108] P.H. Charlton, J. Allen, R. Bailón, S. Baker, J.A. Behar, F. Chen, G.D. Clifford, D. A. Clifton, H.J. Davies, C. Ding, X. Ding, J. Dunn, M. Elgendi, M. Ferdoushi, D. Franklin, E. Gil, M.F. Hassan, J. Hernesniemi, X. Hu, N. Ji, Y. Khan, S. Kontaxis, I. Korhonen, P.A. Kyriacou, P. Laguna, J. Lázaro, C. Lee, J. Levy, Y. Li, C. Liu, J. Liu, L. Lu, D.P. Mandic, V. Marozas, E. Mejía-Mejía, R. Mukkamala, M. Nitzan, T. Pereira, C.C.Y. Poon, J.C. Ramella-Roman, H. Saarinen, M.M.H. Shandhi, H. Shin, G. Stansby, T. Tamura, A. Vehkaoja, W.K. Wang, Y.-T. Zhang, N. Zhao, D. Zheng, T. Zhu, The 2023 wearable photoplethysmography roadmap, Physiol. Meas. 44 (2023) 111001, https://doi.org/10.1088/1361-6579/acead2.
[109] Z. Liu, C. Xiang, Y. Tong, K.H. Li, X. Guan, Transfer Learning Enhanced Blood Pressure Monitoring Based on Flexible Optical Pulse Sensing Patch, ACS Sens. 10 (2025) 2732–2742, https://doi.org/10.1021/acssensors.4c03404.
[110] H.C. Ates, P.Q. Nguyen, L. Gonzalez-Macia, E. Morales-Narváez, F. Güder, J. J. Collins, C. Dincer, End-to-end design of wearable sensors, Nat. Rev. Mater. 7 (2022) 887–907, https://doi.org/10.1038/s41578-022-00460-x.
[111] Y.-J. Wang, L. Wang, Blood pressure and heart rate measurements using fiber bragg grating sensor with optical power detection scheme, Sensors 25 (2025), https://doi.org/10.3390/s25072007.
[112] M.A. Awan, M. Ahmed, B. Wang, A laser doppler blood flow measurement system with a 151.4 dBΩ gain and 0.05% nonlinearity for PAD patients, IEEE Sens. J. 22 (2022) 14196–14204, https://doi.org/10.1109/JSEN.2022.3180927.
[113] R. Kuang, Z. Wang, L. Ma, H. Wang, Q. Chen, A.L. Junior, S. Kumar, X. Li, C. Marques, R. Min, Smart photonic wristband for pulse wave monitoring, 240009-1-, Opto-Electron. Sci. 3 (2024) 240009–240016, https://doi.org/10.29026/oes.2024.240009.
[114] H. Jin, Z. Zheng, Z. Cui, Y. Jiang, G. Chen, W. Li, Z. Wang, J. Wang, C. Yang, W. Song, X. Chen, Y. Zheng, A flexible optoacoustic blood 'stethoscope' for noninvasive multiparametric cardiovascular monitoring, Nat. Commun. 14 (2023) 4692, https://doi.org/10.1038/s41467-023-40181-5.
[115] R.B. Gowda, P. Sharan, S. K, M. Braim, A.N. Alodhayb, An FBG-based optical pressure sensor for the measurement of radial artery pulse pressure, J. Biophotonics 17 (2024) e202400083, https://doi.org/10.1002/jbio.202400083.
[116] A.N.D. Alhussein, M.R.T.M. Qaid, T. Agliullin, B. Valeev, O. Morozov, A. Sakhabutdinov, Fiber Bragg Grating Sensors: Design, Applications, and Comparison with Other Sensing Technologies, Sensors 25 (2025) 2289, https://doi.org/10.3390/s25072289.

[117] A. Konovalov, F. Grebenev, D. Stavtsev, I. Kozlov, V. Gadjiagaev, G. Piavchenko, D. Telyshev, A.Y. Gerasimenko, I. Meglinski, S. Zalogin, A. Artemyev, G. Golodnev, T. Shumeiko, S. Eliava, Real-time laser speckle contrast imaging for intraoperative neurovascular blood flow assessment: Animal experimental study, Sci. Rep. 14 (2024) 1735, https://doi.org/10.1038/s41598-023-51022-2.
[118] M. Ghijsen, T.B. Rice, B. Yang, S.M. White, B.J. Tromberg, Wearable speckle plethysmography (SPG) for characterizing microvascular flow and resistance, Biomed. Opt. Express 9 (2018) 3937–3952, https://doi.org/10.1364/BOE.9.003937.
[119] G.Y. Bae, S.W. Pak, D. Kim, G. Lee, D.H. Kim, Y. Chung, K. Cho, Linearly and Highly Pressure-Sensitive Electronic Skin Based on a Bioinspired Hierarchical Structural Array, Adv. Mater. 28 (2016) 5300–5306, https://doi.org/10.1002/adma.201600408.
[120] Z. Xu, D. Wu, Z. Chen, Z. Wang, C. Cao, X. Shao, G. Zhou, S. Zhang, L. Wang, D. Sun, A flexible pressure sensor with highly customizable sensitivity and linearity via positive design of microhierarchical structures with a hyperelastic model, Microsyst. Nanoeng. 9 (2023) 1–12, https://doi.org/10.1038/s41378-022-00477-w.
[121] T. An, Y. Zhang, J. Wen, Z. Dong, Q. Du, L. Liu, Y. Wang, G. Xing, X. Zhao, Multi-Level Pyramidal Microstructure-Based Pressure Sensors with High Sensitivity and Wide Linear Range for Healthcare Monitoring, ACS Sens. 9 (2024) 726–735, https://doi.org/10.1021/acssensors.3c02001.
[122] S. Wang, W. Deng, T. Yang, Y. Ao, H. Zhang, G. Tian, L. Deng, H. Huang, J. Huang, B. Lan, W. Yang, Bioinspired MXene-Based Piezoresistive Sensor with Two-stage Enhancement for Motion Capture, Adv. Funct. Mater. 33 (2023) 2214503, https://doi.org/10.1002/adfm.202214503.
[123] T. Yang, W. Deng, X. Chu, X. Wang, Y. Hu, X. Fan, J. Song, Y. Gao, B. Zhang, G. Tian, D. Xiong, S. Zhong, L. Tang, Y. Hu, W. Yang, Hierarchically Microstructure-Bioinspired Flexible Piezoresistive Bioelectronics, ACS Nano 15 (2021) 11555–11563, https://doi.org/10.1021/acsnano.1c01606.
[124] J. Wang, J. Shu, M.M. Alam, Z. Gao, Z. Li, R.K.-Y. Tong, Drift-Aware Feature Learning Based on Autoencoder Preprocessing for Soft Sensors, Adv. Intell. Syst. 6 (2024) 2300486, https://doi.org/10.1002/aisy.202300486.
[125] S. Baek, Y. Lee, J. Baek, J. Kwon, S. Kim, S. Lee, K.-P. Strunk, S. Stehlin, C. Melzer, S.-M. Park, H. Ko, S. Jung, Spatiotemporal Measurement of Arterial Pulse Waves Enabled by Wearable Active-Matrix Pressure Sensor Arrays, ACS Nano 16 (2022) 368–377, https://doi.org/10.1021/acsnano.1c06695.
[126] D. Geng, S. Chen, R. Chen, Y. You, C. Xiao, C. Bai, T. Luo, W. Zhou, Tunable Wide Range and High Sensitivity Flexible Pressure Sensors with Ordered Multilevel Microstructures, Adv. Mater. Technol. 7 (2022) 2101031, https://doi.org/10.1002/admt.202101031.
[127] H. Yao, W. Yang, W. Cheng, Y.J. Tan, H.H. See, S. Li, H.P.A. Ali, B.Z.H. Lim, Z. Liu, B.C.K. Tee, Near–hysteresis-free soft tactile electronic skins for wearables and reliable machine learning, Proc. Natl. Acad. Sci. 117 (2020) 25352–25359, https://doi.org/10.1073/pnas.2010989117.
[128] K. Kordas, O. Pitkänen, Frontiers | Piezoresistive Carbon Foams in Sensing Applications, Front. Mater. 6 (2019) 93, https://doi.org/10.3389/fmats.2019.00093.
[129] Y. Zhao, Q. Sun, S. Mei, L. Gao, X. Zhang, Z. Yang, X. Nan, H. Zhang, C. Xue, J. Li, Wearable multichannel-active pressurized pulse sensing platform, Microsyst. Nanoeng. 10 (2024) 1–10, https://doi.org/10.1038/s41378-024-00703-7.
[130] J. Wang, Y. Zhu, Z. Wu, Y. Zhang, J. Lin, T. Chen, H. Liu, F. Wang, L. Sun, Wearable multichannel pulse condition monitoring system based on flexible pressure sensor arrays, Microsyst. & Nanoeng. 8 (2022) 16, https://doi.org/10.1038/s41378-022-00349-3.
[131] X. Wang, G. Wu, X. Zhang, F. Lv, Z. Yang, X. Nan, Z. Zhang, C. Xue, H. Cheng, L. Gao, Traditional Chinese Medicine (TCM)-Inspired Fully Printed Soft Pressure Sensor Array with Self-Adaptive Pressurization for Highly Reliable Individualized Long-Term Pulse Diagnostics, Adv. Mater. 37 (2025) 2410312, https://doi.org/10.1002/adma.202410312.
[132] M. Wang, G. Wang, M. Zheng, L. Liu, C. Xu, Z. Liu, L. He, High-performance flexible piezoresistive pressure sensor based on multi-layer interlocking microstructures, J. Mater. Chem. A 12 (2024) 22931–22944, https://doi.org/10.1039/D4TA03758H.
[133] J. Chen, J. Zhang, J. Hu, N. Luo, F. Sun, H. Venkatesan, N. Zhao, Y. Zhang, Ultrafast-response/recovery flexible piezoresistive sensors with DNA-like double helix yarns for epidermal pulse monitoring, Adv. Mater. 34 (2022) 2104313, https://doi.org/10.1002/adma.202104313.
[134] W. Guo, Z. Ma, Z. Chen, H. Hua, D. Wang, M. Elhousseini Hilal, Y. Fu, P. Lu, J. Lu, Y. Zhang, D. Ho, B.L. Khoo, Thin and soft Ti3C2Tx MXene sponge structure for highly sensitive pressure sensor assisted by deep learning, Chem. Eng. J. 485 (2024) 149659, https://doi.org/10.1016/j.cej.2024.149659.
[135] C. Zhu, J. Wu, J. Yan, X. Liu, Advanced fiber materials for wearable electronics, Adv. Fiber Mater. 5 (2022) 12–35, https://doi.org/10.1007/s42765-022-00212-0.
[136] P. Zhao, Y. Song, P. Xie, F. Zhang, T. Xie, G. Liu, J. Zhao, S.-T. Han, Y. Zhou, All-organic smart textile sensor for deep-learning-assisted multimodal sensing, Adv. Funct. Mater. 33 (2023) 2301816, https://doi.org/10.1002/adfm.202301816.
[137] Y. Guo, H. Liu, D. Wang, Z.M. El-Bahy, J.T. Althakafy, H.M. Abo-Dief, Z. Guo, B. B. Xu, C. Liu, C. Shen, Engineering hierarchical heterostructure material based on metal-organic frameworks and cotton fiber for high-efficient microwave absorber, Nano Res. 15 (2022) 6841–6850, https://doi.org/10.1007/s12274-022-4533-x.
[138] W. Zeng, L. Shu, Q. Li, S. Chen, F. Wang, X.-M. Tao, Fiber-based wearable electronics: A review of materials, fabrication, devices, and applications, Adv. Mater. 26 (2014) 5310–5336, https://doi.org/10.1002/adma.201400633.
[139] Y. Wang, J. Hao, Z. Huang, G. Zheng, K. Dai, C. Liu, C. Shen, Flexible electrically resistive-type strain sensors based on reduced graphene oxide-decorated electrospun polymer fibrous mats for human motion monitoring, Carbon 126 (2018) 360–371, https://doi.org/10.1016/j.carbon.2017.10.034.
[140] S. Mousavi, D. Howard, F. Zhang, J. Leng, C.H. Wang, Direct 3D printing of highly anisotropic, flexible, constriction-resistive sensors for multidirectional proprioception in soft robots, ACS Appl. Mater. & Interfaces 12 (2020) 15631–15643, https://doi.org/10.1021/acsami.9b21816.
[141] M. Zeng, J. Ding, Y. Tian, Y. Zhang, X. Liu, Z. Chen, J. Sun, C. Wu, H. Yin, D. Wei, H. Fan, Phase separation manipulated gradient conductivity for a high-precision flexible pressure sensor, Adv. Funct. Mater. 34 (2024) 2411390, https://doi.org/10.1002/adfm.202411390.
[142] Z. Tan, Q. Hu, B. Yang, W. Liu, Z. Zhang, L. Shu, X. Qiu, Superelastic and highly sensitive biomass-derived piezoresistive aerogels for deep-learning-assisted sensing, Adv. Funct. Mater. 35 (2025) e11831, https://doi.org/10.1002/adfm.202511831.
[143] H. Jeong, Y. Noh, S.H. Ko, D. Lee, Flexible resistive pressure sensor with silver nanowire networks embedded in polymer using natural formation of air gap, Compos. Sci. Technol. 174 (2019) 50–57, https://doi.org/10.1016/j.compscitech.2019.01.028.
[144] R. Qin, M. Hu, X. Li, L. Yan, C. Wu, J. Liu, H. Gao, G. Shan, W. Huang, A highly sensitive piezoresistive sensor based on MXenes and polyvinyl butyral with a wide detection limit and low power consumption, Nanoscale 12 (2020) 17715–17724, https://doi.org/10.1039/D0NR02012E.
[145] Z. Huang, C. Ge, S. Li, M. Cai, Y. Hui, X. Liao, Q. Zeng, Biomimetic Pyrolytic MXene-Based Multifunctional Films with Multi-Level Structure for Wearable Piezoresistive Devices and Bioelectronics, Adv. Funct. Mater. 35 (2025) 2422374, https://doi.org/10.1002/adfm.202422374.
[146] F. Abedheydari, S. Sadeghzadeh, M. Saadatbakhsh, A. Heydariyan, E. Khakpour, Silver-decorated laser-induced graphene for a linear, sensitive, and almost hysteresis-free piezoresistive strain sensor, Sci. Rep. 14 (2024) 28715, https://doi.org/10.1038/s41598-024-80158-y.
[147] Y. Park, H. Luan, K. Kwon, T.S. Chung, S. Oh, J.-Y. Yoo, G. Chung, J. Kim, S. Kim, S.S. Kwak, J. Choi, H.-P. Phan, S. Yoo, H. Jeong, J. Shin, S.M. Won, H.-J. Yoon, Y. H. Jung, J.A. Rogers, Soft, full Wheatstone bridge 3D pressure sensors for cardiovascular monitoring, Npj Flex. Electron. 8 (2024) 1–8, https://doi.org/10.1038/s41528-024-00294-3.
[148] Y. Chang, L. Wang, R. Li, Z. Zhang, Q. Wang, J. Yang, C.F. Guo, T. Pan, First Decade of Interfacial Iontronic Sensing: From Droplet Sensors to Artificial Skins, Adv. Mater. 33 (2021) 2003464, https://doi.org/10.1002/adma.202003464.
[149] Z. Zhu, R. Li, T. Pan, Imperceptible Epidermal–Iontronic Interface for Wearable Sensing, Adv. Mater. 30 (2018) 1705122, https://doi.org/10.1002/adma.201705122.
[150] N. Bai, L. Wang, Y. Xue, Y. Wang, X. Hou, G. Li, Y. Zhang, M. Cai, L. Zhao, F. Guan, X. Wei, C.F. Guo, Graded Interlocks for Iontronic Pressure Sensors with High Sensitivity and High Linearity over a Broad Range, ACS Nano 16 (2022) 4338–4347, https://doi.org/10.1021/acsnano.1c10535.
[151] Z. Luo, J. Chen, Z. Zhu, L. Li, Y. Su, L. Wang, H. Li, Microstructural-PVDF Dielectric Layer Based High-Resolution Flexible Capacitive Pressure Sensor, in: 2021 IEEE 16th International Conference on Nano/Micro Engineered and Molecular Systems (NEMS), IEEE, 2021, pp. 647–651, https://doi.org/10.1109/NEMS51815.2021.9451477.
[152] Y. Zhang, X. Zhou, N. Zhang, J. Zhu, N. Bai, X. Hou, T. Sun, G. Li, L. Zhao, Y. Chen, L. Wang, C.F. Guo, Ultrafast piezocapacitive soft pressure sensors with over 10 kHz bandwidth via bonded microstructured interfaces, Nat. Commun. 15 (2024) 3048, https://doi.org/10.1038/s41467-024-47408-z.
[153] M. Jian, K. Xia, Q. Wang, Z. Yin, H. Wang, C. Wang, H. Xie, M. Zhang, Y. Zhang, Flexible and Highly Sensitive Pressure Sensors Based on Bionic Hierarchical Structures, Adv. Funct. Mater. 27 (2017) 1606066, https://doi.org/10.1002/adfm.201606066.
[154] J.C. Yang, J.-O. Kim, J. Oh, S.Y. Kwon, J.Y. Sim, D.W. Kim, H.B. Choi, S. Park, Microstructured Porous Pyramid-Based Ultrahigh Sensitive Pressure Sensor Insensitive to Strain and Temperature, ACS Appl. Mater. Interfaces 11 (2019) 19472–19480, https://doi.org/10.1021/acsami.9b03261.
[155] R. Qin, J. Nong, K. Wang, Y. Liu, S. Zhou, M. Hu, H. Zhao, G. Shan, Recent Advances in Flexible Pressure Sensors Based on MXene Materials, Adv. Mater. 36 (2024) 2312761, https://doi.org/10.1002/adma.202312761.
[156] Z. Zhan, R. Lin, V.-T. Tran, J. An, Y. Wei, H. Du, T. Tran, W. Lu, Paper/Carbon Nanotube-Based Wearable Pressure Sensor for Physiological Signal Acquisition and Soft Robotic Skin, ACS Appl. Mater. Interfaces 9 (2017) 37921–37928, https://doi.org/10.1021/acsami.7b10820.
[157] F. Basarir, Z. Madani, J. Vapaavuori, Recent Advances in Silver Nanowire Based Flexible Capacitive Pressure Sensors: From Structure, Fabrication to Emerging Applications, Adv. Mater. Interfaces 9 (2022) 2200866, https://doi.org/10.1002/admi.202200866.
[158] S. Chen, Y. Wang, L. Yang, F. Karouta, K. Sun, Electron-induced perpendicular graphene sheets embedded porous carbon film for flexible touch sensors, Nano-Micro Lett. 12 (2020) 136, https://doi.org/10.1007/s40820-020-00480-8.
[159] R. Qin, M. Hu, X. Li, T. Liang, H. Tan, J. Liu, G. Shan, A new strategy for the fabrication of a flexible and highly sensitive capacitive pressure sensor, Microsyst. & Nanoeng. 7 (2021) 100, https://doi.org/10.1038/s41378-021-00327-1.
[160] C.M. Schott, P.M. Schneider, K.-T. Song, H. Yu, R. Götz, F. Haimerl, E. Gubanova, J. Zhou, T.O. Schmidt, Q. Zhang, V. Alexandrov, A.S. Bandarenka, How to Assess and Predict Electrical Double Layer Properties. Implications for Electrocatalysis, Chem. Rev. 124 (2024) 12391–12462, https://doi.org/10.1021/acs.chemrev.3c00806.

[161] I. You, D.G. Mackanic, N. Matsuhisa, J. Kang, J. Kwon, L. Beker, J. Mun, W. Suh, T.Y. Kim, J.B.-H. Tok, Artificial multimodal receptors based on ion relaxation dynamics, Science 370 (2020) 961–965, https://doi.org/10.1126/science.aba5132.
[162] Y. Zheng, T. Lin, N. Zhao, C. Huang, W. Chen, G. Xue, Y. Wang, C. Teng, X. Wang, D. Zhou, Highly sensitive electronic skin with a linear response based on the strategy of controlling the contact area, Nano Energy 85 (2021) 106013, https://doi.org/10.1016/j.nanoen.2021.106013.
[163] H. Tian, Y. Jiang, Y. Song, T. Wang, J. Xue, F. Zhang, Y. Liu, Z. Xue, K. Wang, Y. Zhao, Hierarchical Synergetic Strategy for Iontronic Pressure Sensors with High Sensitivity and Broad Linearity Range, ACS Sens. 10 (2025) 2030–2037, https://doi.org/10.1021/acssensors.4c03238.
[164] X. Cui, J. Chen, W. Wu, Y. Liu, H. Li, Z. Xu, Y. Zhu, Flexible and breathable all-nanofiber iontronic pressure sensors with ultraviolet shielding and antibacterial performances for wearable electronics, Nano Energy 95 (2022) 107022, https://doi.org/10.1016/j.nanoen.2022.107022.
[165] J. Liu, Y. Yang, G. Chen, H. Sun, X. Xie, Y. Hou, L. Zhang, J. Wang, J. Wang, Stretchable and high-performance fibrous sensors based on ionic capacitive sensing for wearable healthcare monitoring, Adv. Sci. 12 (2025) 2412859, https://doi.org/10.1002/advs.202412859.
[166] B. Hong, Y. Xu, J. Tan, Z. Xie, S.Y. Zheng, Q. Wang, Z. Zhou, J. Yang, Skin-mimetic tough polyurethane ionogel for use in soft ionotronics, J. Mater. Chem. C. 11 (2023) 16168–16176, https://doi.org/10.1039/d3tc03661h.
[167] L. Gao, M. Wang, W. Wang, H. Xu, Y. Wang, H. Zhao, K. Cao, D. Xu, L. Li, Highly Sensitive Pseudocapacitive Iontronic Pressure Sensor with Broad Sensing Range, Nano-Micro Lett. 13 (2021) 1–14, https://doi.org/10.1007/s40820-021-00664-w.
[168] Y. Huang, S. Hu, Y. Li, R. Wang, Y. Yang, W. Zhu, Y. Deng, Programmable high-sensitivity iontronic pressure sensors support broad human-interactive perception and identification, Npj Flex. Electron. 9 (2025) 41, https://doi.org/10.1038/s41528-025-00420-9.
[169] Y. Xiao, Y. Duan, N. Li, L. Wu, B. Meng, F. Tan, Y. Lou, H. Wang, W. Zhang, Z. Peng, Multilayer Double-Sided Microstructured Flexible Iontronic Pressure Sensor with a Record-wide Linear Working Range, ACS Sens. 6 (2021) 1785–1795, https://doi.org/10.1021/acssensors.0c02547.
[170] R. Yang, A. Dutta, B. Li, N. Tiwari, W. Zhang, Z. Niu, Y. Gao, D. Erdely, X. Xin, T. Li, H. Cheng, Iontronic pressure sensor with high sensitivity over ultra-broad linear range enabled by laser-induced gradient micro-pyramids, Nat. Commun. 14 (2023) 2907, https://doi.org/10.1038/s41467-023-38274-2.
[171] S.H. Cho, S.W. Lee, S. Yu, H. Kim, S. Chang, D. Kang, I. Hwang, H.S. Kang, B. Jeong, E.H. Kim, S.M. Cho, K.L. Kim, H. Lee, W. Shim, C. Park, Micropatterned Pyramidal Ionic Gels for Sensing Broad-Range Pressures with High Sensitivity, ACS Appl. Mater. Interfaces 9 (2017) 10128–10135, https://doi.org/10.1021/acsami.7b00398.
[172] J. Hilário, B.M. Macucule, P. Wang, W. Yu, C. Meng, Flexible Iontronic Tactile Sensors Based on Silver Nanowire Electrode with Sandpaper-Roughened Surface and Ionic Liquid Gel Electrolyte with Porous Foam Structure for Wearable Sensing Applications, ACS Appl. Electron. Mater. 6 (2024) 4457–4466, https://doi.org/10.1021/acsaelm.4c00522.
[173] Z. Yang, Q. Duan, J. Zang, Y. Zhao, W. Zheng, R. Xiao, Z. Zhang, L. Hu, G. Wu, X. Nan, Z. Zhang, C. Xue, L. Gao, Boron nitride-enabled printing of a highly sensitive and flexible iontronic pressure sensing system for spatial mapping, Microsyst. Nanoeng. 9 (2023) 1–11, https://doi.org/10.1038/s41378-023-00543-x.
[174] J. You, M. Lu, L. Dazhen, M. Gao, R. Zhang, W. Li, F. Lei, W. Ren, G. Li, J. Yang, Anti-Motion Artifacts Iontronic Sensor for Long-Term Accurate Fingertip Pulse Monitoring, Adv. Sci. 12 (2025) 2414425, https://doi.org/10.1002/advs.202414425.
[175] M. Deng, C. Du, J. Fang, C. Xu, C. Guo, J. Huang, K. Li, L. Chen, Y.-T. Zhang, Y. Chang, T. Pan, Flexible adaptive sensing tonometry for medical-grade multi-parametric hemodynamic monitoring, Npj Flex. Electron. 8 (2024) 45, https://doi.org/10.1038/s41528-024-00329-9.
[176] C. Zhang, W. Ouyang, L. Zhang, D. Li, A dual-mode fiber-shaped flexible capacitive strain sensor fabricated by direct ink writing technology for wearable and implantable health monitoring applications, Microsyst. & Nanoeng. 9 (2023) 158, https://doi.org/10.1038/s41378-023-00634-9.
[177] F. Zhuo, Z. Ding, X. Yang, F. Chu, Y. Liu, Z. Gao, H. Jin, S. Dong, X. Wang, J. Luo, Advanced Morphological and Material Engineering for High-Performance Interfacial Iontronic Pressure Sensors, Adv. Sci. 12 (2025) 2413141, https://doi.org/10.1002/advs.202413141.
[178] G. Zhu, R. Yang, S. Wang, Z.L. Wang, Flexible High-Output Nanogenerator Based on Lateral ZnO Nanowire Array, Nano Lett. 10 (2010) 3151–3155, https://doi.org/10.1021/nl101973h.
[179] S. Jiang, X. Zhao, J. Zhang, B. Fang, H. Chen, L. Ma, Z. Ding, J. Wei, N. Hao, Metal-doped functional zinc oxide nanosheets as flexible piezoelectric generator for self-powered mechanical sensing, Sens. Actuators A Phys. 371 (2024) 115337, https://doi.org/10.1016/j.sna.2024.115337.
[180] J. Park, R. Ghosh, M.S. Song, Y. Hwang, Y. Tchoe, R.K. Saroj, A. Ali, P. Guha, B. Kim, S.-W. Kim, M. Kim, G.-C. Yi, Individually addressable and flexible pressure sensor matrixes with ZnO nanotube arrays on graphene, NPG Asia Mater. 14 (2022) 1–13, https://doi.org/10.1038/s41427-022-00386-4.
[181] S. Ma, Y. Kumaresan, A.S. Dahiya, L. Lorenzelli, R.S. Dahiya, Flexible Tactile Sensors Using AlN and MOSFETs Based Ultra-Thin Chips, IEEE Sens. J. 23 (2023) 23988–23994, https://doi.org/10.1109/JSEN.2022.3140651.
[182] X. Chen, K. Parida, J. Wang, J. Xiong, M.-F. Lin, J. Shao, P.S. Lee, A Stretchable and Transparent Nanocomposite Nanogenerator for Self-Powered Physiological Monitoring, ACS Appl. Mater. Interfaces 9 (2017) 42200–42209, https://doi.org/10.1021/acsami.7b13767.
[183] X. Shi, Y. Sun, H. Tian, D. Li, H. Liu, Functional gradient piezoelectric composite nanogenerator for self-powered touch sensor, Phys. Scr. 98 (2023) 125917, https://doi.org/10.1088/1402-4896/ad0695.
[184] M. Waga, T. Matsubara, M. Konyo, T. Takeshita, Y. Takei, T. Kobayashi, S. Tadokoro, Representing Fine Texture of Pencil Hardness by High-Frequency Vibrotactile Equivalence Conversion Using Ultra-Thin PZT-MEMS Vibrators, IEEE Trans. Haptics 17 (2024) 8–13, https://doi.org/10.1109/TOH.2023.3349307.
[185] Z. Meng, H. Zhang, M. Zhu, X. Wei, J. Cao, I. Murtaza, M.U. Ali, H. Meng, J. Xu, Lead Zirconate Titanate (a piezoelectric ceramic)-Based thermal and tactile bimodal organic transistor sensors, Org. Electron. 80 (2020) 105673, https://doi.org/10.1016/j.orgel.2020.105673.
[186] P. Zheng, W. Wei, Z. Liang, B. Qin, J. Tian, J. Wang, R. Qiao, Y. Ren, J. Chen, C. Huang, X. Zhou, G. Zhang, Z. Tang, D. Yu, F. Ding, K. Liu, X. Xu, Universal epitaxy of non-centrosymmetric two-dimensional single-crystal metal dichalcogenides, Nat. Commun. 14 (2023) 592, https://doi.org/10.1038/s41467-023-36286-6.
[187] M. Dai, W. Zheng, X. Zhang, S. Wang, J. Lin, K. Li, Y. Hu, E. Sun, J. Zhang, Y. Qiu, Y. Fu, W. Cao, P. Hu, Enhanced Piezoelectric Effect Derived from Grain Boundary in MoS2 Monolayers, Nano Lett. 20 (2020) 201–207, https://doi.org/10.1021/acs.nanolett.9b03642.
[188] W. Wu, L. Wang, Y. Li, F. Zhang, L. Lin, S. Niu, D. Chenet, X. Zhang, Y. Hao, T. F. Heinz, J. Hone, Z.L. Wang, Piezoelectricity of single-atomic-layer MoS2 for energy conversion and piezotronics, Nature 514 (2014) 470–474, https://doi.org/10.1038/nature13792.
[189] S.A. Han, T.-H. Kim, S.K. Kim, K.H. Lee, H.-J. Park, J.-H. Lee, S.-W. Kim, Point-Defect-Passivated MoS2 Nanosheet-Based High Performance Piezoelectric Nanogenerator, Adv. Mater. 30 (2018) 1800342, https://doi.org/10.1002/adma.201800342.
[190] D.Y. Park, D.J. Joe, D.H. Kim, H. Park, J.H. Han, C.K. Jeong, H. Park, J.G. Park, B. Joung, K.J. Lee, Self-Powered Real-Time Arterial Pulse Monitoring Using Ultrathin Epidermal Piezoelectric Sensors, Adv. Mater. 29 (2017) 1702308, https://doi.org/10.1002/adma.201702308.
[191] J. Li, H. Jia, J. Zhou, X. Huang, L. Xu, S. Jia, Z. Gao, K. Yao, D. Li, B. Zhang, Y. Liu, Y. Huang, Y. Hu, G. Zhao, Z. Xu, J. Li, C.K. Yiu, Y. Gao, M. Wu, Y. Jiao, Q. Zhang, X. Tai, R.H. Chan, Y. Zhang, X. Ma, X. Yu, Thin, soft, wearable system for continuous wireless monitoring of artery blood pressure, Nat. Commun. 14 (2023) 5009, https://doi.org/10.1038/s41467-023-40763-3.
[192] S. Gong, B. Zhang, J. Zhang, Z.L. Wang, K. Ren, Biocompatible Poly(lactic acid)-Based Hybrid Piezoelectric and Electret Nanogenerator for Electronic Skin Applications, Adv. Funct. Mater. 30 (2020) 1908724, https://doi.org/10.1002/adfm.201908724.
[193] S. Anwar, M. Hassanpour Amiri, S. Jiang, M.M. Abolhasani, P.R.F. Rocha, K. Asadi, Piezoelectric Nylon-11 Fibers for Electronic Textiles, Energy Harvesting and Sensing, Adv. Funct. Mater. 31 (2021) 2004326, https://doi.org/10.1002/adfm.202004326.
[194] P. Adhikary, A. Biswas, D. Mandal, Improved sensitivity of wearable nanogenerators made of electrospun Eu3+ doped P(VDF-HFP)/graphene composite nanofibers for self-powered voice recognition, Nanotechnology 27 (2016) 495501, https://doi.org/10.1088/0957-4484/27/49/495501.
[195] B. Sapkota, M.T. Hasan, A. Martin, R. Mahbub, J.E. Shield, V. Rangari, Fabrication and magnetoelectric investigation of flexible PVDF-TrFE/cobalt ferrite nanocomposite films, Mater. Res. Express 9 (2022) 046302, https://doi.org/10.1088/2053-1591/ac6151.
[196] L. Zhang, W. Du, J.-H. Kim, C.-C. Yu, C. Dagdeviren, An emerging era: Conformable ultrasound electronics, Adv. Mater. 36 (2024) 2307664, https://doi.org/10.1002/adma.202307664.
[197] X. Qian, D. Han, L. Zheng, J. Chen, M. Tyagi, Q. Li, F. Du, S. Zheng, X. Huang, S. Zhang, J. Shi, H. Huang, X. Shi, J. Chen, H. Qin, J. Bernholc, X. Chen, L.-Q. Chen, L. Hong, Q.M. Zhang, High-entropy polymer produces a giant electrocaloric effect at low fields, Nature 600 (2021) 664–669, https://doi.org/10.1038/s41586-021-04189-5.
[198] Y. Liu, H. Aziguli, B. Zhang, W. Xu, W. Lu, J. Bernholc, Q. Wang, Ferroelectric polymers exhibiting behaviour reminiscent of a morphotropic phase boundary, Nature 562 (2018) 96–100, https://doi.org/10.1038/s41586-018-0550-z.
[199] X. Lin, F. Yu, X. Zhang, W. Li, Y. Zhao, X. Fei, Q. Li, C. Yang, S. Huang, Wearable piezoelectric films based on MWCNT-BaTiO3/PVDF composites for energy harvesting, sensing, and localization, ACS Appl. Nano Mater. 6 (2023) 11955–11965, https://doi.org/10.1021/acsanm.3c01792.
[200] Y. Ao, L. Jin, S. Wang, B. Lan, G. Tian, T. Xu, L. Huang, Z. Wang, Y. Sun, T. Yang, W. Deng, F. Yang, W. Yang, Dual structure reinforces interfacial polarized MXene/PVDF-TrFE piezoelectric nanocomposite for pressure monitoring, Nano-Micro Lett. 17 (2025) 320, https://doi.org/10.1007/s40820-025-01839-5.
[201] K. Maity, S. Garain, K. Henkel, D. Schmeißer, D. Mandal, Self-Powered Human-Health Monitoring through Aligned PVDF Nanofibers Interfaced Skin-Interactive Piezoelectric Sensor, ACS Appl. Polym. Mater. 2 (2020) 862–878, https://doi.org/10.1021/acsapm.9b00846.
[202] W. Fan, C. Zhang, Y. Liu, S. Wang, K. Dong, Y. Li, F. Wu, J. Liang, C. Wang, Y. Zhang, An ultra-thin piezoelectric nanogenerator with breathable, superhydrophobic, and antibacterial properties for human motion monitoring, Nano Res. 16 (2023) 11612–11620, https://doi.org/10.1007/s12274-023-5413-8.
[203] R.S. Rai, G.J. P, V. Bajpai, M.I. Khan, N. Elboughdiri, A. Shanableh, R. Luque, An eco-friendly approach on green synthesis, bio-engineering applications, and

future outlook of ZnO nanomaterial: A critical review, Environ. Res. 221 (2023) 114807, https://doi.org/10.1016/j.envres.2022.114807.
[204] Y. Chu, J. Zhong, H. Liu, Y. Ma, N. Liu, Y. Song, J. Liang, Z. Shao, Y. Sun, Y. Dong, X. Wang, L. Lin, Human Pulse Diagnosis for Medical Assessments Using a Wearable Piezoelectret Sensing System, Adv. Funct. Mater. 28 (2018) 1803413, https://doi.org/10.1002/adfm.201803413.
[205] S. Ahn, Y. Cho, S. Park, J. Kim, J. Sun, D. Ahn, M. Lee, D. Kim, T. Kim, H. Shin, J.-J. Park, Wearable multimode sensors with amplified piezoelectricity due to the multi local strain using 3D textile structure for detecting human body signals, Nano Energy 74 (2020) 104932, https://doi.org/10.1016/j.nanoen.2020.104932.
[206] W. Fan, G. Zhang, X. Zhang, K. Dong, X. Liang, W. Chen, L. Yu, Y. Zhang, Superior Unidirectional Water Transport and Mechanically Stable 3D Orthogonal Woven Fabric for Human Body Moisture and Thermal Management, Small 18 (2022) 2107150, https://doi.org/10.1002/smll.202107150.
[207] W. Fan, R. Lei, H. Dou, Z. Wu, L. Lu, S. Wang, X. Liu, W. Chen, M. Rezakazemi, T. M. Aminabhavi, Y. Li, S. Ge, Sweat permeable and ultrahigh strength 3D PVDF piezoelectric nanoyarn fabric strain sensor, Nat. Commun. 15 (2024) 3509, https://doi.org/10.1038/s41467-024-47810-7.
[208] K.-Y. Chun, S. Seo, C.-S. Han, Self-Powered, Stretchable, and Wearable Ion Gel Mechanoreceptor Sensors, ACS Sens. 6 (2021) 1940–1948, https://doi.org/10.1021/acssensors.1c00346.
[209] Y. Shi, Y. Guan, M. Liu, X. Kang, Y. Tian, W. Deng, P. Yu, C. Ning, L. Zhou, R. Fu, G. Tan, Tough, Antifreezing, and Piezoelectric Organohydrogel as a Flexible Wearable Sensor for Human–Machine Interaction, ACS Nano 18 (2024) 3720–3732, https://doi.org/10.1021/acsnano.3c11578.
[210] S. Zhou, G. Park, K. Longardner, M. Lin, B. Qi, X. Yang, X. Gao, H. Huang, X. Chen, Y. Bian, H. Hu, R.S. Wu, W. Yue, M. Li, C. Lu, R. Wang, S. Qin, E. Tasali, T. Karrison, I. Thomas, B. Smarr, E.B. Kistler, B.A. Khiami, I. Litvan, S. Xu, Clinical validation of a wearable ultrasound sensor of blood pressure, Nat. Biomed. Eng. (2024) 1–17, https://doi.org/10.1038/s41551-024-01279-3.
[211] R. Fu, L. Tu, Y. Zhou, L. Fan, F. Zhang, Z. Wang, J. Xing, D. Chen, C. Deng, G. Tan, P. Yu, L. Zhou, C. Ning, A Tough and Self-Powered Hydrogel for Artificial Skin, Chem. Mater. 31 (2019) 9850–9860, https://doi.org/10.1021/acs.chemmater.9b04041.
[212] Z. Hu, J. Li, X. Wei, C. Wang, Y. Cao, Z. Gao, J. Han, Y. Li, Enhancing Strain-Sensing Properties of the Conductive Hydrogel by Introducing PVDF-TrFE, ACS Appl. Mater. Interfaces 14 (2022) 45853–45868, https://doi.org/10.1021/acsami.2c13074.
[213] C. Wang, X. Li, H. Hu, L. Zhang, Z. Huang, M. Lin, Z. Zhang, Z. Yin, B. Huang, H. Gong, S. Bhaskaran, Y. Gu, M. Makihata, Y. Guo, Y. Lei, Y. Chen, C. Wang, Y. Li, T. Zhang, Z. Chen, A.P. Pisano, L. Zhang, Q. Zhou, S. Xu, Monitoring of the central blood pressure waveform via a conformal ultrasonic device, Nat. Biomed. Eng. 2 (2018) 687–695, https://doi.org/10.1038/s41551-018-0287-x.
[214] M. Lin, Z. Zhang, X. Gao, Y. Bian, R.S. Wu, G. Park, Z. Lou, Z. Zhang, X. Xu, X. Chen, A. Kang, X. Yang, W. Yue, L. Yin, C. Wang, B. Qi, S. Zhou, H. Hu, H. Huang, M. Li, Y. Gu, J. Mu, A. Yang, A. Yaghi, Y. Chen, Y. Lei, C. Lu, R. Wang, J. Wang, S. Xiang, E.B. Kistler, N. Vasconcelos, S. Xu, A fully integrated wearable ultrasound system to monitor deep tissues in moving subjects, Nat. Biotechnol. 42 (2024) 448–457, https://doi.org/10.1038/s41587-023-01800-0.
[215] C. Wang, B. Qi, M. Lin, Z. Zhang, M. Makihata, B. Liu, S. Zhou, Y. Huang, H. Hu, Y. Gu, Y. Chen, Y. Lei, T. Lee, S. Chien, K.-I. Jang, E.B. Kistler, S. Xu, Continuous monitoring of deep-tissue haemodynamics with stretchable ultrasonic phased arrays, Nat. Biomed. Eng. 5 (2021) 749–758, https://doi.org/10.1038/s41551-021-00763-4.
[216] P.L.M.J. van Neer, L.C.J.M. Peters, R.G.F.A. Verbeek, B. Peeters, G. de Haas, L. Hörchens, L. Fillinger, T. Schrama, E.J.W. Merks-Swolfs, K. Gijsbertse, A.E.C. M. Saris, M. Mozaffarzadeh, J.M. Menssen, C.L. de Korte, J.-L.P.J. van der Steen, A.W.F. Volker, G.H. Gelinck, Flexible large-area ultrasound arrays for medical applications made using embossed polymer structures, Nat. Commun. 15 (2024) 2802, https://doi.org/10.1038/s41467-024-47074-1.
[217] J. Liu, J. Wang, Y. Wang, Z. Wu, H. Sun, Y. Yang, L. Zhang, X. Kou, P. Li, W. Kang, J. Wang, A High-Performance Stretchable Triboelectric Nanogenerator Based on Polytetrafluoroethylene (PTFE) Particles, ENERGY & Environ. Mater. 8 (2025) e12814, https://doi.org/10.1002/eem2.12814.
[218] G. Zhao, Y. Zhang, N. Shi, Z. Liu, X. Zhang, M. Wu, C. Pan, H. Liu, L. Li, Z.L. Wang, Transparent and stretchable triboelectric nanogenerator for self-powered tactile sensing, Nano Energy 59 (2019) 302–310, https://doi.org/10.1016/j.nanoen.2019.02.054.
[219] A new protocol toward high output TENG with polyimide as charge storage layer, Nano Energy 38 (2017) 467–476, https://doi.org/10.1016/j.nanoen.2017.06.017.
[220] Y.-S. Chiu, M. Rinawati, Y.-H. Chang, S. Aulia, C.-C. Chang, L.-Y. Chang, W.-S. Hung, H. Mizuguchi, S.-C. Haw, M.-H. Yeh, Enhancing self-induced polarization of PVDF-based triboelectric film by P-doped g-C3N4 for ultrasensitive triboelectric pressure sensors, Nano Energy 131 (2024) 110207, https://doi.org/10.1016/j.nanoen.2024.110207.
[221] X. Jia, X. Wu, L. Qi, X. Dai, J. Wang, T. Jiang, Z. Hong, CaTiO3/ZnO-PVDF composite-based triboelectric nanogenerators for self-powered gait sensing, Adv. Funct. Mater. 35 (2025) e07124, https://doi.org/10.1002/adfm.202507124.
[222] K. Meng, S. Zhao, Y. Zhou, Y. Wu, S. Zhang, Q. He, X. Wang, Z. Zhou, W. Fan, X. Tan, J. Yang, J. Chen, A Wireless Textile-Based Sensor System for Self-Powered Personalized Health Care, Matter 2 (2020) 896–907, https://doi.org/10.1016/j.matt.2019.12.025.
[223] A.F. Diaz, R.M. Felix-Navarro, A semi-quantitative tribo-electric series for polymeric materials: the influence of chemical structure and properties, J. Electrost. 62 (2004) 277–290, https://doi.org/10.1016/j.elstat.2004.05.005.
[224] C. Yao, T. Sun, S. Huang, M. He, B. Liang, Z. Shen, X. Huang, Z. Liu, H. Wang, F. Liu, H.-J. Chen, X. Xie, Personalized Machine Learning-Coupled Nanopillar Triboelectric Pulse Sensor for Cuffless Blood Pressure Continuous Monitoring, ACS Nano 17 (2023) 24242–24258, https://doi.org/10.1021/acsnano.3c09766.
[225] W. Seung, M.K. Gupta, K.Y. Lee, K.-S. Shin, J.-H. Lee, T.Y. Kim, S. Kim, J. Lin, J. H. Kim, S.-W. Kim, Nanopatterned Textile-Based Wearable Triboelectric Nanogenerator, ACS Nano 9 (2015) 3501–3509, https://doi.org/10.1021/nn507221f.
[226] X. Wang, J. Yang, K. Meng, Q. He, G. Zhang, Z. Zhou, X. Tan, Z. Feng, C. Sun, J. Yang, Z.L. Wang, Enabling the Unconstrained Epidermal Pulse Wave Monitoring via Finger-Touching, Adv. Funct. Mater. 31 (2021) 2102378, https://doi.org/10.1002/adfm.202102378.
[227] Y. Wang, Y. Gao, D. Tan, F. Nip, H. Fu, B. Xu, Stretchable 3D kirigami-structured textiles for high-performance wearable energy harvesting and self-powered sensing, Nano Energy 142 (2025) 111196, https://doi.org/10.1016/j.nanoen.2025.111196.
[228] Y. Jiao, Z. Lin, X. Ma, L. Zhou, X. Guo, Z. Hu, X. Hu, X. Zhao, L. Ding, Y. Hao, J. Chang, High-performance triboelectric nanogenerators based on blade-coating lead halide perovskite film and electrospinning PVDF/graphene nanofiber, Chem. Eng. J. 483 (2024) 149442, https://doi.org/10.1016/j.cej.2024.149442.
[229] W. Ou-Yang, L. Liu, M. Xie, S. Zhou, X. Hu, H. Wu, Z. Tian, X. Chen, Y. Zhu, J. Li, Recent advances in triboelectric nanogenerator-based self-powered sensors for monitoring human body signals, Nano Energy 120 (2024) 109151, https://doi.org/10.1016/j.nanoen.2023.109151.
[230] Y. Zhang, X. Dai, Y. Zhou, J. Shao, L. Zhao, T. Wang, F. Liu, X. Yan, M. Yang, P. Sun, G. Lu, Ultra-thin and sensitive pressure sensor based on MXene/PVDF-HFP composite fiber TENG for self-diagnosis of ligament injuries, Nano Energy 132 (2024) 110372, https://doi.org/10.1016/j.nanoen.2024.110372.
[231] K. Meng, X. Xiao, Z. Liu, S. Shen, T. Tat, Z. Wang, C. Lu, W. Ding, X. He, J. Yang, J. Chen, Kirigami-Inspired Pressure Sensors for Wearable Dynamic Cardiovascular Monitoring, Adv. Mater. 34 (2022) 2202478, https://doi.org/10.1002/adma.202202478.
[232] L. Xie, H. Lei, Y. Liu, B. Lu, X. Qin, C. Zhu, H. Ji, Z. Gao, Y. Wang, Y. Lv, C. Zhao, I. Z. Mitrovic, X. Sun, Z. Wen, Ultrasensitive Wearable Pressure Sensors with Stress-Concentrated Tip-Array Design for Long-Term Bimodal Identification, Adv. Mater. 36 (2024) 2406235, https://doi.org/10.1002/adma.202406235.
[233] F.G. Torres, O.P. Troncoso, G.E. De-la-Torre, Hydrogel-based triboelectric nanogenerators: Properties, performance, and applications, Int. J. Energy Res. 46 (2022) 5603–5624, https://doi.org/10.1002/er.7585.
[234] Z. Cai, X. Xiao, Y. Wei, J. Yin, Stretchable Polymer Hydrogels Based Flexible Triboelectric Nanogenerators for Self-Powered Bioelectronics, Biomacromolecules 26 (2025) 787–813, https://doi.org/10.1021/acs.biomac.4c01709.
[235] H. Zhang, D. Zhang, Z. Wang, G. Xi, R. Mao, Y. Ma, D. Wang, M. Tang, Z. Xu, H. Luan, Ultrastretchable, Self-Healing Conductive Hydrogel-Based Triboelectric Nanogenerators for Human–Computer Interaction, ACS Appl. Mater. Interfaces 15 (2023) 5128–5138, https://doi.org/10.1021/acsami.2c17904.
[236] W. Xu, L.-B. Huang, M.-C. Wong, L. Chen, G. Bai, J. Hao, Environmentally Friendly Hydrogel-Based Triboelectric Nanogenerators for Versatile Energy Harvesting and Self-Powered Sensors, Adv. Energy Mater. 7 (2017) 1601529, https://doi.org/10.1002/aenm.201601529.
[237] H. Sun, Y. Zhao, S. Jiao, C. Wang, Y. Jia, K. Dai, G. Zheng, C. Liu, P. Wan, C. Shen, Environment Tolerant Conductive Nanocomposite Organohydrogels as Flexible Strain Sensors and Power Sources for Sustainable Electronics, Adv. Funct. Mater. 31 (2021) 2101696, https://doi.org/10.1002/adfm.202101696.
[238] H.-Y. Mi, X. Jing, Q. Zheng, L. Fang, H.-X. Huang, L.-S. Turng, S. Gong, High-performance flexible triboelectric nanogenerator based on porous aerogels and electrospun nanofibers for energy harvesting and sensitive self-powered sensing, Nano Energy 48 (2018) 327–336, https://doi.org/10.1016/j.nanoen.2018.03.050.
[239] H. Lv, Z. Wang, Z. Gao, H. Song, Highly stretchable, self-healable, and environment-adaptable ionogel-based high-output triboelectric nanogenerator for self-powered wearable ionotronics, Chem. Eng. J. 509 (2025) 161247, https://doi.org/10.1016/j.cej.2025.161247.
[240] T. Liu, M. Liu, S. Dou, J. Sun, Z. Cong, C. Jiang, C. Du, X. Pu, W. Hu, Z.L. Wang, Triboelectric-Nanogenerator-Based Soft Energy-Harvesting Skin Enabled by Toughly Bonded Elastomer/Hydrogel Hybrids, ACS Nano 12 (2018) 2818–2826, https://doi.org/10.1021/acsnano.8b00108.
[241] Y. Fang, Y. Zou, J. Xu, G. Chen, Y. Zhou, W. Deng, X. Zhao, M. Roustaei, T. K. Hsiai, J. Chen, Ambulatory Cardiovascular Monitoring Via a Machine-Learning-Assisted Textile Triboelectric Sensor, Adv. Mater. 33 (2021) 2104178, https://doi.org/10.1002/adma.202104178.
[242] X. Ran, F. Luo, Z. Lin, Z. Zhu, C. Liu, B. Chen, Blood pressure monitoring via double sandwich-structured triboelectric sensors and deep learning models, Nano Res. 15 (2022) 5500–5509, https://doi.org/10.1007/s12274-022-4172-2.
[243] R. Chen, T. Luo, J. Wang, R. Wang, C. Zhang, Y. Xie, L. Qin, H. Yao, W. Zhou, Nonlinearity synergy: An elegant strategy for realizing high-sensitivity and wide-linear-range pressure sensing, Nat. Commun. 14 (2023) 6641, https://doi.org/10.1038/s41467-023-42361-9.
[244] K.-H. Ha, Z. Li, S. Kim, H. Huh, Z. Wang, H. Shi, C. Block, S. Bhattacharya, N. Lu, Stretchable hybrid response pressure sensors, Matter 7 (2024) 1895–1908, https://doi.org/10.1016/j.matt.2024.04.009.

[245] S. Qin, P. Yang, Z. Liu, J. Hu, N. Li, L. Ding, X. Chen, Triboelectric sensor with ultra-wide linear range based on water-containing elastomer and ion-rich interface, Nat. Commun. 15 (2024) 10640, https://doi.org/10.1038/s41467-024-54980-x.
[246] K. Meng, X. Xiao, W. Wei, G. Chen, A. Nashalian, S. Shen, X. Xiao, J. Chen, Wearable pressure sensors for pulse wave monitoring, Adv. Mater. 34 (2022) 2109357, https://doi.org/10.1002/adma.202109357.
[247] K.-H. Ha, W. Zhang, H. Jang, S. Kang, L. Wang, P. Tan, H. Hwang, N. Lu, Highly Sensitive Capacitive Pressure Sensors over a Wide Pressure Range Enabled by the Hybrid Responses of a Highly Porous Nanocomposite, Adv. Mater. 33 (2021) 2103320, https://doi.org/10.1002/adma.202103320.
[248] Z. Shen, C. Yang, C. Yao, Z. Liu, X. Huang, Z. Liu, J. Mo, H. Xu, G. He, J. Tao, X. Xie, T. Hang, H.-J. Chen, F. Liu, Capacitive–piezoresistive hybrid flexible pressure sensor based on conductive micropillar arrays with high sensitivity over a wide dynamic range, Mater. Horiz. 10 (2023) 499–511, https://doi.org/10.1039/D2MH00892K.
[249] S. Bin Choi, S. Veeralingam, T.D. Khanh, J.S. Choi, K.R. Kishore, S.-B. Jung, J.-W. Kim, Rapid-response hybrid piezo-triboelectric pressure sensor using all-fabric materials for enhanced sensing and power generation, Nano Energy 140 (2025) 111000, https://doi.org/10.1016/j.nanoen.2025.111000.
[250] J.-G. Sun, T.-N. Yang, C.-Y. Wang, L.-J. Chen, A flexible transparent one-structure tribo-piezo-pyroelectric hybrid energy generator based on bio-inspired silver nanowires network for biomechanical energy harvesting and physiological monitoring, Nano Energy 48 (2018) 383–390, https://doi.org/10.1016/j.nanoen.2018.03.071.
[251] J. Wang, J. Xue, Y. Zou, Y. Ma, J. Xu, Y. Li, F. Deng, Y. Wang, K. Xing, Z. Li, T. Zou, A Dual-Modal Wearable Pulse Detection System Integrated with Deep Learning for High-Accuracy and Low-Power Sleep Apnea Monitoring, Adv. Sci. 12 (2025) 2501750, https://doi.org/10.1002/advs.202501750.
[252] S.Z. Hussain, V.P. Singh, M.S.B. Sadeque, S. Yavari, G. Kalimuldina, M. Ordu, Piezoelectric-Triboelectric Hybrid Nanogenerator for Energy Harvesting and Self-Powered Sensing Applications, Small 21 (2025) 2504626, https://doi.org/10.1002/smll.202504626.
[253] P. Samartkit, S. Pullteap, O. Bernal, A non-invasive heart rate and blood pressure monitoring system using piezoelectric and photoplethysmographic sensors, Measurement 196 (2022) 111211, https://doi.org/10.1016/j.measurement.2022.111211.
[254] Z.-J. Liu, T. Xiang, R.-S. Zhou, N. Ji, Y.-T. Zhang, A multi-channel photoplethysmography array with contact-force regulation for tonoarteriographic imaging, OAE Publ. Inc. 3 (2024), https://doi.org/10.20517/chatmed.2023.11.
[255] A. Chandrasekhar, M. Yavarimanesh, K. Natarajan, J.-O. Hahn, R. Mukkamala, PPG sensor contact pressure should be taken into account for cuff-less blood pressure measurement, IEEE Trans. Biomed. Eng. 67 (2020) 3134–3140, https://doi.org/10.1109/TBME.2020.2976989.
[256] M.Y. Ho, H.M. Pham, A. Saeed, D. Ma, WF-PPG: A wrist-finger dual-channel dataset for studying the impact of contact pressure on PPG morphology, Sci. Data 12 (2025) 200, https://doi.org/10.1038/s41597-025-04453-7.
[257] Z. Xu, X. Pan, H. Lu, Q. Lu, Y. Liang, Z. He, Y. Zhu, Y. Yu, W. Wu, X. Han, C. Pan, Surface Energy-Assisted Patterning of Vapor Deposited All-Inorganic Perovskite Arrays for Wearable Optoelectronics, Adv. Sci. 11 (2024) 2402635, https://doi.org/10.1002/advs.202402635.
[258] Z. Du, H.M. Luong, S. Sabury, A.L. Jones, Z. Zhu, P. Panoy, S. Chae, A. Yi, H. J. Kim, S. Xiao, V.V. Brus, G.N. Manjunatha Reddy, J.R. Reynolds, T.-Q. Nguyen, High-Performance Wearable Organic Photodetectors by Molecular Design and Green Solvent Processing for Pulse Oximetry and Photoplethysmography, Adv. Mater. 36 (2024) 2310478, https://doi.org/10.1002/adma.202310478.
[259] B.H. Kang, K. Park, M. Hambsch, S. Hong, H.T. Kim, D.H. Choi, J.H. Lee, S. Kim, H.J. Kim, Skin-conformable photoplethysmogram sensors for energy-efficient always-on cardiovascular monitoring systems, Nano Energy 92 (2022) 106773, https://doi.org/10.1016/j.nanoen.2021.106773.
[260] X. Tang, H. Jiang, Z. Lin, X. Wang, W. Wang, G. Li, Wafer-Scale Vertical 1D GaN Nanorods/2D MoS2/PEDOT:PSS for Piezophototronic Effect-Enhanced Self-Powered Flexible Photodetectors, Nano-Micro Lett. 17 (2024) 56, https://doi.org/10.1007/s40820-024-01553-8.
[261] X. Chen, C. Wang, W. Wei, Y. Liu, S.S. Ge, L. Zhou, H. Kong, Flexible and sensitive pressure sensor with enhanced breathability for advanced wearable health monitoring, Npj Flex. Electron. 9 (2025) 101, https://doi.org/10.1038/s41528-025-00469-6.
[262] Y. Guo, M. Zhong, Z. Fang, P. Wan, G. Yu, A Wearable Transient Pressure Sensor Made with MXene Nanosheets for Sensitive Broad-Range Human–Machine Interfacing, Nano Lett. 19 (2019) 1143–1150, https://doi.org/10.1021/acs.nanolett.8b04514.
[263] Q. Xiang, G. Zhao, T. Tang, H. Zhang, Z. Liu, X. Zhang, Y. Zhao, H. Tan, All-Carbon Piezoresistive Sensor: Enhanced Sensitivity and Wide Linear Range via Multiscale Design for Wearable Applications, Adv. Funct. Mater. 35 (2025) 2418706, https://doi.org/10.1002/adfm.202418706.
[264] J. He, P. Xiao, W. Lu, J. Shi, L. Zhang, Y. Liang, C. Pan, S.-W. Kuo, T. Chen, A Universal high accuracy wearable pulse monitoring system via high sensitivity and large linearity graphene pressure sensor, Nano Energy 59 (2019) 422–433, https://doi.org/10.1016/j.nanoen.2019.02.036.
[265] S. Wang, C. Wang, Y. Zhao, Y. Zhang, Y. Zhang, X. Xu, Q. Lin, K. Yao, Y. Wang, F. Han, Y. Sun, Z. Jiang, Flexible pressure sensors with ultrahigh stress tolerance enabled by periodic microslits, Microsyst. Nanoeng. 10 (2024) 24, https://doi.org/10.1038/s41378-023-00639-4.
[266] C. Zhang, Y. Zhou, C. Ye, Silver nanowires/waterborne polyurethane composite film based piezoresistive pressure sensor for ultrasensitive human motion monitoring, Nanotechnology 35 (2024) 325502, https://doi.org/10.1088/1361-6528/ad4158.
[267] Y. Zhang, J. Yang, X. Hou, G. Li, L. Wang, N. Bai, M. Cai, L. Zhao, Y. Wang, J. Zhang, K. Chen, X. Wu, C. Yang, Y. Dai, Z. Zhang, C.F. Guo, Highly stable flexible pressure sensors with a quasi-homogeneous composition and interlinked interfaces, Nat. Commun. 13 (2022) 1317, https://doi.org/10.1038/s41467-022-29093-y.
[268] Z. Ding, W. Li, W. Wang, Z. Zhao, Y. Zhu, B. Hou, L. Zhu, M. Chen, L. Che, Highly Sensitive Iontronic Pressure Sensor with Side-by-Side Package Based on Alveoli and Arch Structure, Adv. Sci. 11 (2024) 2309407, https://doi.org/10.1002/advs.202309407.
[269] S. Min, D.H. Kim, D.J. Joe, B.W. Kim, Y.H. Jung, J.H. Lee, B.-Y. Lee, I. Doh, J. An, Y.-N. Youn, B. Joung, C.D. Yoo, H.-S. Ahn, K.J. Lee, Clinical Validation of a Wearable Piezoelectric Blood-Pressure Sensor for Continuous Health Monitoring, Adv. Mater. 35 (2023) 2301627, https://doi.org/10.1002/adma.202301627.
[270] X. Wang, Z. Feng, Y. Xia, G. Zhang, L. Wang, L. Chen, Y. Wu, J. Yang, Z.L. Wang, Flexible pressure sensor for high-precision measurement of epidermal arterial pulse, Nano Energy 102 (2022) 107710, https://doi.org/10.1016/j.nanoen.2022.107710.
[271] J. Seong, B.-U. Bak, D. Lee, J. Jin, J. Kim, Tribo-piezoelectric synergistic BaTiO3/PDMS micropyramid, Nano Energy 122 (2024) 109264, https://doi.org/10.1016/j.nanoen.2024.109264.
[272] J.L. Lapum, M. Verkuyl, W. Garcia, O. St-Amant, A. Tan. What is Pulse?, Ryerson University, Toronto, 2018. https://pressbooks.library.torontomu.ca/vitalsign/chapter/what-is-pulse/.
[273] C.W. Tsao, A.W. Aday, Z.I. Almarzooq, A. Alonso, A.Z. Beaton, M.S. Bittencourt, A.K. Boehme, A.E. Buxton, A.P. Carson, Y. Commodore-Mensah, M.S.V. Elkind, K. R. Evenson, C. Eze-Nliam, J.F. Ferguson, G. Generoso, J.E. Ho, R. Kalani, S. S. Khan, B.M. Kissela, K.L. Knutson, D.A. Levine, T.T. Lewis, J. Liu, M.S. Loop, J. Ma, M.E. Mussolino, S.D. Navaneethan, A.M. Perak, R. Poudel, M. Rezk-Hanna, G.A. Roth, E.B. Schroeder, S.H. Shah, E.L. Thacker, L.B. VanWagner, S.S. Virani, J. H. Voecks, N.-Y. Wang, K. Yaffe, S.S. Martin, on behalf of the American Heart Association Council on Epidemiology and Prevention Statistics Committee and Stroke Statistics Subcommittee, Heart Disease and Stroke Statistics—2022 Update: A Report From the American Heart Association, Circulation 145 (2022) e153–e639, https://doi.org/10.1161/CIR.0000000000001052.
[274] P.J. Podrid, F.J. Venditti, P.A. Levine, M.D. Klein, The role of exercise testing in evaluation of arrhythmias, Am. J. Cardiol. 62 (1988) H24–H33, https://doi.org/10.1016/0002-9149(88)90337-2.
[275] V.D.A. Corino, R. Laureanti, L. Ferranti, G. Scarpini, F. Lombardi, L.T. Mainardi, Detection of atrial fibrillation episodes using a wristband device, Physiol. Meas. 38 (2017) 787, https://doi.org/10.1088/1361-6579/aa5dd7.
[276] H. Ouyang, J. Tian, G. Sun, Y. Zou, Z. Liu, H. Li, L. Zhao, B. Shi, Y. Fan, Y. Fan, Z. L. Wang, Z. Li, Self-Powered Pulse Sensor for Antidiastole of Cardiovascular Disease, Adv. Mater. 29 (2017), https://doi.org/10.1002/adma.201703456.
[277] J. Wasserlauf, C. You, R. Patel, A. Valys, D. Albert, R. Passman, Smartwatch Performance for the Detection and Quantification of Atrial Fibrillation, Circulation Arrhythmia Electrophysiology 12 (2019) e006834, https://doi.org/10.1161/CIRCEP.118.006834.
[278] S.A. Lubitz, A.Z. Faranesh, C. Selvaggi, S.J. Atlas, D.D. McManus, D.E. Singer, S. Pagoto, M.V. McConnell, A. Pantelopoulos, A.S. Foulkes, Detection of Atrial Fibrillation in a Large Population Using Wearable Devices: The Fitbit Heart Study, Circulation 146 (2022) 1415–1424, https://doi.org/10.1161/CIRCULATIONAHA.122.060291.
[279] S. Qiu, Y. Li, C. Dai, S. Wu, X. Chen, N. Ji, G. Fang, Y. Yam, C.C.L. Wang, N. Zhao, A textile-based alignment-free electrophysiological sensing sleeve for comprehensive cardiovascular monitoring, Microsyst. & Nanoeng. 11 (2025) 228, https://doi.org/10.1038/s41378-025-01088-x.
[280] Z. Ma, H. Hua, C. You, Z. Ma, W. Guo, X. Yang, S. Qiu, N. Zhao, Y. Zhang, D. Ho, B.P. Yan, B.L. Khoo, FlexiPulse: A machine-learning-enabled flexible pulse sensor for cardiovascular disease diagnostics, Cell. Rep. Phys. Sci. 4 (2023) 101690, https://doi.org/10.1016/j.xcrp.2023.101690.
[281] A.J. Shah, N. Isakadze, O. Levantsevych, A. Vest, G. Clifford, S. Nemati, Detecting heart failure using wearables: a pilot study, Physiol. Meas. 41 (2020) 044001, https://doi.org/10.1088/1361-6579/ab7f93.
[282] A.G. Bonomi, L.M. Eerikäinen, F. Schipper, R.M. Aarts, H.M. De Morree, L. Dekker, Detecting episodes of brady- and tachycardia using photoplethysmography at the wrist in free-living conditions: 44th Computing in Cardiology Conference (CinC 2017), Comput. Cardiol. 44 (2017), https://doi.org/10.22489/CinC.2017.271-329.
[283] R. Mukkamala, S.G. Shroff, C. Landry, K.G. Kyriakoulis, A.P. Avolio, G.S. Stergiou, The Microsoft Research Aurora Project: Important Findings on Cuffless Blood Pressure Measurement, Hypertension 80 (2022) 534–540, https://doi.org/10.1161/HYPERTENSIONAHA.122.20410.
[284] H. Korkalainen, J. Aakko, B. Duce, S. Kainulainen, A. Leino, S. Nikkonen, I. O. Afara, S. Myllymaa, J. Töyräs, T. Leppänen, Deep learning enables sleep staging from photoplethysmogram for patients with suspected sleep apnea, Sleep 43 (2020) zsaa098, https://doi.org/10.1093/sleep/zsaa098.
[285] Y. Zheng, Z. Zhan, Q. Chen, J. Chen, J. Luo, J. Cai, Y. Zhou, K. Chen, W. Xie, Highly Sensitive Perovskite Photoplethysmography Sensor for Blood Glucose Sensing Using Machine Learning Techniques, Adv. Sci. 11 (2024) 2405681, https://doi.org/10.1002/advs.202405681.
[286] A. Beros, J. Sluyter, A. Hughes, B. Hametner, S. Wassertheurer, R. Scragg, Arterial stiffness and incident chronic kidney disease: a large population-based cohort study, J. Nephrol. 37 (2024) 1241–1250, https://doi.org/10.1007/s40620-024-01968-x.

[287] M. Briet, P. Boutouyrie, S. Laurent, G.M. London, Arterial stiffness and pulse pressure in CKD and ESRD, Kidney Int. 82 (2012) 388–400, https://doi.org/10.1038/ki.2012.131.
[288] L.L. Cooper, B.R. Prescott, V. Xanthakis, E.J. Benjamin, R.S. Vasan, N. M. Hamburg, M.T. Long, G.F. Mitchell, Association of Aortic Stiffness and Pressure Pulsatility With Noninvasive Estimates of Hepatic Steatosis and Fibrosis: The Framingham Heart Study, Arterioscler. Thromb. Vasc. Biol. 44 (2024) 1704–1715, https://doi.org/10.1161/ATVBAHA.123.320553.
[289] L. Zou, G. Liu, Multiscale Bidirectional Temporal Convolutional Network for Sleep Apnea Detection Based on Wearable Photoplethysmography Bracelet, IEEE J. Biomed. Health Inform. 28 (2024) 1331–1340, https://doi.org/10.1109/JBHI.2023.3335658.
[290] Q. Shen, X. Yang, L. Zou, K. Wei, C. Wang, G. Liu, Multitask Residual Shrinkage Convolutional Neural Network for Sleep Apnea Detection Based on Wearable Bracelet Photoplethysmography, IEEE Internet Things J. 9 (2022) 25207–25222, https://doi.org/10.1109/JIOT.2022.3195777.
[291] T. Chen, J. Zhang, Z. Xu, S.J. Redmond, N.H. Lovell, G. Liu, C. Wang, Energy-Efficient Sleep Apnea Detection Using a Hyperdimensional Computing Framework Based on Wearable Bracelet Photoplethysmography, IEEE Trans. Biomed. Eng. 71 (2024) 2483–2494, https://doi.org/10.1109/TBME.2024.3377270.
[292] K. Markov, M. Elgendi, V. Birrer, C. Menon, Interpretable feature-based machine learning for automatic sleep detection using photoplethysmography, Npj Biosensing 2 (2025) 24, https://doi.org/10.1038/s44328-025-00041-2.
[293] K. Kotzen, P.H. Charlton, S. Salabi, L. Amar, A. Landesberg, J.A. Behar, SleepPPG-Net: A Deep Learning Algorithm for Robust Sleep Staging From Continuous Photoplethysmography, IEEE J. Biomed. Health Inform. 27 (2023) 924–932, https://doi.org/10.1109/JBHI.2022.3225363.
[294] G. Kocabay, H. Hasdemir, M. Yildiz, Evaluation of pulse wave velocity in systemic lupus erythematosus, rheumatoid arthritis and Behçet's disease, J. Cardiol. 59 (2012) 72–77, https://doi.org/10.1016/j.jjcc.2011.09.004.
[295] E. Almeida-Gutierrez, P. Garcia-De La Torre, A. Acevedo-Melendez, J. Torres-Rosales, A. Pacheco-Lopez, K. Lupercio-Mora, R.C. Garcia-Mendez, G. Borrayo-Sanchez, G. Saturno-Chiu, P5347Pulse wave velocity is associated with cognitive impairment in older adults with heart disease, Eur. Heart J. 40 (2019) ehz746.0314, https://doi.org/10.1093/eurheartj/ehz746.0314.
[296] W. Nanyue, Y. Youhua, H. Dawei, L. Jia, L. Tongda, S. Zengyu, C. Yanping, Wangjia Xueliyuan, Comparative study of pulse-diagnosis signals between 2 kinds of liver disease patients based on the combination of unsupervised learning and supervised learning, IEEE Int. Conf. Bioinforma. Biomed. 2013 (2013) 260–262, https://doi.org/10.1109/BIBM.2013.6732688.
[297] W. Nanyue, Y. Youhua, H. Dawei, X. Bin, L. Jia, L. Tongda, X. Liyuan, S. Zengyu, C. Yanping, W. Jia, Pulse Diagnosis Signals Analysis of Fatty Liver Disease and Cirrhosis Patients by Using Machine Learning, Sci. World J. 2015 (2015) 859192, https://doi.org/10.1155/2015/859192.
[298] J. Wang, S. Liu, Q. Cao, S. Wu, J. Niu, R. Zheng, L. Bie, Z. Xin, Y. Zhu, S. Wang, H. Lin, T. Wang, M. Xu, J. Lu, Y. Chen, Y. Xu, W. Wang, G. Ning, Y. Xu, M. Li, Y. Bi, Z. Zhao, New definition of metabolic dysfunction-associated fatty liver disease with elevated brachial-ankle pulse wave velocity and albuminuria: a prospective cohort study, Front. Med. 16 (2022) 714–722, https://doi.org/10.1007/s11684-021-0888-8.
[299] V.W.-S. Wong, G.L.-H. Wong, G.W.-K. Yip, A.O.-S. Lo, J. Limquiaco, W.C.-W. Chu, A.M.-L. Chim, C.-M. Yu, J. Yu, F.K.-L. Chan, J.J.-Y. Sung, H.L.-Y. Chan, Coronary artery disease and cardiovascular outcomes in patients with non-alcoholic fatty liver disease, Gut 60 (2011) 1721–1727, https://doi.org/10.1136/gut.2011.242016.
[300] Z. Zhang, Y. Zhang, L. Yao, H. Song, A. Kos, A sensor-based wrist pulse signal processing and lung cancer recognition, J. Biomed. Inform. 79 (2018) 107–116, https://doi.org/10.1016/j.jbi.2018.01.009.
[301] X.F. Teng, Y.T. Zhang, Continuous and noninvasive estimation of arterial blood pressure using a photoplethysmographic approach, Proc. 25th Annu. Int. Conf. IEEE Eng. Med. Biol. Soc. 4 (2003) 3153–3156, https://doi.org/10.1109/IEMBS.2003.1280811.
[302] F. Miao, N. Fu, Y.-T. Zhang, X.-R. Ding, X. Hong, Q. He, Y. Li, A Novel Continuous Blood Pressure Estimation Approach Based on Data Mining Techniques, IEEE J. Biomed. Health Inform. 21 (2017) 1730–1740, https://doi.org/10.1109/JBHI.2017.2691715.
[303] C. Yi, C. Jian, J. Wenqiang, Continuous blood pressure measurement based on photoplethysmography, 2019 14th IEEE Int. Conf. Electron. Meas. & Instrum. (ICEMI) (2019) 1656–1663, https://doi.org/10.1109/ICEMI46757.2019.9101774.
[304] G. Slapničar, N. Mlakar, M. Luštrek, Blood Pressure Estimation from Photoplethysmogram Using a Spectro-Temporal Deep Neural Network, Sensors 19 (2019) 3420, https://doi.org/10.3390/s19153420.
[305] M. Elgendi, F. Haugg, R.R. Fletcher, J. Allen, H. Shin, A. Alian, C. Menon, Recommendations for evaluating photoplethysmography-based algorithms for blood pressure assessment, Commun. Med. 4 (2024) 140, https://doi.org/10.1038/s43856-024-00555-2.
[306] S. González, W.-T. Hsieh, T.P.-C. Chen, A benchmark for machine-learning based non-invasive blood pressure estimation using photoplethysmogram, Sci. Data 10 (2023) 149, https://doi.org/10.1038/s41597-023-02020-6.
[307] L. Alzubaidi, J. Zhang, A.J. Humaidi, A. Al-Dujaili, Y. Duan, O. Al-Shamma, J. Santamaría, M.A. Fadhel, M. Al-Amidie, L. Farhan, Review of deep learning: concepts, CNN architectures, challenges, applications, future directions, J. Big Data 8 (2021) 53, https://doi.org/10.1186/s40537-021-00444-8.
[308] C. El Hajj, P.A. Kyriacou, Recurrent neural network models for blood pressure monitoring using PPG morphological features, 2021 43rd Annu. Int. Conf. IEEE Eng. Med. & Biol. Soc. (EMBC) (2021) 1865–1868, https://doi.org/10.1109/EMBC46164.2021.9630319.
[309] C. Sideris, H. Kalantarian, E. Nemati, M. Sarrafzadeh, Building continuous arterial blood pressure prediction models using recurrent networks, IEEE Int. Conf. Smart Comput. (SMARTCOMP) 2016 (2016) 1–5, https://doi.org/10.1109/SMARTCOMP.2016.7501681.
[310] G. Keren, B. Schuller, Convolutional RNN: An enhanced model for extracting features from sequential data, in: 2016 International Joint Conference on Neural Networks (IJCNN), IEEE, 2016, pp. 3412–3419, https://doi.org/10.1109/IJCNN.2016.7727636.
[311] J. Liu, S. Hu, Y. Wang, Q. Hu, D. Wang, C. Yang, A Lightweight Hybrid Model Using Multiscale Markov Transition Field for Real-Time Quality Assessment of Photoplethysmography Signals, IEEE J. Biomed. Health Inform. 28 (2024) 1078–1088, https://doi.org/10.1109/JBHI.2023.3331975.
[312] C. Ma, P. Zhang, F. Song, Y. Sun, G. Fan, T. Zhang, Y. Feng, G. Zhang, KD-Informer: A Cuff-Less Continuous Blood Pressure Waveform Estimation Approach Based on Single Photoplethysmography, IEEE J. Biomed. Health Inform. 27 (2023) 2219–2230, https://doi.org/10.1109/JBHI.2022.3181328.
[313] M. Mäkynen, G.A. Ng, X. Li, F.S. Schlindwein, T.C. Pearce, Compressed Deep Learning Models for Wearable Atrial Fibrillation Detection through Attention, Sensors 24 (2024) 4787, https://doi.org/10.3390/s24154787.
[314] K. Rishi Vardhan, S. Vedanth, G. Poojah, K. Abhishek, M. Nitish Kumar, V. Vijayaraghavan, BP-Net: Efficient Deep Learning for Continuous Arterial Blood Pressure Estimation using Photoplethysmogram, 2021 20th IEEE Int. Conf. Mach. Learn. Appl. (ICMLA) (2021) 1495–1500, https://doi.org/10.1109/ICMLA52953.2021.00241.
[315] T. Islam, Md.S. Hafiz, J.R. Jim, Md.M. Kabir, M.F. Mridha, A systematic review of deep learning data augmentation in medical imaging: Recent advances and future research directions, Healthc. Anal. 5 (2024) 100340, https://doi.org/10.1016/j.health.2024.100340.
[316] P. Antiperovitch, D. Mortara, J. Barrios, R. Avram, K. Yee, A.N. Khaless, A. Cristal, G. Tison, J. Olgin, Continuous atrial fibrillation monitoring from photoplethysmography: Comparison between supervised deep learning and heuristic signal processing, JACC Clin. Electrophysiol. 10 (2024) 334–345, https://doi.org/10.1016/j.jacep.2024.01.008.
[317] N.J. van Steijn, I.S. Blommestijn, S. Blok, S. Pepplinkhuizen, G.A. Somsen, R. E. Knops, L. Breukel, J.G.P. Tijssen, I.I. Tulevski, P.M. Croon, M.M. Winter, Enhanced detection and prompt diagnosis of atrial fibrillation using apple watch, JACC 87 (2026) 1714–1728, https://doi.org/10.1016/j.jacc.2025.11.032.
[318] S. Zuo, L. Zhou, H. Feng, et al., Validation of Smartwatches Integrated With Photoplethysmography for Continuous Evaluation of Atrial Fibrillation Burden, JACC Clin. Electrophysiol. (2026), https://doi.org/10.1016/j.jacep.2026.03.036.
[319] E. Hellou, T. Jamal, E. Zuroff, P. Kalhor, M. Delgado-Lelievre, M. Manzato, L. O. Lerman, A. Lerman, E. Kachel, Z. Zoghby, Performance of a cuffless photoplethysmography-based device for continuous monitoring of blood pressure after cardiac surgery: A preliminary validation study, J. Human. Hypertens. 39 (2025) 894–902, https://doi.org/10.1038/s41371-025-01082-w.
[320] D.H. Nguyen, P.C.-P. Chao, H.F. Yan, T.-Y. Tu, C.-H. Cheng, T.-P. Phan, Predicting blood pressures for pregnant women by PPG and personalized deep learning, IEEE J. Biomed. Health Inform. 29 (2025) 5–16, https://doi.org/10.1109/JBHI.2024.3386707.
[321] C. Ma, L. Guo, H. Zhang, Z. Liu, G. Zhang, DiffCNBP: lightweight diffusion model for IoMT-based continuous cuffless blood pressure waveform monitoring using PPG, IEEE Internet Things J. 12 (2025) 61–80, https://doi.org/10.1109/JIOT.2024.3460382.
[322] J. Liu, H. Zhu, W. Xiang, S. Hu, Q. Hu, D. Wang, H. Yang, Z. Mao, F. Xu, C. Yang, An IoMT-driven framework for precision cardiovascular assessment incorporating multiscale perspectives and microfiber bragg grating, IEEE Internet Things J. 12 (2025) 4050–4064, https://doi.org/10.1109/JIOT.2024.3483450.
[323] L. Yuan, X. Gao, R. Kang, X. Zhang, X. Meng, X. Li, X. Li, Flexible strain sensors based on an interlayer synergistic effect of nanomaterials for continuous and noninvasive blood pressure monitoring, ACS Appl. Mater. Interfaces 16 (2024) 26943–26953, https://doi.org/10.1021/acsami.4c04134.
[324] K.-H. Huang, F. Tan, T.-D. Wang, Y.-J. Yang, A highly sensitive pressure-sensing array for blood pressure estimation assisted by machine-learning techniques, Sensors 19 (2019) 848, https://doi.org/10.3390/s19040848.
[325] C. Liu, F. Ma, Q. Sun, Q. Hu, W. Tong, X. Guo, R. Hu, P. Liu, Y. Huang, X. Hao, W. Ma, Y. Zhang, Highly sensitive flexible capacitive pressure sensor based on a multicross-linked dual-network ionic hydrogel for blood pressure monitoring applications, ACS Appl. Mater. Interfaces 16 (2024) 34042–34056, https://doi.org/10.1021/acsami.4c04686.
[326] Y. Wu, Y. Li, X. Wang, P. Guo, H. Luo, X. Li, X. Zhu, J. Yang, Intelligent ring for dynamic pulse wave monitoring using fine tubular triboelectric nanogenerators, Nano Energy 134 (2025) 110581, https://doi.org/10.1016/j.nanoen.2024.110581.
[327] C. Yao, S. Liu, X. Xu, P. Yun, T. Zhang, T. Sun, M. He, B. Liang, M. Li, S. Huang, Y. Li, Y. Wang, H. Chen, X. Xie, Long-term used continuous blood pressure monitoring via personalized object transfer learning architecture enhanced triboelectric pulse sensors, Adv. Funct. Mater. 35 (2025) 2418318, https://doi.org/10.1002/adfm.202418318.
[328] S. Tian, L. Wang, R. Zhu, A flexible multimodal pulse sensor for wearable continuous blood pressure monitoring, Mater. Horiz. 11 (2024) 2428–2437, https://doi.org/10.1039/D3MH01999C.

[329] L. Li, S. Sheng, Y. Liu, J. Wen, C. Song, Z. Chen, W. Xu, Z. Zhang, W. Fan, C. Chen, Q. Sun, P.-P. Shum, Automatic and continuous blood pressure monitoring via an optical-fiber-sensor-assisted smartwatch, PhotoniX 4 (2023) 1–14, https://doi.org/10.1186/s43074-023-00099-z.
[330] A.E. Schutte, Wearable cuffless blood pressure tracking: when will they be good enough? J. Human. Hypertens. 38 (2024) 669–672, https://doi.org/10.1038/s41371-024-00932-3.
[331] J.-R. Hu, D.Y. Park, N. Agarwal, M. Herzig, G. Ormseth, M. Kaushik, D.M. Giao, R.-A.N. Turkson-Ocran, S.P. Juraschek, The Promise and Illusion of Continuous, Cuffless Blood Pressure Monitoring, Curr. Cardiol. Rep. 25 (2023) 1139–1149, https://doi.org/10.1007/s11886-023-01932-4.
[332] R. Mukkamala, S.G. Shroff, K.G. Kyriakoulis, A.P. Avolio, G.S. Stergiou, Cuffless Blood Pressure Measurement: Where Do We Actually Stand? Hypertension 82 (2025) 957–970, https://doi.org/10.1161/HYPERTENSIONAHA.125.24822.
[333] R.S. Kasbekar, S. Ji, E.A. Clancy, A. Goel, Optimizing the input feature sets and machine learning algorithms for reliable and accurate estimation of continuous, cuffless blood pressure, Sci. Rep. 13 (2023) 7750, https://doi.org/10.1038/s41598-023-34677-9.
[334] W. Wang, P. Mohseni, K.L. Kilgore, L. Najafizadeh, PulseDB: A large, cleaned dataset based on MIMIC-III and VitalDB for benchmarking cuff-less blood pressure estimation methods, Front. Digit. Health 4 (2023) 1090854, https://doi.org/10.3389/fdgth.2022.1090854.
[335] Y. Yao, Y. Wang, Y. Liu, Y. Yu, X. Wang, T. Wang, B. Zheng, M. Yan, Association of perioperative step count tracked by a wristband with surgical outcomes in minimally invasive lung cancer surgery: A prospective observational study, Frontiers in Medicine 12 (2025) 1590327, https://doi.org/10.3389/fmed.2025.1590327.
[336] S.R. Greysen, K.J. Waddell, M.S. Patel, Exploring wearables to focus on the "sweet spot" of physical activity and sleep after hospitalization: Secondary analysis, JMIR mHealth uHealth 10 (2022) e30089, https://doi.org/10.2196/30089.
[337] T.J. Daskivich, J. Houman, M. Lopez, M. Luu, P. Fleshner, K. Zaghiyan, S. Cunneen, M. Burch, C. Walsh, G. Paiement, T. Kremen, H. Soukiasian, A. Spitzer, T. Jackson, H.L. Kim, A. Li, B. Spiegel, Association of wearable activity monitors with assessment of daily ambulation and length of stay among patients undergoing major surgery, JAMA Netw. Open. 2 (2019) e187673, https://doi.org/10.1001/jamanetworkopen.2018.7673.
[338] A. Rajkomar, E. Oren, K. Chen, A.M. Dai, N. Hajaj, M. Hardt, P.J. Liu, X. Liu, J. Marcus, M. Sun, P. Sundberg, H. Yee, K. Zhang, Y. Zhang, G. Flores, G. E. Duggan, J. Irvine, Q. Le, K. Litsch, A. Mossin, J. Tansuwan, D. Wang, J. Wexler, J. Wilson, D. Ludwig, S.L. Volchenboum, K. Chou, M. Pearson, S. Madabushi, N. H. Shah, A.J. Butte, M.D. Howell, C. Cui, G.S. Corrado, J. Dean, Scalable and accurate deep learning with electronic health records, Npj Digit. Med. 1 (2018) 18, https://doi.org/10.1038/s41746-018-0029-1.
[339] W.K. Wang, R. Yang, C. Pang, K. Natarajan, N. Liu, D. McDuff, D.J. Slotwiner, F. Wang, M. McDermott, X. Xu, Beyond the clinic: A large-scale evaluation of augmenting EHR with wearable data for diverse health prediction, arXiv Preprint arXiv:2509.22920 (2025).
[340] C.V.F. Pereira, E.M. de Oliveira, A.D. de Souza, Machine learning applied to edge computing and wearable devices for healthcare: systematic mapping of the literature, Sensors 24 (2024), https://doi.org/10.3390/s24196322.
[341] D. Duncker, W.Y. Ding, S. Etheridge, P.A. Noseworthy, C. Veltmann, X. Yao, T. J. Bunch, D. Gupta, Smart wearables for cardiac monitoring—real-world use beyond atrial fibrillation, Sensors 21 (2021) 2539, https://doi.org/10.3390/s21072539.
[342] V.-T. Tran, C. Riveros, P. Ravaud, Patients' views of wearable devices and AI in healthcare: Findings from the ComPaRe e-cohort, npj Digit. Med. 2 (2019) 53, https://doi.org/10.1038/s41746-019-0132-y.
[343] K. Sel, D. Osman, N. Huerta, A. Edgar, R.I. Pettigrew, R. Jafari, Continuous cuffless blood pressure monitoring with a wearable ring bioimpedance device, npj Digit. Med. 6 (2023) 1–11, https://doi.org/10.1038/s41746-023-00796-w.
[344] D. Kireev, K. Sel, B. Ibrahim, N. Kumar, A. Akbari, R. Jafari, D. Akinwande, Continuous cuffless monitoring of arterial blood pressure via graphene bioimpedance tattoos, Nat. Nanotechnol. 17 (2022) 864–870, https://doi.org/10.1038/s41565-022-01145-w.
[345] K.-H. Ha, H. Huh, Z. Li, N. Lu, Soft capacitive pressure sensors: trends, challenges, and perspectives, ACS Nano 16 (2022) 3442–3448, https://doi.org/10.1021/acsnano.2c00308.